IOWA STATE UNIVERSITY
Digital Repository

2002

Analytical applications of ionic liquids and determination of cell viability using capillary electrophoresis coupled with laser-induced fluorescence detection

Lingfeng (Brian) He
Iowa State University

Follow this and additional works at: https://lib.dr.iastate.edu/rtd

Part of the Analytical Chemistry Commons, and the Microbiology Commons

Recommended Citation

INFORMATION TO USERS

This manuscript has been reproduced from the microfilm master. UMI films the text directly from the original or copy submitted. Thus, some thesis and dissertation copies are in typewriter face, while others may be from any type of computer printer.

The quality of this reproduction is dependent upon the quality of the copy submitted. Broken or indistinct print, colored or poor quality illustrations and photographs, print bleedthrough, substandard margins, and improper alignment can adversely affect reproduction.

In the unlikely event that the author did not send UMI a complete manuscript and there are missing pages, these will be noted. Also, if unauthorized copyright material had to be removed, a note will indicate the deletion.

Oversize materials (e.g., maps, drawings, charts) are reproduced by sectioning the original, beginning at the upper left-hand corner and continuing from left to right in equal sections with small overlaps.

Analytical applications of ionic liquids and determination of cell viability using capillary

electrophoresis coupled with laser-induced fluorescence detection

by

Lingfeng (Brian) He

A dissertation submitted to the graduate faculty

in partial fulfillment of the requirements for the degree of

DOCTOR OF PHILOSOPHY

Major: Analytical Chemistry

Program of Study Committee:
Daniel W. Armstrong, Major Professor
Bonita A. Glatz
Robert S. Houk
William S. Jenks
Edward S. Yeung

Iowa State University

Ames, Iowa

2002

UMI Number: 3073451

UMI®

Graduate College
Iowa State University

This is to certify that the doctoral dissertation of

Lingfeng He

has met the dissertation requirements of Iowa State University

Signature was redacted for privacy.

Major Professor

Signature was redacted for privacy.

For the Major Program

This dissertation is dedicated to

My grandparents

My parents Longhua He and Juying Su,

My wife Xuerong Gao

My children

TABLE OF CONTENTS

PART TWO. DETERMINATION OF CELL VIABILITY USING CAPILLARY ELECTROPHORESIS COUPLED WITH LASER-INDUCED FLUORESCENCE DETECTION

ACKNOWLEDGEMENT

Pursuing a Ph.D degree is a long journey for me both physically and spiritually. Now when I look back my pathway, my heart is full of thanks and appreciations. I would like to express my sincere gratitude to my advisor, Professor Daniel W. Armstrong, for his guidance, inspiration, encouragement, and patience during the past five years. Without him, I may not experience and enjoy the fantastic things about scientific research. To my current POS committee – Dr. Bonita A. Glatz, Dr. William S. Jenks, Dr. Robert S. Houk, and Dr. Edward S. Yeung, and previous POS committee – Dr. Dennis C. Johnson, thank you all for your time, and encouragement. It is my honor to have you serve as my committee members. I would also like to thank Dr. Armstrong's research group in University of Missouri-Rolla and Iowa State University for their valuable intellectual input and support over the years. Your caring friendships are memorable and warm my heart for my whole life. I want to express my special thanks to Dr. Armstrong's secretaries – Marry Jo and Anglia for taking care of those trivial but important things for me.

I will always be indebted to so many visiting scholars in Dr. Armstrong's laboratory, including Alain, Marco, Yuqi, Eve, Juraj, Sam, Fanming, etc. No matter what we did, discussing, arguing, having lunch, or chatting, I always enjoyed the time we spent together. My thanks are also extended to Dr Yeung's research group for their generous support and friendship.

I would especially like to thank my beloved wife Xuerong for truly being my rock. Whenever I need her, she is always there for me. She is a gift from God. I would also like to thank my whole family and my wife's family for standing by my side all the time. Never has one person been blessed with such wonderful families.

May God bless and be with everyone of you.

The financial support from University of Missouri-Rolla and Iowa State University for this work is gratefully appreciated.

INTRODUCTION

Newly developed ionic liquids that are air and moisture stable have been subject to an increasing number of scientific investigations. Their recent applications include novel solvent systems and catalysts for organic synthesis, versatile electrolytes for electrochemical studies, and liquid-liquid extraction solvents. The potential usage of ionic liquids could be vast. The purpose of the first part of this dissertation is to address the novel applications of ionic liquids in the field of analytical chemistry. In this part, the author's research can be divided into two directions: (a) examining the chromatographic performance of ionic liquids as gas chromatography (GC) stationary phases or solvents for GC stationary phases; (b) synthesizing new ionic liquids and testing their properties as matrices for matrix-assisted laser desorption/ionization (MALDI) mass spectrometry.

In addition to multiple applications of ionic liquids, we also became interested in developing an effective instrumental method to assess the viability of microorganisms and mammalian cells. Since existing techniques, such as plate count methods, flow cytometry, etc., are either laborious or too expensive, highly efficient and more affordable methods are needed. Therefore, the second part of this dissertation is focused on the feasibility of using capillary electrophoresis (CE), in combination with fluorescent labeling technique, to determine cell viability. The author first adapted the recently developed highly efficient microbial CE method and viable fluorescence staining method to determine the viability of bacteria and yeast, and then carried out the potency study of animal sperm using a similar CE approach.

This dissertation is presented as two independent parts. Each part begins with a general introduction and literature review of recent progress in the specific research area. The following chapters are arranged in such a way that the related published papers or manuscripts are presented as separate chapters. All these chapters are presented in publication format. References for each chapter are independent and appear at the end of the chapter. The last chapter is general conclusions covering both parts of this dissertation.

PART ONE

ANALYTICAL APPLICATIONS OF IONIC LIQUIDS

CHAPTER 1

GENERAL INTRODUCTION AND LITERATURE REVIEW

1.1. INTRODUCTION

Ionic liquids (ILs) are a class of solvents in which every entity is an ion. To avoid confusion with inorganic molten salts, which are generally thought to be high-melting, highly viscous and very corrosive media, the term "ionic liquid" is specifically selected to refer to a class of organic salts with low melting points (< 100 °C). Ionic liquids are not new; some of them have been known for many years, for instance, ethylammonium nitrate ($[EtNH_3][NO_3]$), which has a melting point of 12 °C, was first described in 1914 [1]. Because of their moisture-sensitivity, and thermal and chemical instability, ionic liquids didn't receive extensive attention at first. In the past two decades, their promise as an alternative reaction medium (solvent) has increased the interest in this field [2-9]. The important discovery was that 1,3-dimethylimidazolium [10,11] and N-alkylpyridinium [12,13] salts of common weakly coordinating anions (such as BF_4^-, PF_6^-, $CF_3SO_3^-$, etc) are liquid at or near room temperature. Although the reason why these salts have such low melting point is not well understood, it is believed that the asymmetry of the cation and the type of anion play major roles [14,15]. The structures of some important cations and anions in ionic liquids are shown in Figure 1.1 and some physical properties of ionic liquids containing fluoroanions are given in Table 1.1.

Ionic liquids possess several favorable solvent properties: (a) they are good solvents, with moderate viscosities for a wide range of inorganic, organic and polymeric chemicals, (b) they are often composed of poorly coordinating ions, so they have the potential to be highly polar yet weakly coordinating solvents, (c) many of the newly discovered ionic liquids are air- and water-stable. They are immiscible with a number of organic solvents and provide a nonaqueous, polar alternative for biphasic systems. Hydrophobic ionic liquids can also be used as immiscible polar phases with water. (d) Ionic liquids have no detectable vapor pressure, hence they may be used in high-vacuum systems and eliminate environmental problems associated with production of volatile organic carbons (VOCs). These features of ionic liquids, together with other useful properties including high conductivity. wide electrochemical window (ca. 4 Volt), tolerance to strong acids, and excellent thermal and chemical stability, initiated a range of active research on the potential applications of ionic liquids as solvents and catalysts for organic synthesis [7,8], and versatile electrolytes for electrochemical studies [16-22]. 1-Alkyl-3-methylimidazolium based ionic liquids (such as
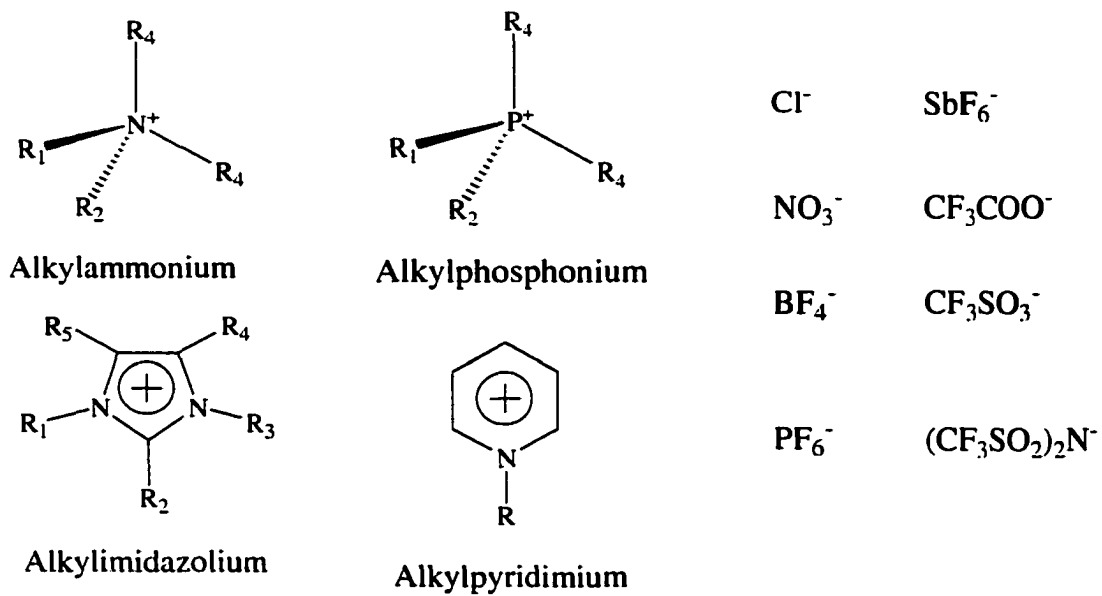
Figure 1.1. The structures of some important cations and anions.

Table 1.1. The melting point (m. p.), density, viscosity and conductivity of some ionic liquids containing fluoroanions (in the order of conductivity).[a]
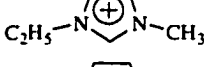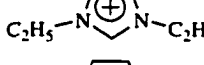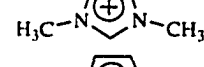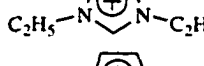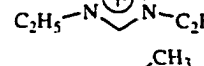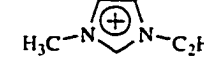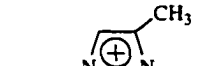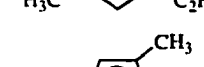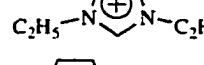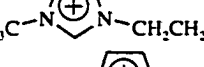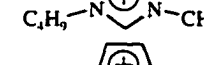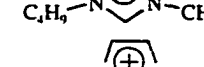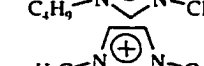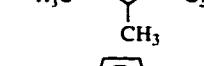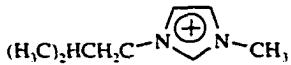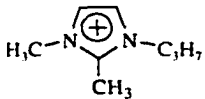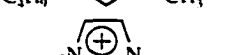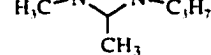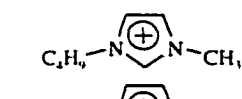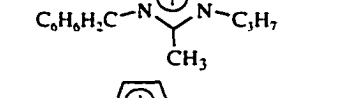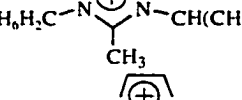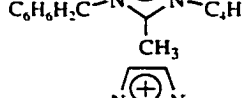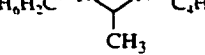
Cation	Anion	m. p. (K)	Density (gcm^{-3})	Viscosity (cP)	Conductivity (Sm^{-1})
C_2H_5–N⊕N–CH_3	F(HF)$_n^-$	183	1.13 (298 K)	4.9 (298 K)	12 (298 K)
C_2H_5–N⊕N–CH_3	BF_4^-	288	1.24 (295 K)	37.7 (295 K)	1.4 (298 K)
C_2H_5–N⊕N–CH_3	CF_3COO^-	259	1.285 (295 K)	35 (293 K)	0.96 (293 K)
C_2H_5–N⊕N–CH_3	$CF_3SO_3^-$	264	1.38 (298 K)	42.7 (298 K)	0.92 (298 K)
C_2H_5–N⊕N–CH_3	$(CF_3SO_2)_2N^-$	270	1.520 (295 K)	34 (293 K)	0.88 (293 K)
C_2H_5–N⊕N–C_2H_5	$(CF_3SO_2)_2N^-$	287	1.452 (294 K)	35 (293 K)	0.85 (293 K)
H_3C–N⊕N–CH_3	$(CF_3SO_2)_2N^-$	295	1.559 (295 K)	44 (293 K)	0.84 (293 K)
C_2H_5–N⊕N–C_2H_5	$CF_3SO_3^-$	296	1.330 (295 K)	53 (293 K)	0.75 (293 K)
C_2H_5–N⊕N–C_2H_5	CF_3COO^-	223-243 g^b	1.250 (295 K)	43 (293 K)	0.74 (293 K)
H_3C–N⊕N–C_2H_5 (CH$_3$)	$(CF_3SO_2)_2N^-$	270	1.470 (295 K)	37 (293 K)	0.66 (293 K)
H_3C–N⊕N–C_2H_5 (CH$_3$)	$CF_3SO_3^-$	279	1.334 (293 K)	51 (293 K)	0.64 (293 K)
C_2H_5–N⊕N–C_2H_5 (CH$_3$)	$(CF_3SO_2)_2N^-$	251	1.432 (296 K)	36 (293 K)	0.62 (293 K)
H_3C–N⊕N–$CH_2CH_2OCH_3$	$(CF_3SO_2)_2N^-$	223-243	1.496 (295 K)	54 (293 K)	0.42 (293 K)
C_4H_9–N⊕N–CH_3	$(CF_3SO_2)_2N^-$	269	1.429 (292 K)	52 (293 K)	0.39 (293 K)
C_4H_9–N⊕N–CH_3	$CF_3SO_3^-$	289	1.290 (293 K)	90 (293 K)	0.37 (293 K)
C_4H_9–N⊕N–CH_3	CF_3COO^-	223-243 g^b	1.209 (294 K)	73 (293 K)	0.32 (293 K)
H_3C–N⊕N–C_2H_5 (CH$_3$)	$(CF_3SO_2)_2N^-$	293	1.495 (294 K)	88 (293 K)	0.32 (293 K)
C_3H_7–N⊕N–C_2H_5	$CF_3SO_3^-$	275	1.27		0.27 (298 K)

Table 1.1. (Continued)

Cation	Anion	m. p. (K)	Density (gcm^{-3})	Viscosity (cP)	Conductivity (Sm^{-1})
(H$_3$C)$_2$HCH$_2$C—imidazolium—CH$_3$	(CF$_3$SO$_2$)$_2$N$^-$	223-243 g^b	1.428 (293 K)	83 (293 K)	0.26 (293 K)
H$_3$C—imidazolium(CH$_3$)—C$_3$H$_7$	(CF$_3$SO$_2$)$_2$N$^-$				0.252 (298 K)
C$_2$H$_5$—imidazolium—C$_2$H$_5$	CF$_3$COO$^-$	223-243	1.183 (296 K)	89 (293 K)	0.25 (293 K)
C$_4$H$_9$—imidazolium—CH$_3$	BF$_4^-$	192	1.17 (303 K)	233 (303 K)	0.173 (298.5 K)
C$_4$H$_9$—imidazolium—CH$_3$	PF$_6^-$	212	1.37 (303 K)	312 (303 K)	0.146 (298.5 K)
C$_2$H$_5$—imidazolium—CH$_3$	(CF$_3$SO$_2$)$_3$C$^-$				0.13 (295 K)
C$_4$H$_9$—imidazolium—CH$_3$	CF$_3$(CF$_2$)$_2$CO$^-$	223-243 ^{b}	1.333 (295 K)	182 (293 K)	0.10 (293 K)
H$_3$C—imidazolium—CH$_2$CF$_3$	(CF$_3$SO$_2$)$_2$N$^-$	223-243	1.656 (293 K)	248 (293 K)	0.098 (293 K)
C$_4$H$_9$—imidazolium—C$_2$H$_5$	CF$_3$(CF$_2$)$_3$SO$_3^-$	294	1.427 (291 K)	323 (293 K)	0.053 (293 K)
H$_3$C—imidazolium(CH$_3$)—C$_3$H$_7$	(CF$_3$SO$_2$)$_3$C$^-$				0.046 (298 K)
C$_4$H$_9$—imidazolium—CH$_3$	CF$_3$(CF$_2$)$_3$SO$_3^-$	293	1.473 (291 K)	373 (293 K)	0.045 (293 K)
C$_6$H$_6$H$_2$C—imidazolium(CH$_3$)—C$_3$H$_7$	(CF$_3$SO$_2$)$_2$N$^-$	not crystallized			0.0059 (293 K)
C$_6$H$_6$H$_2$C—imidazolium(CH$_3$)—CH(CH$_3$)(C$_2$H$_5$)	(CF$_3$SO$_2$)$_2$N$^-$	not crystallized			0.0037 (293 K)
C$_6$H$_6$H$_2$C—imidazolium(CH$_3$)—C$_4$H$_9$	(CF$_3$SO$_2$)$_2$N$^-$	not crystallized			0.0029 (293 K)
C$_6$H$_6$H$_2$C—imidazolium(CH$_3$)—C$_4$H$_9$	(CF$_3$SO$_2$)$_2$N$^-$	not crystallized			0.0027 (293 K)
C$_4$H$_9$—imidazolium—C$_2$H$_5$	(CF$_3$SO$_2$)$_2$N$^-$	223-243			no data

^{a} Data are taken from ref. 9.

^{b} g stands for glass transition temperature.

1-butyl-3-methylimidazolium hexafluorophosphate [BMIM][PF$_6$]) are considered attractive alternatives to toxic, flammable volatile organic solvents for "clean processes" and "green chemistry" [3,23]. Several reviews have been published on the physico-chemical properties and applications of ionic liquids in organic synthesis [6-8].

Given their properties, ionic liquids could be used to advantage in a variety of separation methods. When employed in solvent extraction processes, the negligible vapor pressure and low flammability of room temperature ionic liquids (RTIL), are important advantages over conventional organic solvents. Recently RTILs were considered as a water-immiscible phase in liquid-liquid extraction [24]. The distribution ratios for substituted-benzene derivatives between RTIL and water were approximately an order of magnitude less than the corresponding octanol / water partition coefficients. Although there was a rough correlation between these systems, there was a clear polarity difference [24]. For metal ion separations, Dai and co-workers found large distribution coefficient values for extraction of strontium nitrate from aqueous solutions into disubstituted imidazolium hexafluorophos-phates and bis[(trifluoromethyl)sulfonyl]amides by dicyclohexano-18-crown-6 (DC18C6) [25]. Rogers and co-workers reported the extraction of sodium, cesium, and strontium nitrates from aqueous solutions into 1-butyl-, 1-hexyl-, and 1-octyl-3-methylimidazolium hexafluorophosphates by 18-crown-6, DC18C6, and 4,4'(5')-di(*tert*-butylcyclohexano)-18-crown-6 [26]. Subsequently, Rogers and co-workers described "task specific" RTILs containing metal ion chelating units and their use in the solvent extraction of cadmium (II) and mercury (II) chlorides [27]. Very recently, Bartsch's group sysmatically studied the influence of structural variations of the 1-alkyl-3-methylimidazolium-based ionic liquids on the selectivity and efficiency of competitive alkali metal salt extraction by crown ether DC18C6 [28]. Another use of RTILs is as running electrolytes in capillary electrophoresis (CE). Using a CE method involving 1-alkyl-3-methylimidazolium-based ionic liquids, Stalcup *et al.* successfully resolved and identified phenolic compounds found in grape seed extracts [29].

Our initial interest in RTILs stemmed from their unusual combination of properties, i.e., volatility, viscosity, solubility, and polarity. Our interest was further enhanced when it was found that RTILs could solubilize a number of complex organic molecules of interest to the separation community (such as, cyclodextrins and macrocyclic antibiotics). Because of their unique ionic composition, wide liquid range (300 °C in some cases) and relatively good thermal stability, ionic liquids are potentially useful liquid stationary phases for gas chromatography (GC) and may provide unusual selectivity compared to conventional polymeric nonionic GC stationary phases presently in use. Therefore, the first chapter of this

dissertation will focus on examining ionic liquids as stationary phases for gas-liquid chromatography, while the following chapter explores the potential applications of ionic liquids as stationary phase solvents for methylated cyclodextrins in gas chromatography.

In a different context, it is well known that, in matrix-assisted laser desorption/ionization mass spectrometry (MALDI), the properties of the matrix are crucial for a successful analysis [30-51]. The general properties of effective matrixes for MALDI include: they must dissolve (liquid matrix) or co-crystallize (solid matrix) with the sample, strongly absorb the laser light, remain in the condensed phase under high-vacuum conditions, stifle both chemical and thermal degradation of the sample, and promote the ionization of the sample via any of a number of mechanisms [33-37]. Although both solids and liquids have been used as MALDI matrixes, solid matrixes are more widely utilized. They have the advantages of having low vapor pressure and in being simple, single-component systems with indigenous UV chromophores. Unfortunately, the analytes cannot be uniformly dispersed throughout the solid matrix. Both the solute and impurities segregate in the matrix, resulting in a considerable degree of heterogeneity and poor reproducibility. Conversely, liquid matrixes produce more homogeneous solutions and better shot-to-shot reproducibility. Their inherent volatility, however, results in a dynamic, changing, uncontrolled matrix. In addition, liquid matrixes usually do not contain the desired UV chromophore. Consequently, other components must be added to make up for this deficiency [35,52-55]. An ideal matrix for MALDI may be an UV-absorbing liquid that has little or no vapor pressure and promotes ionization as well or better than do the current solid matrixes.

We noticed that ionic liquids match these requirements quite well: they have no effective vapor pressure, which is important for mass spectral applications; they are good solvents for a variety of chemicals; and it is easy to incorporate appropriate chromophores into and adjust the physico-chemical properties of ionic liquids. Obviously, these properties mean that ionic liquids may have potential as novel matrices for MALDI. The third chapter of the dissertation will investigate ionic liquids as MALDI matrices for the analysis of peptides, proteins and polymers.

1.2. LITERATURE REVIEW

1.2.1. Ionic Liquids as GC Stationary Phases

The majority of stationary phases employed in gas-liquid chromatography (GC or GLC) are molecular liquids which retain solutes through all types of intermolecular forces, such as dispersion (instantaneous dipole-induced dipole forces), orientation (dipole-dipole forces), induction (dipole-induced dipole forces), and hydrogen bonding (complexation) interactions. The last three forces are selective interactions which may be utilized to separate substances of similar volatility [63]. Ionic liquids contain additional selective intermolecular forces due to the presence of charge-bearing groups. The forces between ions are strong, promote order in the liquid state, and are potentially useful for enhancing the separation of polar solutes.

Before the introduction of novel alkylimidazolium- and alkylpyridimium-based ionic liquids, a variety of salts had been used in GC for various purposes [56-82]. These salts can be classified into three categories: inorganic salts, inorganic hydrated melts, and organic molten salts. Inorganic salts have been used mainly in the form of additives to modify the selectivity of liquid phases [56]. Notable examples are the use of silver salts to improve the separation of saturated and unsaturated hydrocarbons and metal chelates, such as nickel (II) bis-3-heptafluorobutyryl-(IR)-camphorate for the separation of structural, configurational, and optical isomers [56,57]. It is also common practice to use inorganic salts as adsorbent deactivating agents in gas-solid chromatography [57]. Less frequently, inorganic salts have been used as adsorbing packing or as layers in open-tubular column gas-solid chromatography [58-61]. Low-melting-point inorganic salt eutectic mixtures have also been successfully used to separate volatile metal halides that were either too involatile or too reactive for analysis using conventional column packings [56,62]. The application of inorganic salts to the separation of organic solutes, however, was less successful owing primarily to low solubility of organic solutes in them and also because many solutes undergo chemical transformation in molten salt systems [63].
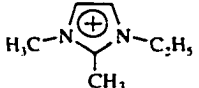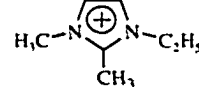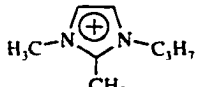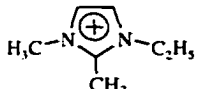
Compared to other salts, inorganic hydrated melts received much less attention as GC stationary phases. They are molten salts in which a cation (generally) has a filled or nearly filled coordination shell of water molecules. The water is tightly bound in the inner coordination sphere of the cation, which forms part of the lattice structure of the melt, and thus provide considerable stability to the system. Water vapor is not lost from the melt until temperatures well above the normal boiling point of water are reached. Poole, et al., used

calcium nitrate tetrahydrate as stationary phase in packed GC column and separated hydrocarbons and some substituted benzene derivatives [64]. Berezkin, et al, have been used crystal hydrates maintained in dynamic equilibrium with water steam-conditioned carrier gas to separate polar solutes [65,66].

Organic molten salts, also referred to as liquid organic salts in the literature, are defined as ionic liquids in this dissertation if their melting points are below 100 °C. In the early development of ionic liquid GC stationary phases, the dominant cations contained in organic molten salts are alkylammonium and alkylphosphonium (Figure 1.1). Unlike inorganic molten salts, the organic molten salts have lower melting-points, a significant capacity to dissolve a wide range of organic compounds, and lower chemical reactivity. In addition, they provide greater variability in the properties of the individual ions available for study. Therefore, many problems associated with the poor wetting characteristics and limited solubility of organic solutes in inorganic melts could be overcome by using organic molten salts [63]. The first application of organic molten salts as stationary phases for GC was reported by Barber *et al.*. These authors investigated the retention properties of a wide range of solutes on the stearate salts of the bivalent metals manganese, cobalt, nickel, copper, and zinc [67]. Since late 1970s, Poole and other groups published a series of papers on using organic molten salts as GC stationary phases [63,64,68-82]. Their studies were focused on characterization of the solvent properties of organic molten salts and the retention mechanisms of organic solutes on these ionic phases. Based on their results, a few conclusions can be drawn. First, organic molten salts can be classified as highly polar stationary phases for GC. Second, the interactions between solutes and organic molten salts are characterized by weak dispersive interactions, strong orientation interactions, and a wide range of proton donor/acceptor capabilities, which are usually absent in molecular GC stationary phases. Third, the dominant retention mechanism is gas-liquid phase partitioning and only in the case of the alkanes, alcohols, and benzaldehyde is gas-liquid phase adsorption important [63,83].

Although alkylammonium- and alkylphosphonium-based ionic liquids have had some success when used as stationary phases for GC, their usefulness is limited by their relatively narrow liquid ranges, thermal instability and unsatisfactory wettability towards fused silica surfaces. These are extremely important factors for the development of open tubular GC columns. Newer ionic liquids containing alkylimidazolium or alkyl-pyridimium cations have improved properties and are more suitable as GC stationary phases. These statements are supported by a recent study showing that alkylimidazolium ionic liquids have wider liquid range and better thermal stability (see Table 1.2) [84].

Table 1.2. The melting points and decomposing temperatures of some alkylimidazolium and alkylammonium salts.[a]

Cation	Anion	Melting Point (°C)	Decomposing Temp. (°C)	Liquid Range (°C)
$(C_2H_5)_4N^+$	Cl^-	36.5 [b]	264	227.5
$H_3C-N^\oplus N-C_2H_5$ (imidazolium)	Cl^-	89	281	192
$H_3C-N^\oplus N-C_3H_7$ (imidazolium)	Cl^-	60	281	221
$H_3C-N^\oplus N-C_2H_5$, CH_3 (imidazolium)	Cl^-	188	290	102
$(C_2H_5)_4N^+$	BF_4^-	72	412	340
$H_3C-N^\oplus N-C_2H_5$ (imidazolium)	BF_4^-	11	450	439
$(C_2H_5)_4N^+$	PF_6^-	70	388	318
$H_3C-N^\oplus N-C_2H_5$ (imidazolium)	PF_6^-	62	481	419
$H_3C-N^\oplus N-C_3H_7$ (imidazolium)	PF_6^-	40	440	400
$H_3C-N^\oplus N-C_2H_5$, CH_3 (imidazolium)	PF_6^-	196	500	304
$(C_2H_5)_4N^+$	$(CF_3SO_2)_2N^-$	104	399	295
$(C_4H_9)_4N^+$	$(CF_3SO_2)_2N^-$	90	388	298
$H_3C-N^\oplus N-C_2H_5$ (imidazolium)	$(CF_3SO_2)_2N^-$	-15	453	468
$H_3C-N^\oplus N-CH(CH_3)_2$ (imidazolium)	$(CF_3SO_2)_2N^-$	16	409	393
$H_3C-N^\oplus N-C_3H_7$, CH_3 (imidazolium)	$(CF_3SO_2)_2N^-$	15	462	447
$(C_2H_5)_4N^+$	$(C_2F_5SO_2)_2N^-$	83	397	314
$H_3C-N^\oplus N-C_2H_5$ (imidazolium)	$(C_2F_5SO_2)_2N^-$	-1	462	463
$H_3C-N^\oplus N-C_2H_5$, CH_3 (imidazolium)	$(C_2F_5SO_2)_2N^-$	25	420	395
$(C_2H_5)_4N^+$	$(CF_3SO_2)_3C^-$	46	397	351
$(C_4H_9)_4N^+$	$(CF_3SO_2)_3C^-$	59	398	339
$H_3C-N^\oplus N-C_2H_5$ (imidazolium)	$(CF_3SO_2)_3C^-$	39	430	391

[a] Data are taken from ref 84.

[b] This is the melting point for tetraethyl ammonium chloride tetrahydrate.

1.2.2. Characterization of GC Stationary Phases

Gas-liquid chromatographic stationary phases are generally characterized in terms of solvent strength (polarity) and solvent selectivity. In molecular solvents, the solvent strength or polarity of a solvent is determined by its solvation behavior which in turn depends on the action of intermolecular forces (Coulombic, orientational, inductive, dispersion, and charge-transfer forces, as well as hydrogen-bonding forces) between the solvent and the solute [85]. Ionic liquids are even more complicated, since both cations and anions can have their own distinct properties and interactions. Attempts were made to correlate the polarity of a solvent to its physical parameters, e.g. dielectric constant, refractive index and dipole moment. As often has been found, the solvent polarity cannot be defined simply using any of these macroscopic solvent parameters, and specific solvent-solute interactions must be taken into account. This led to the development of empirical scales of solvent polarity. Empirical parameters can be derived from the effect of a solvent on a solvent-dependant standard process (the rate of a chemical reaction, and the absorption of light by a solvatochromic dye) by determining the rate constants or absorption/emission maxima, respectively.

The most comprehensive solvent scale to date is probably the E_T scale which was mainly established by Dimroth and Reichardt [87]. In this system, solvatochromic Reichardt's dye (2,4,6-triphenylpyridinium-N-4-(2,6-diphenylphenoxide) betaine) (Figure 1.2) is used as the test substance, which exhibits an extremely large solvatochromic shift in its charge transfer (CT) absorption band, from λ_{max} = 810 nm in diphenyl ether to λ_{max} = 453 nm in water. The solvatochromism arises from unequal, differential solvation of the highly dipolar zwitterionic ground state compared with the less dipolar first excited state. The position of the CT absorption of the dye is strongly influenced by the ability of the solvent to act as a hydrogen bond donor (HBD) to the phenoxide oxygen atom [88]. The transition energy for the CT absorption may be calculated from the position of λ_{max} using the relationship (Eq.1.1)
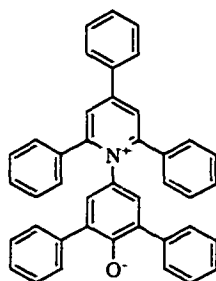
Figure 1.2. Structure of Reichardt's dye.

$$E_T(30) \: / \: \text{kcal mol}^{-1} = 28591 \: / \: (\lambda_{max} \: / \: \text{nm}) \qquad\qquad (1.1)$$

For convenience these values are often normalized to give a parameter E_T^N, where $E_T^N = 0.0$ for tetramethylsilane, and 1.0 for water. The E_T^N values of some ionic liquids and some common solvents are summarized in Table 1.3. Note that, E_T^N scale is only suitable for comparing the solvent properties of ionic liquids and non-ionic solvents that are liquid at about room temperature. The polarity values of some ionic liquids determined by other polarity scales, including π^* scale of dipolarity/polarization, the α-scale of hydrogen-bond donor acidity, the β-scale of hydrogen-bond basicity, and Ω-scale, are also listed in Table 1.3 for the sake of comparison [89]. Generally, the polarity of ionic liquids appears to be largely cation controlled, while the hydrogen bond donor strength is entirely anion dependent. The alkylimidazolium ionic liquids are less polar than methanol but more polar than acetonitrile [88].

In the case of gas chromatography, the polarity and selectivity of a stationary phase can be easily determined by analyzing the retention of a variety of probe compounds. GC can provide more useful information about the solvent properties of an ionic liquid, since it recognizes the intimacy of the solute-solvent relationship based on the solute behavior. The magnitude of individual solute-stationary phase interactions is commonly described as stationary phase selectivity, whereas, the weighted average of all possible intermolecular interactions for the stationary phase represents the stationary phase polarity. The empirical Rohrchneider scale [90], which was later modified by McReynolds [91], is the most widely used classification scale. The scale is based on the principle that intermolecular forces are additive. Individual contributions to retention of a solute can be evaluated from the difference in retention index (Kovats index) values of a series of test solute probes measured on the liquid phase to be characterized and on squalane. Squalane is used as a nonpolar reference phase.

The retention index, originally proposed by Kovats [92-94] and later refined by Ettre [95], uses the linear relationship that exists between the logarithm of retention parameters and the number of carbon atoms within a homologous series. It is commonly expressed on a uniform scale of homologous n-alkanes. The retention index of a substance is equal to 100 times the carbon number of a hypothetical n-alkane with the same retention parameter (time, volume, etc.). The retention scale is made up of the n-alkanes with retention index values equal to 100 times the carbon number of the n-alkane. The retention index of a substance X is typically calculated by coinjection of bracketing n-alkanes differing by one carbon number and using Eq.1.2:

Table 1.3. Solvent polarity measurements of some ionic liquids (in the order of E_T^N value).[a]
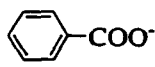
Cation	Anion	E_T^N	π^*	α	β	Ω
$(C_3H_7)_2NH_2^+$	SCN^-	1.006	1.16	0.97	0.39	
$C_2H_5(CH_3)CHNH_3^+$	SCN^-	1.006	1.28	0.91		
H_2O		1.000	1.09	1.17	0.47	0.869
$C_2H_5NH_3^+$	NO_3^-	0.954	1.24	0.85	0.46	0.82
$C_4H_9NH_3^+$	SCN^-	0.948	1.23	0.92		
$C_3H_7NH_3^+$	NO_3^-	0.923	1.17	0.88	0.52	
$(C_4H_9)_3NH^+$	NO_3^-	0.802	0.97	0.84		
$H_3C-N\overset{\oplus}{[]}N-C_4H_9$ (imidazolium)	ClO_4^-	0.684				0.67
$H_3C-N\overset{\oplus}{[]}N-C_4H_9$ (imidazolium)	BF_4^-	0.673	1.09	0.73	0.72	0.66
$H_3C-N\overset{\oplus}{[]}N-C_4H_9$ (imidazolium)	$CF_3SO_3^-$	0.667				0.65
$H_3C-N\overset{\oplus}{[]}N-C_4H_9$ (imidazolium)	PF_6^-	0.667	0.91	0.77	0.41	0.68
CH_3CH_2OH		0.654	0.54	0.75	0.75	0.718
$H_3C-N\overset{\oplus}{[]}N-C_4H_9$ (imidazolium)	$(CF_3SO_2)_2N^-$	0.642				
$H_3C-N\overset{\oplus}{[]}N-C_4H_9$ (imidazolium)	Cl^-		1.17	0.41	0.95	
$CH_3CH_2NH_3^+$	Cl^-	0.636				
$H_3C-N\overset{\oplus}{[]}N-C_8H_{17}$ (imidazolium)	PF_6^-	0.633	0.88	0.58	0.46	
$H_3C-N\overset{\oplus}{[]}N-C_8H_{17}$ (imidazolium)	$(CF_3SO_2)_2N^-$	0.630				

Table 1.3. (Continued)

Cation	Anion	E_T^N	π^*	α	β	Ω
H$_3$C–N⊕N–C$_8$H$_{17}$ (imidazolium)	Cl⁻		1.09	0.33	0.90	
(C$_3$H$_7$)$_4$N⁺	◯–NH(CH$_2$)$_2$SO$_3$⁻	0.62	1.08	0.34	0.80	
H$_3$C–N⊕N–C$_4$H$_9$ (imidazolium)	CF$_3$CO$_2$⁻	0.620				
(C$_4$H$_9$)$_4$N⁺	◯–NH(CH$_2$)$_2$SO$_3$⁻	0.62	1.01	0.34	0.98	
(C$_5$H$_{11}$)$_4$N⁺	◯–NH(CH$_2$)$_2$SO$_3$⁻	0.58	1.00	0.15	0.91	
(C$_2$H$_5$)$_4$N⁺	NO$_3$⁻	0.460				
CH$_3$CN		0.460	0.75	0.19	0.31	0.692
(C$_2$H$_5$)$_4$N⁺	Cl⁻	0.454				
(C$_6$H$_{13}$)$_4$N⁺	◯–COO⁻	0.420				
CH$_3$CH$_2$OCH$_2$CH$_3$		0.117	0.27	0.00	0.47	0.466
cyclohexane		0.009	0.00	0.00	0.00	0.595

[a] Data are taken from ref. 89.

$$I = 100 \, n + 100 \, (\log R_X - \log R_n) / (\log R_{n+1} - \log R_n) \qquad (1.2)$$

where R is the retention parameter (adjusted retention time, adjusted retention volume, specific retention volume, partition coefficient, *etc.*), n is carbon number of the *n*-alkane eluting before substance X, and $n + 1$ is carbon number of the *n*-alkane eluting directly after substance X. One of the most easily measured parameters in chromatography is the adjusted retention time. In theory, the retention index of a substance should depend only on the stationary phase and the column temperature and should be independent of other column variables (chromatographic support material, flow rate, column efficiency, *etc.*). In fact, the retention index is only independent of column variables when the *n*-alkanes and the substance are retained by the same retention mechanism, namely partitioning. This is not true in many cases and the retention index may be subject to systematic errors.

McReynolds proposed that ten probes were sufficient to adequately characterize the intermolecular interactions which controlled solute retention. Benzene (X') measures dispersive interactions with weak proton acceptor properties, butanol (Y') measures orientation interactions with both proton donor and acceptor capabilities, 2-pentanone (Z') measures orientation properties with proton acceptor but not proton donor capabilities, nitropropane (U') measures orientation interactions, and pyridine (S') measures weak orientational interactions with strong proton acceptor but not proton donor capabilities. Iodobutane, 2-methyl-2-pentanol, 2-octyne, p-dioxane, and cis-hydrindene represent the remaining five test probes. The Rohrchneider-McReynolds scheme further assumes that the energy for each type of intermolecular interaction is proportional to a value a to e characteristic of each test probe and a value X' to S' characteristic of the liquid stationary phase. The retention index difference, ΔI, is given by Eq. 1.3.

$$\Delta I = aX' + bY' + cZ' + dU' + eS' \qquad (1.3)$$

To evaluate the five phase constants a value of 1.0 is assigned to each of the probe constants in turn. For benzene, the probe constants are a = 1 and b = c = d = e. The stationary phase value X' is obtained from

$$X' = \Delta I \, (\text{Benzene}) = I_{TP} \, (\text{Benzene}) - I_{SQ} \, (\text{Benzene}) \qquad (1.4)$$

where I_{TP} (probe) is the retention index for the specified test probe on the stationary phase being evaluated and I_{SQ} (probe) refers to the retention index for the probe on the nonpolar

squalane reference phase. By repeating the above procedure using butanol, 2-pentanone, nitropropane and pyridine the remaining four stationary phase constants can be determined. Today, virtually all new liquid stationary phases are characterized in terms of the Rohrchneider-McReynolds scale. Column manufacturers customarily quote Rohrchneider-McReynolds constants for each stationary phase marketed to aid in the selection of phases for particular applications. In our work, two ionic liquid, 1-butyl-3-methylimidazolium chloride ([BuMIm][Cl]) and 1-butyl-3-methylimidazolium chloride hexafluorophosphate ([BuMIm] [PF$_6$]), were evaluated as GC stationary phases using the Rohrchneider-McReynolds scale.

1.2.3. Ionic Liquids as MALDI Matrices

Like electrospray ionization (ESI), Matrix-assisted Laser Desorption / Ionization (MALDI) is a tremendously successful method for analyzing polar, nonvolatile, and thermally labile biomolecules and synthetic polymers with high molecular weight [96-103]. It is applicable over a wide mass range (up to 500 kDa for biological materials and 1.5 million Da for synthetic polymers), requiring femtomoles or less of analyte while consuming only a small fraction of sample applied to the target [30,45,49,102-109]]. The operating principles and a typical configuration of a MALDI instrument with a TOF mass spectrometer are illustrated in Figure 1-1.3. MALDI's success is due in large part to the development of a number of effective matrixes and an increased understanding of their role and use [30-51]. MALDI matrixes are found to function at least in three ways: (a) the analyte is diluted in the high-molar excess of matrix forming a "matrix solution". This prevents analyte molecules from aggregating and reduces strong molecular interactions. (b) The matrix has a strong absorption at the wavelength of the incident laser light and transfers the laser energy to the analyte in a controllable way, because excess heat energy is rapidly dissipated by the sublimation of "matrix solution" and by fragmentation of the matrix, which protects the analyte molecules from bond cleavage. (c) Analyte ionization is promoted by matrix-involved photochemical reactions.

The analyte is either co-crystallized with a solid matrix or dissolved in a liquid matrix in a molar ratio of analyte to matrix in the range of 1:100-1:50,000. Normally, matrix solutions are prepared in water, water-acetonitrile, or water-alcohol mixtures at a concentration of 5-10 mg/ml depending on the solubility of the matrix. The analyte is prepared at a concentration of about 0.1 mg/ml and in a solvent that is miscible with the matrix solution (for peptides or proteins, aqueous 0.1% trifluoroacetic acid is frequently used). The matrix and analyte solutions are mixed to give a final matrix-to-analyte molar ratio of approximately 5,000:1 and a final volume of 0.5-2 μl. The mixture is applied to a
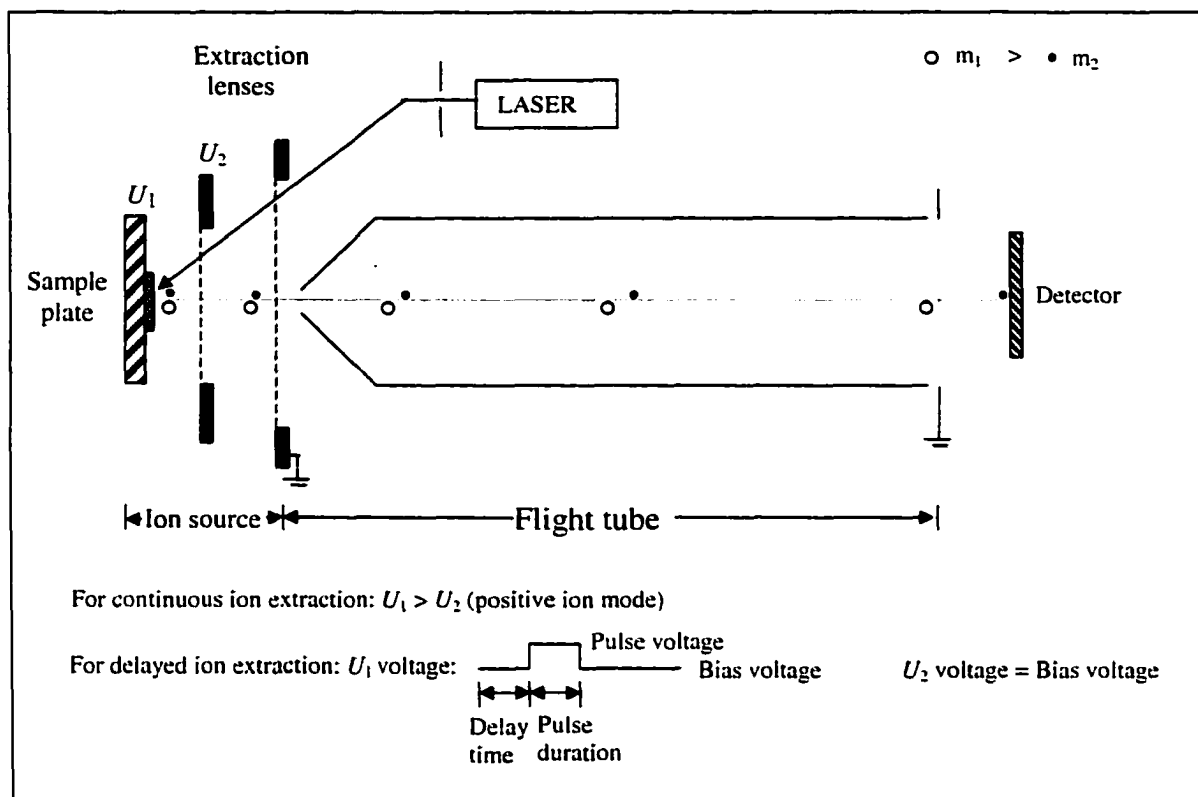
Figure 1.3. Schematic of a linear MALDI-TOF-MS with a MALDI source interfaced to a TOF mass spectrometer. Analytes are co-deposited with a large excess of matrix on a sample plate. Laser radiation is focused onto the sample probe to effect ionization. The ions formed at the sample plate are captured by the electric field in the ion source and accelerated toward the detector through the flight tube. All ions drift through the flight tube at different velocities, and are separated into different ion packets based on their m/z. The laser pulse triggers the clock in the transient recorder that measures the time of flight for different ions. The recorded time spectra can be converted into mass spectra.

stainless steel MALDI-MS sample plate and allowed to dry by either ambient evaporation heating with a stream of warm air or under vacuum. During the drying process, the analyte and matrix co-deposit from solution on the sample plate. Special attention should be given to sample preparation, as it may affect the quality of the data, especially when using solid matrix [42,110-112].

MALDI matrices usually are small organic molecules, used either independently or in a mixture in such a way as to produce the best mass spectra. It should be noted that a matrix that is optimal for one type of sample (proteins or peptides) may not be effective for other types of samples (e.g., synthetic polymers or RNA and DNA fragments) (see Table 1.3). Hence, a variety of different matrixes have been developed for a wide range of samples and the search for new matrix compounds has not stopped since the inception of MALDI-MS [51,113]. The commonly used MALDI matrices are summarized in Table 1.3. In general, these matrices fall into three groups according to their chemical properties: organic acids (derivatives of benzoic acid, cinnamic acid, and related aromatic carboxylic acids, etc.) [30-32], neutral compounds (2,4,6-trihydroxy acetophenone, dithranol, etc.) or elemental sub-micron powders (such as cobalt, graphite, porous silicon) [43,104,114], and basic compounds (p-nitroaniline) [38]. Alternatively, based on their physical state, MALDI matrices can be classified into two groups, i.e. solid and liquid matrices.

As mentioned earlier, a liquid matrix is preferable for MALDI analyses, since it has advantages, such as continuous and homogeneous sampling, point-to-point and shot-to-shot signal reproducibility, and the opportunity to control sample chemistry [115-117]. Unfortunately, the application of liquid matrix is confined by its lack of suitable chromophores and high vacuum instability. In Chapter 3, it is demonstrated that the problems encountered by traditional MALDI matrixes can be overcome by using special ionic liquid matrixes. Nearly 40 different ionic liquids were synthesized and evaluated as MALDI matrices for the analysis of peptides, proteins and polymers.

Table 1.4. Chemical names, trivial names, structures, states and applications of some frequently used MALDI matrices.

Matrix	Structure	State	Usable wavelength	Application
2,5-Dihydroxy benzoic acid (DHBA, or Gentisic acid)		Solid	266 nm, 337 nm, 355 nm, 2.79 µm, 2.94 µm, 10.6 µm	Peptides, proteins, lipids, oligonucleotides, polar synthetic polymers, oligosaccharides
Trans-3,5-dimethoxy-4-hydroxy cinnamic acid (Sinapic acid or Sinapinic acid, SA)		Solid	266 nm, 337 nm, 355 nm, 2.79 µm, 2.94 µm, 10.6 µm	Peptides, proteins, and glycoproteins
Trans-3-methoxy-4-hydroxy cinnamic acid (Ferulic acid, FA)		Solid	355 nm	Synthetic polymers
4-Hydroxy-α-cyano-cinnamic acid (CHCA)		Solid	337 nm, 2.94 µm	Peptides, proteins, lipids, oligonucleotides, synthetic polymers
Nicotinic acid (NA)		Solid	266 nm, 337 nm, 2.94 µm, 10.6 µm.	Proteins, oligonucleotides
Picolinic acid		Solid	266 nm	Proteins
3-Hydroxypicolinic acid (HPA or 3HPA)		Solid	337 nm, 355 nm	Nucleic acids, glycoproteins, oligonucleotides
2,4,6-Trihydroxy acetophenone (2,4,6-THAP)		Solid	337 nm	Oligonucleotides, oligosaccharides
1,8,9-Anthracenetriol (Dithranol)		Solid	337 nm	Synthetic polymers
All-trans-Retinoic acid		Solid	337 nm	Synthetic polymers
6-Aza-2-thiothymine (ATT)		Solid	337 nm	Oligonucleotides, nucleic acids
2-(4-Hydroxyphenylazo)-benzoic acid (HABA)		Solid	355 nm	Synthetic polymers
Succinic acid		Solid	2.94 µm, 10.6 µm	Peptides, proteins
Glycerol		Liquid	2.79 µm, 2.94 µm, 10.6 µm	Nucleic acids
p-Nitroaniline / glycerol		Liquid	337 nm	Proteins, carbohydrates, oligonucleotides
Graphite / glycerol			337 nm	Proteins, oligosaccharides, synthetic polymers
Cobalt powder / glycerol			337 nm	Oligosaccharides, pharmaceuticals, surfactants.

REFERENCES

1. Walden, P. *Bull. Acad. Imper. Sci (St. Petersburg)* 1914, 1800.
2. Bradley, D. *Chem. Ind.* **1999**, February 1, 86.
3. Freemantle, M. *C&E News* **1998**, March 30, 32-38.
4. Freemantle, M. *C&E News* **2000**, May 15, 37-50.
5. Chauvin, Y.; Olivier-Bourbigou, H. *Chemtech* **1995**, September, 26-30.
6. Holbrey, J. D.; Seddon, K. R. *Clean Prod. Proc.* **1999**, 1, 223-236.
7. Welton, T. *Chem. Rev.* **1999**, 99, 2071-2083.
8. Wasserscheid, P.; Keim, W. *Angew. Chem. Int. Ed. Engl.* **2000**, 39, 3772-3789.
9. Hagiwara, R.; Ito, Y. *J. Fluorine Chem.* **2000**, 105, 221-227.
10. Wilkes, J. S.; Levisky, J. A.; Wilson, R. A.; Hussey, C. L. *Inorg. Chem.* **1982**, 21, 1263-1264.
11. Wilkes, J. S.; Zaworotko, M. J. *J. Chem. Soc., Chem. Commun.* **1992**, 965-967.
12. Hurley, F. H.; Wier, T. P. *J. Electrochem. Soc.* **1951**, 98, 203-206.
13. Chum, H. L.; Koch, V. R.; Miller, L. L.; Osteryoung, R. A. *J. Am. Chem. Soc.* **1975**, 97, 3264.
14. Larsen, A. S.; Holbrey, J. D.; Tham, F. S.; Reed, C. A. *J. Am. Chem. Soc.* **2000**, 122, 7264-7272.
15. Pernak, J.; Czepukowicz, A. *Ind. Eng. Chem. Res.* **2001**, 40, 2379-2383.
16. Bonhôte, P.; Dias, A.-P.; Armond, M.; Papageorgiou, N.; Kalyanasundaram, K.; Grätzel, M. *Inorg. Chem.* **1996**, 35, 1168.
17. Papageorgiou, N.; Athanassov, Y.; Armand, M.; Bonhôte, P.; Pettersson, H.; Azam, A.; Grätzel, M. *J. Electrochem. Soc* **1996**, 143, 3099.
18. Carlin, R.T.; Long, H.C. De; Fuller, J.; Trulove, P.C. *J. Electrochem. Soc* **1994**, 141, L73.
19. Koch, V.R.; Nanjundiah, C.; Appetecchi, G.B.; Scrosati, B. *J. Electrochem. Soc.* **1995**, 142, L116.
20. V.R. Koch, L.A. Dominey, C. Nanjundiah and M.J. Ondrechen. *J. Electrochem. Soc.* **1996**, 143, 788.
21. A.B. McEwen, S.F. McDevitt and V.R. Koch. *J. Electrochem. Soc.* **1997**, 144, L84.
22. J. Fuller, R.T. Carlin and R.A. Osteryoung. *J. Electrochem. Soc.* **1997**, 144, 3881.
23. Freemantle, M. *Chem. Eng. News* **1999**, 79, 23-24.
24. Huddleston, J. G.; Willauer, H. D.; Swatloski, R. P.; Visser, A. E.; Rogers, R. D. *Chem. Commun.* **1998**, 1765.
25. Dai, S.; Ju, Y. H.; Barnes, C. E. *J. Chem. Soc., Dalton Trans.* **1999**, 1201.

26. Visser, A. E.; Swatloski, R. P.; Reichert, W. M.; Griffin, S. T.; Rogers, R. D. *Ind. Eng. Chem. Res.* **2000**, *39*, 3596.

27. Visser, A. E.; Swatloski, R. P.; Reichert, W. M.; Mayton, R.; Sheff, S.; Wierzbicki, A.; Davis, J. H., Jr.; Rogers, R. D. *J. Chem. Soc., Chem. Commun.* **2001**, 135.

28. Chun, A.; Dzyuba, S. V.; Bartsch, R. A. *Anal. Chem.* **2001**, 73, 3737-3741.

29. Yanes, E. G.; Gratz, S. R.; Baldwin, M. J.; Robinson, S. E.; Stalcup, A. M. *Anal. Chem.* **2001**, 73, 3838-3844.

30. Karas, M.; Hillenkamp, F. *Anal. Chem.* **1988**, *60*, 2299-2301.

31. Beavis, R. C.; Chait, B. T. *Rapid Commun. Mass Spectrom.* **1989**, *3*, 432-435.

32. Beavis, R. C.; Chait, B. T. *Anal. Chem.* **1990**, *62*, 1836-1840.

33. Dominic Chan, T. W.; Colburn, A. W.; Derrick, P. T. *Org. Mass Spectrom.* **1992**, *27*, 53-56.

34. Cornett, D. S.; Duncan, M. A.; Amster, I. J. *Anal. Chem.* **1993**, *65*, 5, 2608-2613.

35. Williams, J. B.; Gusev, A. I.; Hercules, D. M. *Macromolecules* **1996**, *29*, 8144-8150.

36. Caldwell, K. L.; Murray, K. K. *Appl. Surf. Sci.* **1998**, 127-129, 242-247.

37. Zenobi, R.; Knockenmuss, R. *Mass Spectrom. Rev.* **1998**, *17*, 337-366.

38. Fitzgerald, M. C.; Parr, G. R.; Smith, L. M. *Anal. Chem.* **1993**, *65*, 2608-2613.

39. Huberty, M. C.; Vath, J. E.; Yu, W.; Martin, S. A. *Anal. Chem.* **1993**, *65*, 2791-2800.

40. Juhasz, P.; Biemann, K. *Proc. Natl. Acad. Sci. U.S.A.* **1994**, *91*, 4333-4337.

41. Beeson, M. D.; Murray, K. K.; Russell, D. H. *Anal. Chem.* **1995**, *67*, 1981-1986.

42. Cohen, S. L.; Chait, B. T. *Anal. Chem.* **1996**, *68*, 31-37.

43. Dale, M. J.; Knockenmuss, R.; Zenobi, R. *Anal. Chem.* **1996**, *68*, 3321-3329.

44. Gimon-Kinsel, M.; Preston-Schaffter, L. M.; Kinsel, G. R.; Russell, D. H. *J. Am. Chem. Soc.* **1997**, *119*, 2534-2540.

45. Limback, P. A. *Spectroscopy* **1998**, *13*, 16-27

46. Williams, T. L., Fenselau, C. *Eur. Mass Spectrom.* **1998**, *4*, 379-383

47. Asara, J. M.; Allison, J. *J. Am. Soc. Mass Spectrom.* **1999**, *10*, 35-44.

48. Kirpekar, F.; Berkenkamp, S.; Hillenkamp, F. *Anal. Chem.* **1999**, *71*, 2334-2339.

49. Sporns, P.; Wang, J. *Food Res. Int.* **1998**, *31*, 181-189.

50. Ring, S., Rudich, Y. *Rapid Commun. Mass Spectrom.* **2000**, *14*, 515-519

51. Zhang, L.-K.; Gross, M. L. *J. Am. Soc. Mass Spectrom.* **2000**, *11*, 854-865.

52. Cornett, D.S.; Duncan, M.A.; Amster, I.J. *Anal. Chem.* **1993**, 65, 2608-2613.

53. Williams, J.B.; Gusev, A.L.; Hercules, D.M. *Macromolecules* **1996**, 29, 8144-8150.

54. Kolli, K.V.S.; Orlando, R. *Rapid Commun. Mass Spectrom.* **1996**, 10, 923-926.

55. Chan, T-W. D.; Colburn, A.W.; Derrick, P.J. *Org. Mass Spectrom.* **1992**, 27, 53-56.

56. Baiulescu, C. E.; Llie, V. A. *Stationary Phases in Gas Chromatography.* Pergamon Press, Oxford, 1975.

57. Poole, C. F.; Schuette, S. A. *Contemporary Practice of Chromatography*. Elsevier, Amsterdam, 1984.

58. Baiulescu, C. E.; Llie, V. A. *Anal. Chem.* **1972**, *44*, 1490-1495.

59. Bhattachajee, A.; Basu, A. N. *J. Chromatogr.* **1972**, 71, 534-539.

60. Ober, A. G.; Cooke, M.; Nickless, G. *J. Chromatogr.* **1980**, 196, 237-244.

61. Wishousky, T. I.; Grob, R. L.; Zacchei, A. G. *J. Chromatogr.* **1982**, 249, 1-18.

62. Juvet, R. S.; Shaw, V. R.; Khan, M. A. *J. Am. Chem. Soc.* **1969**, *91*, 3788-3792.

63. Poole, C.F.; Furton, K. G.; Kersten, B. R. *J. Chromatogr. Sci.* **1986**, 24, 400-409.

64. Poole, C.F.; Bulter, H.T.; Coddens, M.E.; Dhanesar, S.C.; Pacholec, F. *J. Chromatogr.* **1984**, 289, 299-320.

65. Berezkin, V.G.; Alishoyev, V.R.; Victorova, E.N.; Gavrichev, V.S.; Fateeva, V.M. *Chromatographia.* **1982**, 16, 126.

66. Berezkin, V.G.; Alishoyev, V.R.; Victorova, E.N.; Gavrichev, V.S.; Fateeva, V.M. *J. High Resolut. Chromatogr. Chromatogr.Commun.* **1983**, 6, 42.

67. Barber, D.E.; Philips, C.S.G.; Tusa, G.F.; Verdin, A. *J. Chem. Soc.* **1959**, 18-24.

68. Pachole, F.; Butler, H. T.; Poole, C.F. *Anal. Chem.* **1982**, 54, 1938-1941.

69. Dhanesar, S.C.; Coddens, M.E.; Poole, C.F. *J. Chromatogr.* **1985**, 324, 415-421.

70. Furton, K.G.; Poole, C. F. *J. Chromatogr.* **1985**, 349, 235.

71. Coddens, M.E.; Furton, K.G.; Poole, C.F. *J. Chromatogr.* **1986**, 356, 59.

72. Furton, K.G.; Poole, C. F. *Anal. Chem.* **1987**, 59, 1170.

73. Furton, K.G.; Poole, C. F. Kersten, B.R. *Anal. Chim. Acta.* **1987**, 192, 255.

74. Furton, K.G.; Poole, S.K.; Poole, C. F. *Anal. Chim. Acta.* **1987**, 192, 49-61.

75. Poole, S.K.; Furton, K.G.; Poole, C.F. *J. Chromatogr. Sci.* **1988**, 26, 67-73.

76. Pomaville, R.M.; Poole, S.K.; Davis, L.J.; Poole, C.F. *J. Chromatogr.* **1988**, 438, 1.

77. Pomaville, R.M.; Poole, C.F. *Anal. Chem.* **1988**, 60, 1103.

78. Pomaville, R.M.; Poole, C.F. *J. Chromatogr.* **1989**, 468, 261-278.

79. Poole, S.K.; Shetty, P.H.; Poole, C.F. *Anal. Chim. Acta.* **1989**, 218, 241-264.

80. Shetty, P.H.; Poole, S.K.; Poole, C.F. *Anal. Chim. Acta.* **1990**, 236, 51-61.

81. Poole, S.K.; Poole, C.F. *Analyst* **1995**, 120, 289-294.

82. Arancibia, E.L.; Cartells, R.C.; Nardillo, A.M. *J. Chromatogr.* **1987**, 398, 21-29.

83. Morales, R.; Blacnco, C.; Furton, K.G. *Talanta* **1993**, 40, 1541-1549.

84. Ngo, H.L.; LeCompte, K.; Hargens, L.; McEwen, A.B. *Thermorchim. Acta* **2000**, 97-102, 357-358.

85. Reichardt, C. *Angew. Chem., Int. Ed. Engl.*, **1965**, 4, 29-40.

86. Reichardt, C. *Solvents and Solvent Effects in Organic Chemistry* (2nd ed). VCH: Weinheim, 1988.

87. Reichardt, C. *Chem. Rev.* **1994**, 94, 2319-2358.

88. Muldoon, M.J.; Gordon, C.M.; Dunkin, I.R. *J. Chem. Soc., Perkin Trans. 2* **2001**, 433-435.

89. Welton, T. unpulished manuscript.

90. Rohrschneider, L. *J. Chromatogr.* **1966**, 22, 6.

91. McReynolds, W.R. *J. Chromatogr.* **1970**, 8, 685.

92. Kovats, E. *Helv. Chim. Acta* **1958**, 41, 1915.

93. Kovats, E. *Z. Anal. Chem.* **1961**, 181, 351.

94. Kovats, E. *Helv. Chim. Acta* **1963**, 46, 2705.

95. Ettre, L.S. *Chromatographia.* **1974**, 7, 261.

96. Macfarlane, R. D.; Torgerson, D. F. *Science* **1976**, *191*, 920-923.

97. Armstrong, D. W.; Sequin, R.; McNeal, C. J.; Macfarlane, R. D.; Fendler, J. H. *J. Am. Chem. Soc.* **1978**, *100*, 4605-4606.

98. Benninghoven, A.; Sichtermann, W. K. *Anal. Chem.* **1978**, *50*, 1180-1184.

99. Barber, M.; Bordoli, R. S.; Sedgwick, R. S.; Tyler, A. N. *J. Chem. Soc., Chem. Commun.* **1981**, *325* - 327.

100. Blakely, C. R.; Carmody, J. J.; Vestal, M. L. *Anal. Chem.* **1980**, *52*, 1636-1641

101. Whitehouse, C. M.; Dreyer, R. N.; Yamashita, M.; Fenn, J. B. *Anal. Chem.* **1985**, *57*, 675-679.

102. Cotter, R. J. *Anal. Chim. Acta* **1987**, *195*, 45-59.

103. Hillenkamp, F.; Karas, M.; Beavis, R. C.; Chait, B. T. *Anal. Chem.* **1991**, *63*, 1193A-1203A.

104. Tanaka, K.; Waki, H.; Ido, y.; Akita, s.; Yoshida, Y.; Yoshida, T. *Rapid Commun. Mass Spectrom.* **1988**, 2, 151-153.

105. Karas, M.; Bahr, U. *NATO ASI Series, Series C.* **1997**, 54 (Selected Topics in Mass Spectrometry in the Biomolecular Sciences), 33-53.

106. Sporns, P.; Abell, D.C. *Trends Food Sci. Technol.* **1996**, 187-190.

107. Wu, K.J.; Odom, R.W. *Anal. Chem.* **1998**, 70, 456A-461A.

108. Berkenkamp, S.; Kirpekar F.; Hillenkamp, F. *Science* **1998**, 281, 260-262.

109. Schriemer, D.C.; Li, L. *Anal. Chem.* **1996**, 68, 2721-2725.

110. Dogruel, D.; Nelson, R.W.; Williams, P. *Rapid Commun. Mass Spectrom.* **1996**, 10, 801-804.

111. Yalcin, T.; Dai, Y.; Li, L. *J. Am. Soc. Mass Spectrom.* **1998**, 9, 1303-1310.

112. Schriemer, D.C.; Li, L. *Anal. Chem.* **1997**, 69, 4169-4175.

113. Mechref, Y.; Novotny, M. *J. Am. Soc. Mass Spectrom.* **1998**, 9, 1293-1302.

114. Kinumi, T.; Saisu, T.; Takayama, M.; Niwa, H. *J. Mass Spectrom.* **2000**, 35, 417-422.

115. Williams, J.B.; Gusev, A.L.; Hercules, D.M. *Macromolecules* **1996**, 29, 8144-8150.

116. Kolli, K.V.S.; Orlando, R. *Rapid Commun. Mass Spectrom.* **1996**, 10, 923-926.

117. Williams, T.L.; Fenselau, C. *Eur. Mass Spectrom.* **1998**, 4, 379-383.

CHAPTER 2

EXAMINATION OF IONIC LIQUIDS AND THEIR INTERANTION WITH MOLECULES, WHEN USED AS STATIONARY PHASES IN GAS CHROMATOGRAPHY

A paper published in Analytical Chemistry[1]

Daniel W. Armstrong, Lingfeng He, and Yan-Song Liu

ABSTRACT

Stable room-temperature ionic liquids (RTILs) have been used as novel reaction solvents. They can solubilize complex polar molecules such as cyclodextrins and glycopeptides. Their wetting ability and viscosity allow them to be coated onto fused silica capillaries. Thus, 1-butyl-3-methylimidazolium hexafluorophosphate and the analogous chloride salt can be used as stationary phases for gas chromatography (GC). Using inverse GC, one can examine the nature of these ionic liquids via their interactions with a variety of compounds. The Rohrschneider-McReynolds constants were determined for both ionic liquids and a popular commercial polysiloxane stationary phase. Ionic liquid stationary phases seem to have a dual nature. They appear to act as a low-polarity stationary phase to nonpolar compounds. However, molecules with strong proton donor groups, in particular, are tenaciously retained. The nature of the anion can have a significant effect on both the solubilizing ability and the selectivity of ionic liquid stationary phases. It appears that the unusual properties of ionic liquids could make them beneficial in many areas of separation science.

2.1. INTRODUCTION

Room-temperature ionic liquids that are air and moisture stable have been subject to an increasing number of scientific investigations [1-10]. Their use as novel solvent systems for organic synthesis has received a good deal of attention [2-9]. Most recently, polyether-based ionic liquids were shown to be viable solvents for electrochemical studies [10]. Room-temperature ionic liquids (RTILs) resemble ionic melts of metallic salts in that, essentially, every entity in the solution is an ion. RTILs have several properties that could make them useful in a variety of chemical processes. For example, they are good solvents for many organic, inorganic, and polymeric substances. Many RTILs are immiscible with water and nonpolar organic solvents. They have a liquid range of 300 °C and good thermal stability. The viscosity of RTILs can vary considerably, but they have no effective vapor pressure. Finally, they are very accessible, given their ease of preparation from relatively inexpensive materials [3,5,11].

Given their properties, room-temperature ionic liquids could be used to advantage in a variety of separation methods. Recently they were considered as a water-immiscible phase in liquid-liquid extraction [11]. Because of environmental concerns with volatile organic carbon (VOC), the RTILs were considered attractive alternatives (given their lack of vapor pressure). The distribution ratios for a variety of analytes between RTIL and water were approximately an order of magnitude less than the corresponding octanol/water partition coefficients [11]. Although there was a rough correlation between these systems, there was a clear polarity difference [11].

Our interest in RTILs initially was aroused by their unusual combination of properties (i.e., volatility, viscosity, solubility, and polarity). Our interest was further enhanced when it was found that RTILs could solubilize a number of complex organic molecules of interest to the separation community. For example, the solubility of some cyclodextrins and macrocyclic antibiotics is summarized in Table 2.1. Also, we believed that gas-liquid chromatography (GLC) could be an attractive way to evaluate differences in various RTILs as well as their interactions with a variety of molecules. In this initial work we examine two ionic liquids by using them as stationary phases in gas-liquid chromatography. Also, they are evaluated as unusual stationary phases.

Table 2.1. Approximate solubility of some compounds in [BuMIm][Cl], [BuMIm][PF₆], and [BuMIm][BF₄][a]

Compounds	Solubility (%, w/w)		
	[BuMIm][Cl]	[BuMIm][PF₆]	[BuMIm][BF₄]
α-Cyclodextrin	30	<1	<1
β-Cyclodextrin	21	<1	<1
γ-Cyclodextrin	30	<1	<1
2,3-Dimethyl-β-cyclodextrin	12	<1	10
2,6-Di-O-methyl-β-cyclodextrin	3	28	5
Permethyl-β-cyclodextrin	34	16	<1
Avoparcin	8	<1	<1
Rifamycin	3	<1	5
Teicoplanin	~10	<1	<1
Vancomycin	~15	<1	<1

[a] [BuMIm][Cl] is 1-butyl-3-methylimidazolium chloride. [BuMIm][PF₆] is 1-butyl-3-methy- limidazolium hexafluorophosphate and [BuMIm][BF₄] is 1-butyl-3-methylimidazolium tetra- fluoroborate.

2.2. EXPERIMENTAL SECTION

2.2.1. Materials

1-Methylimidazole, chlorobutane, hexafluorophosphoric acid, sodium tetrafluoro-borate, squalane, anhydrous ethyl ether, anhydrous dichloromethane, and all test solutes were purchased from Aldrich (Milwaukee, WI) or Fluka Chemical Co. (Ronkonkoma, NY). HPLC grade ethyl acetate was purchased from Fisher (St. Louis, MO). Hexafluorophosphonic acid is a corrosive, toxic solution and must be handled with care.

All untreated fused silica capillary tubing (0.25-mm i.d.) was obtained from Supelco (Bellefonte, PA). DB-5 column (30 m × 0.25-mm i.d., film thickness 0.25 μm), obtained from J & W Scientific (Folson, CA), was cut into two pieces, each one of 15-m length.

2.2.2. Methods

The synthesis of 1-butyl-3-methylimidazolium chloride ([BuMIm][Cl]), 1-butyl-3-methylimidazolium hexafluorophosphate ([BuMIm][PF$_6$]), and 1-butyl-3-methyl-imidazolium tetrafluoroborate ([BuMIm][BF$_4$]) were reported elsewhere [3,5,11]. Briefly, [BuMIm][Cl] was prepared by adding equal amounts (0.5 mol) of 1-methylimidazole and chlorobutane to a round-bottomed flask fitted with a reflux condenser and reacting them for 48-72 h at 70 °C. The resulting viscous liquid was allowed to cool to room temperature and then was washed three times with 50-mL portions of ethyl acetate. After the last washing, the remaining ethyl acetate was removed by heating the liquid to 70 °C under vacuum. [BuMIm][PF$_6$] was prepared from [BuMIm][Cl] by slowly adding hexafluorophosphoric acid (0.13 mol) to a solution of [BuMIm][Cl] (0.1 mol) in 100 mL of water. After stirring for 12 h, the lower liquid portion was washed with water until the washings were no longer acidic. The ionic liquid was heated under vacuum at 70 °C to remove any excess water. The yield was >80%.

Before coating, 15-m fused silica capillary tubing was subjected to a sodium chloride pretreatment as reported by Huang et al [12]. The capillary then was coated by the static method using a solution of 0.15% (w/v) of the stationary phase materials in dichloromethane at 40 °C. Coated columns were flushed with dry helium gas for 60 min, then conditioned from 30-100 °C at 0.5 °C/min. After conditioning for 8-10 hours, column efficiency was tested with naphthalene at 100 °C. The [BuMIm][PF$_6$] column had 1900 plates/m, while the [BuMIm][Cl] column had 1700 plates/m.

All test solutes were dissolved in ethyl ether. A Hewlett-Packard model 5890 series II was used for all separations. Split injection and flame ionization detection were utilized. The injector and detector were held at 222 °C, and helium was used as the carrier gas. The Kováts retention indices and the Rohrschneider-McReynolds constants were determined for these capillary columns as reported previously [13].

2.3. RESULTS AND DISCUSSION

Table 2.2 lists the Kováts retention indexes of the first five McReynolds solutes on a squalane reference column, a commercial DB-5 bonded-phase column, and two columns containing ionic liquid stationary phases. The largest Kováts index was for butanol on the [BuMIm][Cl] column. The lowest values for all five solutes were obtained on the squalane reference column followed by the commercial DB-5 column (Table 2.2).

Table 2.3 gives the Rohrschneider-McReynolds constants of the five reference analytes on five different columns. The data for the first four stationary phases were generated in this study while the values for OV-22 [phenyl methyl diphenylpolysiloxane (65% phenyl)] were taken from the literature for the purpose of comparison [14]. The average of the five Rohrschneider-McReynolds constants is sometimes used as an approximate polarity scale. However, the individual constants must be considered in order to evaluate different contributions to retention. The respective constants (Table 2.3) are thought to measure: dispersive interactions (X); proton donor and acceptor capabilities plus dipolar interactions (Y); dipolar interactions plus weak proton acceptor, but not proton donor capabilities (Z); dipolar interactions (U); and strong proton acceptor (but not donor) capabilities (S) [14]. Unlike many GLC stationary phases which have smaller variations in these constants, the ionic liquids show considerable differences (Table 2.3). In particular, proton donor and dipolar interactions appear to be very strong, followed by proton acceptor capabilities. Also, simply changing the nature of the anion has a significant effect on the magnitude of the individual interactions but not on the overall "average polarity" (Table 2.3).

Another interesting facet of the ionic liquids, when used as GLC stationary phases, is that they appear to have a dual nature. This is illustrated in Figure 2.1. Analytes that are relatively nonpolar and are not acidic nor basic, tend to separate on ionic liquid stationary phases in much the same manner (and with similar retention) as on relatively nonpolar stationary phases, such as DB-5 (see compounds 1, 2, 3, 6, and 8 in Figure 2.1A and B). Conversely, highly polar molecules and proton-donor molecules (particularly weak acids)

. . .

Table 2.2. Kovátes indices of the five first test solutes at 100 °C

Column[a]	Benzene	Butanol	2-Pentanone	Nitro-propane	Pyridine
Squalane	656	600	629	655	700
DB-5	682	666	700	748	763
[BuMIm][Cl]	730	1037	742	900	912
[BuMIm][PF$_6$]	763	851	807	963	944

[a] The DB-5 column has a stationary phase of (5%-phenyl)-methyl-polysilxane. [BuMIm][Cl] is 1-butyl-3-methylimidazolium chloride. [BuMIm][PF$_6$] is 1-butyl-3-methylimidazolium hexafluorophosphate.

Table 2.3. Rohrschneider-McReynolds constants of the five first test solutes at 100 ° C

Column[a]	X[c]	Y[c]	Z[c]	U[c]	S[c]	Av[c]
Squalane	0	0	0	0	0	0
DB-5	27	66	71	93	63	64
[BuMIm][Cl]	74	437	113	245	212	216
[BuMIm][PF$_6$]	107	251	178	308	244	218
OV-22[b]	160	188	191	283	253	215

[a] The DB-5 column has a stationary phase of (5%-phenyl)-methyl-polysilxane. [BuMIm][Cl] is 1-butyl-3-methylimidazolium chloride. [BuMIm][PF$_6$] is 1-butyl-3-methylimidazolium hexafluorophosphate. The OV-22 column has a stationary phase of phenylmethyldiphenyl-polysiloxane (65% phenyl).

[b] Obtained from ref. 14.

[c] X is benzene, Y is butanol, Z is 2-pentanone, U is nitropropane, and S is pyridine. Av is the average of the five values for each stationary phase.
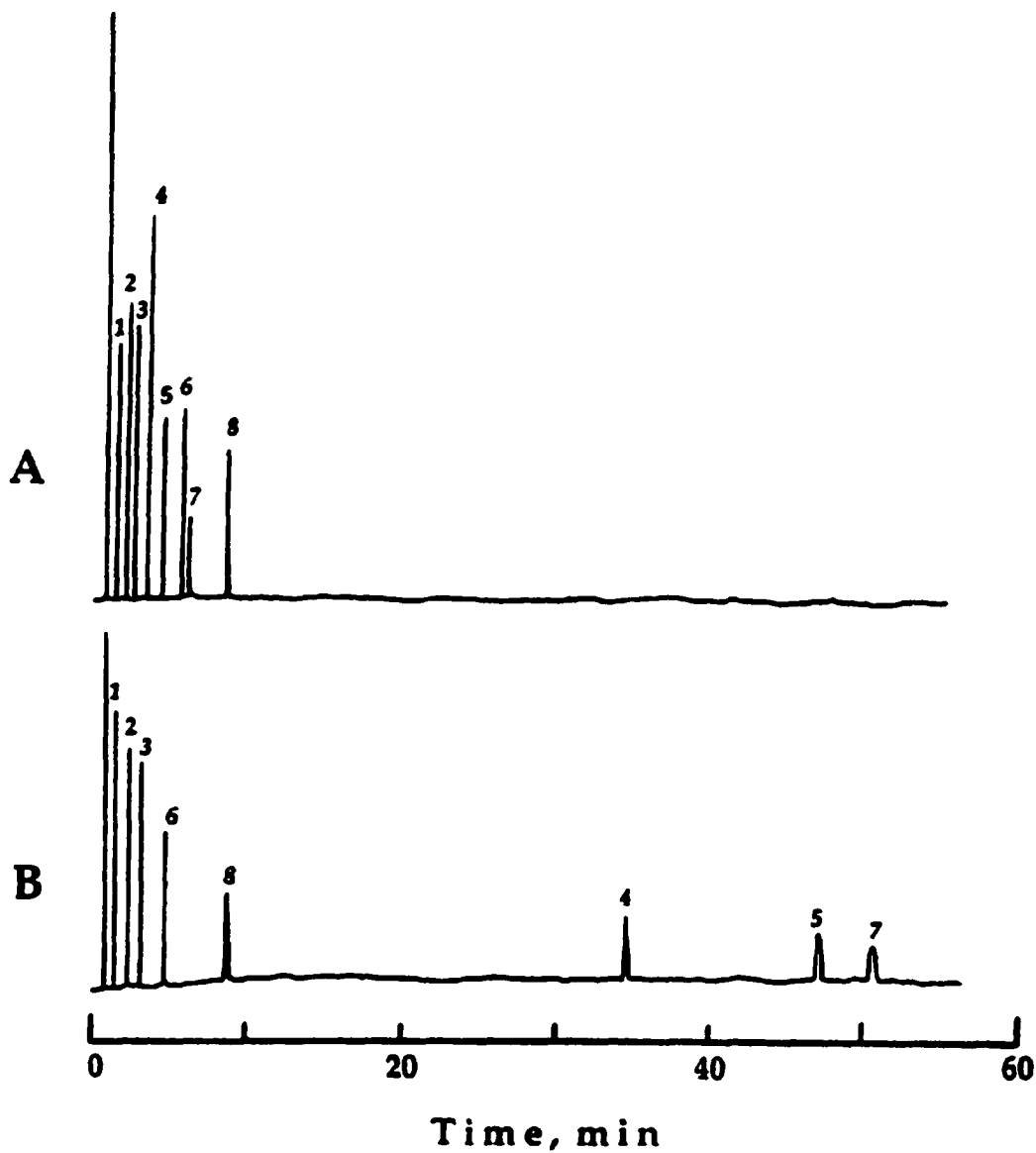
Figure 2.1. Chromatograms comparing the retention and separation of eight compounds on the same size GC columns (15 m × 0.25-mm i.d.) and under identical conditions (isothermal at 100 °C and a pressure of 9 psi). Column A is a commercial DB-5 column, and Column B utilizes the ionic liquid [BuMIm][PF$_6$] as the stationary phase. The test compounds are: 1, butyl acetate; 2, n-heptanol, 3, p-dichlorobenzene, 4, o-cresol, 5, 2,5-dimethylphenol, 6, n-dodecane, 7, 4-chloroaniline, and 8, n-tridecane.

have very different retention behavior (Figure 2.1B). These types of molecules are strongly retained by the ionic liquid stationary phases (Figure 2.1) and in some cases are not eluted under these test conditions (see the phenols, carboxylic acids, and diols in Table 2.4). Some of the larger proton-acceptor analytes (i.e., the amines) also show this type of behavior, but not to the same extent as the acids. The strong proton donor and acceptor effects observed for ionic liquids in this work support a previous report by Elaiwi et al [15].

Table 2.4 lists the retention factors for a variety of compounds on GLC columns containing two different ionic liquid stationary phases as well as squalane and the DB-5 stationary phase. The more nonpolar and nonionizable compounds are listed toward the beginning of Table 2.4, while the ionizable and more polar compounds are listed afterward. All four GLC columns tended to have similar retention factors for the neutral, less polar compounds. The relative retention on the ionic liquid stationary phases increases with the more polar alcohols and formamids. This increase is even more dramatic for the amines and particularly the phenols and organic acids (Table 2.4). The observed retention behavior corresponds well with that predicted by the previously mentioned Rohrschneider-McReynolds constants. Also apparent from the data in Table 2.4 is that the nature of the anionic portion of the ionic liquids can have a profound effect on retention and selectivity.

2.3.1. Effect of the Anion.

The cationic portion of both ionic liquids in this study consists of the 1-butyl-3-methylimidazolium ion (see Experimental Section and Tables 2.2-2.4). Both ionic liquids have approximately the same average polarity (see the "Average" in Table 2.3). However, it is clear from the data in Table 2.4 that there are significant differences in the chloride versus the hexafluorophosphate ionic liquids. The data show that some classes of compounds interact more strongly with the hexafluorophosphate ionic liquid, while other classes of compounds interact more strongly with the chloride-containing ionic liquid (Table 2.4). Indeed, it appears that GLC may be a very useful tool to study differences in the properties of various ionic liquids as well as how they interact with molecules.

Molecules that do not contain good proton-donating or -accepting groups (e.g., aliphatic and aromatic compounds, esters, aldehydes, and ketones) are more strongly retained on the [BuMIm][PF$_6$] stationary phase. This is true even for the more polar haloalkanes. However, all compounds with proton-donor groups (e.g., alcohols, diols, phenols, and carboxylic acids) interact much more strongly with the chloride-containing [BuMIm][Cl] ionic liquid (Table 2.4). Amines also prefer the [BuMIm][Cl].

Table 2.4. Comparison of retention factors (*k'*) of solutes eluted from GLC columns containing ionic liquid, squalane, and (5%-Phenyl)-methylphenylsiloxane (DB-5) stationary phase [a]

Compounds	Squalane	DB-5	[BuMIm]-[Cl]	[BuMIm]-[PF$_6$]	Compounds	Squalane	DB-5	[BuMIm]-[Cl]	[BuMIm]-[PF$_6$]
(A) Paraffins (100 °C)					(E) Alcohols (25-80 °C at 1 °C/min) / Diols (80 °C)				
n-Heptane	0.2	0.1	0.08	0.1	Methanol	-0.17	-0.17	6.7	0.8
n-Octane	0.5	0.3	0.2	0.3	Ethanol	0.0	-0.08	6.7	1.1
n-Nonane	1.0	0.6	0.4	0.6	n-Propanol	0.04	0.21	10.4	2.3
n-Decane	2.2	1.3	0.8	1.2	n-Butanol	0.6	1.0	15.1	4.7
n-Undecane	4.7	2.5	1.7	2.5	n-Pentanol	2.1	2.6	16.0	8.1
n-Dodecane	8.4	4.8	3.6	4.4	2-Hexanol	3.5	3.3	19.1	8.4
					3-Heptanol	8.2	5.7	20.0	12.1
(B) Substituted Alkanes (25-80 °C at 1 °C/min)					n-Heptanol	12.0	8.2	24.1	18.1
Acetonitrile	-0.1	0.08	1.1	2.7	3-Octanol	15.3	8.9	29.5	18.9
Propionitrile	0.2	0.3	6.7	3.3	Glycol	0.08	0.3		26.2
1-Chlorobutane	0.9	0.7	0.5	0.7	1,3-Butanediol	0.6	1.2		39.2
1-Chloropentane	2.8	2.1	1.7	2.2	1,2-Pentanediol	1.1	2.0		42.5
1-Chlorohexane	6.3	4.5	4.5	5.5					
1-Chlorooctane	16.5	10.9	16.7	18.1	(F) Amines (100 °C)				
					N-Butylamine	0.08	0.09	0.2	0.1
(C) Aromatics (Nonionizable) (100 °C)					1,5-Dimethylhexylamine	1.3	1.0	5.1	1.1
Benzene	0.8	0.7	0.7	1.2	n-Octylamine	1.8	2.0		6.3
p-Dichlorobenzene	2.1	1.6	1.6	2.2	n-Decylamine	11.9	3.1		15.2
m-Dichlorobenzene	2.4	1.8	1.9	2.7	Aniline	1.1	1.3	37.8	12.6
Toluene	2.8	1.7	2.0	3.0	Benzylmethylamine	1.7	1.6		6.5
p-Xylene	7.3	3.2	4.9	7.2	Benzylethylamine	3.4	2.0		12.7
m-Xylene	7.4	3.2	4.9	7.2	Benzylpropylamine	4.5	2.8		11.0
o-Xylene	8.5	3.5	6.1	8.8	m-Chloroaniline	3.3	3.3	46.8	17.5
Nitrobenzene	2.4	2.5	5.3	9.6	p-Chloroaniline	4.5	5.4	122.4	56.3
m-Dimethylbenzene	20.0	6.3	15.2	16.6	1-Ethylpropylamine	0.2	0.04	3.1	0.6
3-Chloronitrobenzene	7.0	6.1	11.2	17.3	Diethylamine	0.6	0.5	2.0	1.0
4-Chloronitrobenzene	7.3	6.5	15.4	21.2	N,N-Ethyldimethylamine	1.5	1.4	13.2	8.5
Naphthalene	30.3	8.8	33.1	35.0					

Table 2.4. (Continued)

Compounds	Squalane	DB-5	[BuMIm]-[Cl]	[BuMIm]-[PF₆]	Compounds	Squalane	DB-5	[BuMIm]-[Cl]	[BuMIm]-[PF₆]
1,7-Dimethylnaphthalene	37.2	18.5	23.2	41.3	(G) Phenols (100 °C)				
1,3-Dimethylnaphthalene	39.2	18.5	24.4	43.0	m-Nitrophenol	3.7	3.3		14.1
1,6-Dimethylnaphthalene	39.2	18.8	24.4	43.0	2,6-Dimethylphenol	3.0	3.3		18.6
1,4-Dimethylnaphthalene	43.5	20.6	27.1	47.6	o-Cresol	1.5	2.1		39.3
1,5-Dimethylnaphthalene	44.2	20.9	27.7	48.5	Phenol	0.7	1.3		45.8
1,2-Dimethylnaphthalene	46.3	22.4	30.2	54.1	2,5-Dimethylphenol	3.2	3.9		54.2
1,8-Dimethylnaphthalene	53.7	25.2	37.0	63.6	p-Cresol	1.6	2.5		61.0
					m-Cresol	1.6	2.5		64.3
(D) Aldehyes (25 C) / Amides (100 °C) / Esters (30-60 °C at 0.5 °C/min) / Ketones (25-60 °C at 1 °C/min)					2,3-Diemthylphenol	3.5	4.8		65.8
					3,5-Diemthylphenol	3.8	4.6		89.1
2-Methylbutylaldehyde	0.7	1.0	0.8	1.9	3,4-Diemthylphenol	4.0	5.4		114.0
Valeraldehyde	1.1	1.5	1.3	3.1	m-Chlorophenol	3.2	6.2		241.9
Formamide	0.0	0.2		19.7	p-Dhlorophenol	3.2	6.2		254.5
N-Methylformamide	0.1	0.3	27.3	12.3					
N,N-Dimethylformamide	0.2	0.3	1.0	4.3	(H) Carboxylic Acids (100 °C)				
Methyl acetate	0.0	0.08	0.1	0.5	Acetic acid	0.0	0.04		3.1
Ethyl acetate	0.2	0.4	0.3	0.9	Propionic acid	0.07	0.13		3.8
Isopropyl acetate	0.5	0.8	0.4	1.1	2-Chloropropionic acid	0.3	0.9		
n-Propyl acetate	1.0	1.4	0.9	2.1	Dichloroacetic acid		9.0		
n-Butyl acetate	3.4	3.8	2.4	4.6	Benzoic acid				
Acetone	-0.1	0.0	0.2	0.9					
2-Butanone	0.2	0.4	0.5	1.7					
2-Pentanone	0.9	1.1	1.1	3.0					
3-Chloro-2-butanone	1.1	1.6	3.2	5.4					
4-Methyl-2-pentanone	1.7	1.9	1.7	3.9					

ᵃ Whenever no value is reported, this indicates that the solute was eluted under the indicated condition.

An examination of the Rohrschneider-McReynolds constants (Table 2.3) confirms the experimental observations in Table 2.4. The constant for proton-donor activity (i.e., the Y terms in Table 2.3) was far and away the most dominant feature of [BuMIm][Cl]. Conversely, constants for dispersive and dipolar interactions (i.e., the X and U terms in Table 2.3) were more prominent for [BuMIm][PF$_6$]. Clearly, GLC can be a useful tool to evaluate and compare ionic liquids. As indicated in this study, one can focus on the nature of specific anions (or cations in other instances). Such information could be useful in a number of areas other than separations, where knowledge of salt-organic interactions and/or relative-ion behaviors is important.

The only compounds that were retained to a greater extent on the less polar squalane and DB-5 columns than on the ionic liquid columns were the unsubstituted alkanes, the smaller chloroalkanes, and a few of the esters, aldehydes, and ketones.

2.4. CONCLUSIONS

Room-temperature ionic liquids (RTILs) act as nonpolar stationary phases when separating nonpolar analytes or somewhat polar analytes that are not proton-donor or -acceptor molecules. However, they act in the opposite manner (i.e., are highly interactive and retentive) when used to separate molecules with somewhat acidic or basic functional groups. Thus, molecules with proton-donor or -acceptor characteristics tend to be spatially resolved, as a group, from nonpolar analytes. The dual nature of ionic liquid stationary phases also is evident from the Rohrschneider-McReynolds constants. Inverse GLC also is a good way to examine the nature of different ionic liquids. It is apparent that the chloride-containing ionic liquid interacted much more strongly with proton-donor and -acceptor molecules. The hexafluorophosphate-containing ionic liquid tended to be somewhat less polar and interacted more strongly with nonpolar solutes. GLC with ionic liquids is an effective way to study differences in ions as well to study interactions between ions and organic molecules. RTILs often can solubilize complex macrocyclic molecules such as cyclodextrins and their derivatives and macrocyclic antibiotics. As a result of their novel properties, RTILs may be useful in many separation methods.

ACKNOWLEDGEMENT

REFERENCES

1. Osteryoung, R. A. Molten Salt Chemistry: An Introduction and Selected Application; Mamantov, G., Marassi, R., Eds.; *NATO ASI Ser., Ser. C* **1987**, *202*, 329.

2. Wilkes, J. S.; Levisky, J. A.; Wilson, R. A.; Hussey, C. L. *Inorg. Chem.* **1982**, *21*, 1263.

3. Wilkes, J. S.; Zaworotko, M. J. *J. Chem. Soc., Chem. Commun.* **1992**, 965.

4. Chauvin, Y.; Oliver-Bourbigou, H. *CHEMTECH* **1995**, *Sept. 26*.

5. Suarez, P. A. Z.; Dullius, J. E. L.; Einloft, S.; DeSouza, R. F.; Dupont, J. *Polyhedron* **1996**, *15*, 1217.

6. Adams, C. J.; Earle, M. J.; Roberts, G.; Seddon, K. R. *Chem. Commun.* **1998**, 2097.

7. Earle, M. J.; McCormac, P. B.; Seddon, K. R. *Chem. Commun.* **1998**, 2245.

8. Dyson, P. J.; Ellis, D. J.; Parker, D. G.; Welton, T. *Chem. Commun.* **1999**, 25.

9. Freemantle, M. *Chem. Eng. News* **1999**, *Jan. 4*, 23.

10. Dickinson, V, E.; Williams, M. E.; Hendrickson, S. M.; Masui, H.; Murray, R. W. *J. Am. Chem. Soc.* **1999**, *121*, 613. 11.

11. Huddleston, J. G.; Willauer, H. D.; Swatloski, R. P.; Visser, A. E.; Rogers, R. D. *Chem. Commun.* **1998**, 1765.

12. Huang, A., Nan, N.; Chen, M.; Pu, X.; Tang, H.; Sun, Y. *Acta Sci. Nat. Univ. Pekin.* **1988**, *24*, 425.

13. Berthod, A.; Zhou, E. Y., Le, K.; Armstrong, D. W. *Anal. Chem.* **1995**, *67*, 849.

14. McReynolds, W. O. *J. Chromatogr. Sci.* **1970**, *8*, 685.

15. Elaiwi, A.; Hitchcock, P. B.; Seddon, K. R.; Srinivasan, N.; Tan, Y.-M.; Welton, T.; Zora, J. A. *J. Chem. Soc., Dalton Trans.* **1995**, 3467.

CHAPTER 3

IONIC LIQUIDS AS STATIONARY PHASE SOLVENTS FOR METHYLATED CYCLODEXTRINS IN GAS CHROMATOGRAPHY

A paper published in Chromatographia[1]

Alain Berthod / Lingfeng He / Daniel W. Armstrong

KEY WORDS

Gas chromatography, chiral separation, methylated cyclodextrin, room temperature ionic liquids, 1-butyl-3-methylimidazolium chloride.

SUMMARY

Room temperature ionic liquids (RTIL) are molten salts with melting points well below room temperature. 1-butyl-3-methylimidazolium chloride is a typical example of such RTIL. It was used as a solvent to dissolve permethylated-β-cyclodextrin (BPM) and dimethylated-β-cyclodextrin (BDM) to prepare stationary phases for capillary columns in gas chromatography for chiral separation. The RTIL containing columns were compared to commercial columns containing the same chiral selectors. A set of 64 chiral compounds separated by the commercial BPM column was tested on the RTIL BPM column. Only 21 were enantioresolved. Similarly, a set of 80 compounds separated by the commercial BDM column was passed on the RTIL BDM column with only 16 positive separations. It is proposed that the imidazolium ion pair could make an inclusion complex with the cyclodextrin cavity, blocking it for chiral recognition. All the chiral compounds recognized by the RTIL columns had their asymmetric carbon that was part of a ring structure. The retention factors of the derivatized solutes were lower on the RTIL columns than those obtained on the commercial equivalent column. The peak efficiencies obtained with the RTIL capillary were significantly higher than that obtained with the commercial column. These observations may contribute to the knowledge of the mechanism of cyclodextrin-based GC enantioselective separations.

3.1. INTRODUCTION

Salts whose melting point is below normal room temperature, exhibit liquid behavior at 20 °C. These molten salts are called room temperature ionic liquids (RTIL). They are relatively cheap and easy to prepare. They have a liquid range of 200 to 300 °C, a good thermal stability and practically no vapor pressure. RTILs are good solvents, but are themselves sparingly miscible with water and non-polar organic solvents. Due to their physico-chemical properties, RTILs have been extensively investigated as potential candidates as alternative solvents in liquid-liquid extractions and chemical reactions, or as electrolytes for use in batteries, photoelectrochemical cells, electroplating and capacitors [1-4].

In a recent work two RTILs, 1-butyl-3-methylimidazolium hexafluorophosphate ([BuMI] [PF_6^-]) and [BuMI] chloride were evaluated as a stationary phase in capillary gas chromatography (GC) [5]. It was found that the two RTILs have a dual nature when used as GC stationary phases. They act as a low polarity stationary phase to nonpolar compounds and oppositely, they tenaciously retain molecules with proton donor or acceptor groups such as hydroxyl, phenol or amino groups. Table 3.1 lists the Rohrschneider-McReynolds constants of the two RTILs along with that of other GC stationary phases. The two [BuMI] salts have interesting solvent capabilities. They were able to solubilize between 12 and 34% w/w of various cyclodextrins (CDs) used as chiral selectors in chromatography [6-8].

In this work, two chiral stationary phases (CSP) were prepared by dissolving two chiral selectors in a RTIL. The two CSPs were coated on the internal wall of capillary tubes that could be used as columns in GC. A variety of volatile chiral compounds containing widely different functionalities were used as test solutes on the RTIL-based CSP columns and on the commercial columns containing the same CD chiral selector. The results obtained on the columns allow comparing the chromatographic figures of merit: selectivity, efficiency and resolution. Our main goal is to evaluate, from an analytical chemistry point of view, the capability of RTILs as solvents for stationary phases in GC and especially for chiral CD selectors. The results also provide information that could help understand better the mechanism of CD-based GC enantioselective separations.

3.2. EXPERIMENTAL

3.2.1. RTIL Preparation

1-butyl-3-methylimidazolium chloride ($C_8H_{15}N_2Cl$, m.w. 174.5) was synthesized by reacting 1-methylimidazole (Aldrich, Milwaukee, WI, USA) with chlorobutane (Aldrich) in equimolecular amount in a round-bottomed flask for 2 to 3 days at 70°C. The raw [BuMI][Cl] RTIL was cooled to room temperature and washed with ethyl acetate portions. The [BuMI][Cl] RTIL was a pale yellow very viscous liquid at 25°C. The yield was higher than 85% [5].

1-3.2.2. Chiral Stationary Phase Preparation

Permethylated β-cyclodextrin (BPM) and 2,6-dimethyl-β-cyclodextrin (BDM) were the two chiral selectors obtained from Astec (Whippany, NJ, USA). In 1 g of the [BuMI][Cl] liquid, 323 mg of BPM were dissolved forming 1.323 g of a 26.4% *w/w* BPM solution in the RTIL that will be used as the CSP to prepare the BPM containing columns. Similarly, 383 mg of BDM were dissolved in 1 g of RTIL to obtain 1.383 g of a 27.7% *w/w* BDM solution in the RTIL. This later solution was used to prepare the BDM containing columns.

3.2.3. Capillary Column Preparation

Coils of untreated fused silica capillary tubing (250 μm i.d.) coated by a brown polyimide layer were purchased from Supelco (Bellafonte, PA). 10-m portions of capillary tubing were cut to prepare the columns. The commercial capillary columns that were used as references were coated with a ~25% *w/w* BDM or BPM in polydimethylsiloxane with a 0.250 μm film thickness. In a 10-m column with a 250 μm i.d., a 0.250 μm film thickness corresponds to 2 mm³ of CSP or 2.2 mg (CSP density is about 1.1 g.cm⁻³). The 10-m capillary internal volume is 0.491 cm³. It is necessary to prepare a dichloromethane solution containing 2.2 mg of CSP in 0.491 cm³ that is a 0.45% *w/v* solution. The capillaries were coated by the static method using the 0.45% *w/v* CSP solution in dichloromethane at 40°C as already described [5]. The efficiencies of the coated columns were tested with naphthalene at 100°C and found to be in the 17000-20000 plate range (HETP within 500 and 600 μm).

3.2.4. Test Solutes

68 test solutes were tested on the BPM columns and 80 on the BDM columns. They were all chiral compounds with a variety of functionalities. The alcohols, phenols, carboxylic acids and amines were derivatized by trifluoroacetic anhydride before injection. The ketones, ethers, esters, amides, and the halogenated, insaturated, aromatic and cyclic compounds were injected as received. All these chiral compounds were obtained from Sigma or Aldrich. The chiral test solutes were selected because they were previously enantioseparated by the BPM or BDM columns or by both [5, 8, 9]. All test solutes were dissolved in ethyl ether and analyzed on the RTIL containing chiral columns and on the corresponding commercial columns with identical chromatographic conditions (temperature and carrier gas average velocity).

3.2.5. Instrumentation

The commercial chiral columns were obtained from Astec. They were a 20 m (250 µm i.d.) Chiraldex B-PM (ref. 76023) column and a 20 m (250 µm i.d.) Chiraldex B-DM (ref. 77021) column. They contained respectively the permethylated β-CD and 2,6-O-dimethylated β-CD chiral selectors dissolved in a polydimethylsiloxane polymer coated in a 0.25 µm layer thickness. A Hewlett-Packard model 5890 series II GC chromatograph was used for all separations. A split injector (split ratio 1/100) and a flame ionization detector were maintained at 222 °C and used with helium carrier gas.

3.3. RESULTS AND DISCUSSION

3.3.1. Polarity of the RTIL

Table 3.1 lists the Rohrschneider-McReynolds polarity indexes of the [BuMI][Cl] solvent stationary phase compared to different other materials used as GC stationary phases. The unique polarity behavior of RTIL is clearly shown by these indexes. The Y index of the RTILs is much higher than the corresponding index of classical stationary phases. For example, the Y value of [BuMI][Cl] is 437 and the corresponding value for the 65% phenyl PS phase (OV22) with a similar average polarity is only 188, 60% lower (Table 3.1). The Y parameter is related to the proton donor and acceptor capabilities of the phase and to the dipolar interactions [5, 10]. It explains the capability of RTIL stationary phases to retain tenaciously phenols, alcohols, free carboxylic acids and amines, all compounds with a strong proton donor or acceptor functionality, as recently described in our previous work [5].

Table 3.1. Rohrschneider-McReynolds constants for RTILs and other GC stationary phases

GC stationary phase	X (Benzene)	Y (Butanol)	Z (2-Pentanone)	U (Nitropropane)	S (Pyridine)	Average
PS[1]	16	55	44	65	42	44
PS 5% phenyl[2]	32	72	65	98	65	66
PS 65% phenyl[3]	160	188	191	283	253	215
[BuMI] [Cl⁻][4]	74	437	113	245	212	216
[BuMI] [PF₆⁻][4]	107	251	178	308	244	218
Zinc stearate[5]	61	231	59	98	544	199

1) PS = polydimethylsiloxane, trade names: OV1, DB-1, SE30, HP-1, CP Sil 5 CB.
2) Trade names: SE52, OV5, HP-5, DB-5, CP Sil 8 CB.
3) Trade names: OV22, TAP-CB, Rtx65.
4) Data from ref. [5].
5) Zinc octadecanoate was a GC stationary phase used below 160 °C.

The four other parameters, X, Z, U and S of the RTIL stationary phases are lower than the corresponding value of the classical OV22 stationary phase. For comparison the Rohrschneider-McReynolds indexes of zinc stearate, a GC stationary phase used on some occasions, are also listed in Table 3.1. Zinc stearate is a salt melting around 130 °C. Its Y value, 231, is also higher than that of a classical stationary phase. Its S value is also very high, 544, due to the proton affinity of the carboxylate anion. Its three other indexes, X, Z and U are low, with values comparable to the 5% phenyl phase (OV 5 in Table 3.1).

This unique polarity of the [BuMI][Cl] RTIL stationary phase should be taken into account when it is used as a solvent for chiral selectors. Many chiral alcohols, amines, acids, phenols were enantioseparated on CD-based CSP [9]. If the analyzed solutes contain proton donor or acceptor functionalities, it is likely that strong interactions with these groups will dominate the separation and interactions with the chiral selector may be minimal. When these functionalities were present, the solute was derivatized. It was shown that chiral recognition is better in GC working at reduced temperature [9]. This further motivates for derivatization of polar groups: it converts most strong proton donor or acceptor functionalities (alcohols, amines, carboxylic acids) in very weak proton donor or acceptor groups (esters or amides) and makes the solute more volatile and less retained at moderate working temperature.

3.3.2. Enantiomer Separation

Of the 68 chiral compounds whose enantiomers were separated by the Chiraldex B-PM, only 21 were also enantio-separated with the RTIL containing BPM stationary phase. That is about one out of three compounds (31%). Table 3.2 lists the chromatographic data obtained for the 21 successful separations. Only 16 out of 80 compounds enantio-separated by the Chiraldex B-DM columns (20%) were separated by the analogue RTIL containing BPM column. Tables 3.3 lists the results obtained for the 16 compounds. Strikingly, with no exception, all the enantiomers that were separated by the two RTIL capillary columns contained a ring as a part of their asymmetric center. The full set of compounds listed in Tables 3.2 and Table 3.3 contains chiral compounds with a ring, thereby increasing rigidity about the stereogenic center since at least two of its four different substituents cannot rotate freely. The original sets of 68 compounds (BPM column) or 80 compounds (BDM column) contained the Tables 3.2 and Tables 3.3 listed compounds plus many chiral molecules that were not cyclic. All of them were enantioseparated by the Chiraldex columns but none of the compounds with independent, noncyclic substituents were enantioresolved by the RTIL containing columns. It seems that the rigidity about the stereogenic center produced by the

Table 3.2. Chromatographic results obtained with the BPM columns

Compound	Temp °C	Chiraldex B-PM 20 m column					[BuMI][Cl] + BPM (26.4% w/w) 10 m column				
		k_1	k_2	α	Rs	N plates	k_1	k_2	α	Rs	N plates
2-Ethoxy tetrahydrofuran	30	5.08	5.70	1.12	1.0	1900	3.24	3.37	1.04	0.8	11200
2,5-Dimethoxy tetrahydrofuran	30	10.8	13.1	1.21	1.5	1200	8.21	9.03	1.10	1.25	3350
Dihydro-5-(hydroxymethyl)-2(3H)-furanone	100	18.3	18.8	1.03	1.3	15000	67.0	71.2	1.06	1	4400
α-Ionone	100	20.9	22.7	1.09	1.8	8400	21.2	22.4	1.06	1.5	12300
3,4-Dihydro-2-methoxy-2H-pyran	25	21.8	24.2	1.11	0.8	1139	12.3	13.0	1.06	0.5	1500
2,3-Dihydro-7a-methyl-3-isopropylpyrrolo [2,1,-b] oxazol-5(7aH)-one	90	23.4	25.6	1.10	2.8	16500	25.7	26.7	1.04	1.3	18800
2-Propynyloxy-2H-pyran	50	23.6	24.7	1.05	1.0	8800	19.1	19.4	1.02	0.5	19400
α-Pinene	25	27.0	31.4	1.16	1.1	900	15.8	16.9	1.07	1.2	5000
4-Methyl-1-tetralone	100	33.7	36.2	1.07	1.6	8500	35.1	36.3	1.03	1.2	21500
Camphene	25	37.0	38.5	1.04	0.7	5200	10.2	11.3	1.11	0.9	1400
β-Pinene	30	42.2	44.1	1.04	0.9	7200	25.8	26.7	1.03	1	15300
cis-Pinane	25	42.8	45.5	1.06	0.7	2100	27.7	29.5	1.06	1.5	10200
Pulegone	60	56.5	61.1	1.08	1.6	7000	41.5	42.8	1.03	1	18500
Fenchone	40	59.6	61.7	1.04	0.7	6800	27.7	28.7	1.04	1	13600
cis-4-Acetoxy-2-cyclopenten-1-ol	50	65.3	95.9	1.47	6.5	4800	48.7	58.1	1.19	3.1	5100
2-Methylpiperidine	40	69.4	81.7	1.18	1.8	1900	30.4	31.6	1.04	1	11400
trans-2-Phenyl-cyclohexanol	80	71.4	77.9	1.09	3.5	26100	54.7	56.7	1.04	1.1	15600
3-Chloro-2-norbornanone	60	72.8	82.0	1.13	1.5	2600	70.4	74.1	1.05	1.1	7500
Me-3-(terbutoxycarbonyl)-2,2-dimethyl-4-oxazolidinecarboxylate	80	79.3	85.3	1.08	3.3	34100	88.6	92.6	1.04	1.25	13300
2,3-Dihydro-7a-methyl-3-phenylpyrrolo [2,1,-b] oxazol-5(7aH)-one	110	120.5	134.4	1.12	5.0	34200	301.8	310.6	1.03	1	19500
2-Acetyl-5-norbornene	40	139.8	144.2	1.03	0.8	10816	55.7	58.4	1.05	0.9	6000

Isotherm conditions. k_1 and k_2 are the retention factors of the first and second eluting enantiomer, respectively. α and Rs are the selectivity and resolution factors, respectively. N is the plate number of the last eluting peak. Compounds sorted by increasing retention factors on the Chiraldex B-PM column.

Table 3.3. Chromatographic results obtained with the BDM columns

Compounds	Temp. °C	Chiraldex B-DM 20 m column					[BuMI][Cl] + BDM (27.7% w/w) 10 m column				
		k_1	k_2	α	Rs	N	k_1	k_2	α	Rs	N
2-Ethoxy tetrahydrofuran	30	11.22	14.7	1.31	2.1	1100	3.53	3.70	1.05	1.1	14200
1,3,5-Trimethylcyclohexene	25	20.8	23.7	1.14	1.1	1200	7.05	7.18	1.02	0.7	30500
2,5-Dimethoxy tetrahydrofuran	30	21.6	28.8	1.33	3.25	2200	7.14	7.66	1.07	1.3	7000
1,3,5-Trimethylcyclohexene	25	29.5	29.7	1.01	0.3	2300	7.43	7.67	1.03	1.0	20300
α-Ionone	100	33.45	37.9	1.13	2.2	5070	20.0	20.5	1.02	1.0	39000
α-Pinene	30	37.05	42.5	1.15	1.25	1400	10.0	10.3	1.03	1.1	22800
β-Pinene	30	46.36	52.0	1.12	1.2	1800	16.1	16.5	1.02	0.9	30000
γ-Nonaroic lactone	100	48.5	54.6	1.13	1.8	3850	21.8	22.3	1.02	0.9	27500
Limonene	30	73.5	83.4	1.13	1.9	3700	36.9	37.5	1.02	0.7	31800
cis-4-Acetoxy-2-cyclopenten-1-ol	60	82.5	99.3	1.20	9.8	4900	51.3	54.8	1.07	1.4	7500
Dihydro-5-(hydroxymethyl)-2(3H)-furanone	100	86.6	118.6	1.37	2.3	900	67.3	69.8	1.04	0.8	7900
2-Methylpiperidine	30	91.0	104.6	1.15	2.4	4900	45.8	47.4	1.03	0.7	7400
4-Methyl-1-tetralone	90	142.7	160.8	1.13	1.6	2900	54.1	55.5	1.03	1.1	30800
Pulegone	50	179.5	213.1	1.19	3.5	6600	66.1	67.8	1.03	1.0	25600
2-Acetyl-5-norbornene	40	254.3	303.2	1.19	2.2	2500	58.2	60.3	1.04	1.2	19000
3-Chloro-2-norbornanone	50	260.6	299.6	1.15	1.7	2400	106.1	108.3	1.02	0.7	19000

Isotherm conditions. k_1 and k_2 are the retention factors of the first and second eluting enantiomer, respectively. α and Rs are the selectivity and resolution factors, respectively. N is the plate number of the last eluting peak. Compounds sorted by increasing retention factors on the Chiraldex B-DM column.

cycle is needed to obtain chiral recognition with methylated β-CDs dissolved in [BuMI][Cl] RTIL. This condition may be necessary, but it is not sufficient since 26 compounds containing a ring linking two bonds of the asymmetric center were not separated by the BPM-RTIL column and 41 compounds with a ring were not separated by the BDM-RTIL column.

In a previous mechanistic study of the chiral recognition by derivatized CDs in GC, we demonstrated that at least two different mechanisms could produce enantioselective separations [8]. One mechanism was when chiral molecules were forming a dominant enantioselective inclusion complex. It could be called "use of the inside of the CD cavity". The second mechanism did not involve such complex and used external CD interactions to separate the two enantiomers. It could be called "use of the outside of the CD molecule". Most enantiomeric pairs are separated by a combination of mechanisms [8]. The inclusion formation was characterized by good enantioselective factors and slow kinetics (low efficiency, broad peaks) and easy overloading. The chiral recognition without inclusion complexation showed low enantioselective factors (partial resolution) but fast kinetics (high efficiency). Given the results of this study (i.e., partial enantioselectivity and, as will be exposed, high efficiency), we suspected that one of the enantio-recognition mechanisms, the inclusion complex formation, may be hindered by the RTIL that is made of ion pairs small enough to fit in the CD cavity. Using the electrophoretic method [11], the association constants of [BuMI][Cl] with BDM and BPM chiral selectors were found to be 15 ± 3 M^{-1} and 20 ± 4 M^{-1}, respectively, in a methanol 10% v/v - 50 mM pH 7 phosphate buffer 90% v/v electrolyte phase. These binding constants in solution are not extremely high, but they mean that an inclusion complex of the RTIL ion pair is possible in the CD cavity. NMR experiments with RTIL and the CDs (without solvent to displace) would give the exact binding constants that are likely higher than the values obtained in methanol-buffer solutions. It should be noted that the CSPs we used contained more than 70% w/w [BuMI][Cl] or about 22 RTIL ion pairs per β-CD molecule.

If inclusion complexation takes place between RTIL ion pairs and the methylated β-CD molecules, the enantiorecognition capabilities of the later would be greatly reduced: the formation of solute inclusion complex may be highly reduced or completely suppressed. However, the second mechanism for CD chiral recognition is not affected by the RTIL-CD complex formation: the outside of the CD molecule is perfectly available [8]. We suggest that the RTIL-CD complex formation could even be a useful phenomenon if one wishes to do mechanistic studies of chiral recognition by CD via external associations. Tables 3.2 and 3.3 show that in most cases, the enantioselectivity factors were lower with the RTIL stationary

phases than with the Chiraldex columns. Since most solutes are enantiorecognized by a combination of the two mechanisms (internal and external CD interactions), this may indicate that partial inclusion complexation is useful in the chiral recognition mechanism. A given enantiomer has more affinity for both the CD cavity and the CD outside wall. In the few cases where the enantioselectivity factors were higher with the RTIL stationary phases than with the Chiraldex columns, it can be speculated that the inclusion of an enantiomer provides a negative contribution to the overall enantioselectivity factor of that particular enantiomeric pair (e.g., dihydro-5-(hydroxymethyl)-2(3H)-furanone or camphene in Table 3.2; 1,3,5-trimethylcyclohexene in Table 3.3). A given enantiomer of these molecules may have more affinity for the outside of the CD molecule and less for the CD cavity than the other enantiomer. Here again an NMR study of the CD-solute complex formation would give the exact answer.

3.3.3. Solute Retention

The solute retentions were compared using the retention factor, k:

$$k = (t_k - t_o) / t_o \qquad (3.1)$$

which compensates for differences in column lengths. Figure 3.1 shows the $k_{chiraldex}/k_{RTIL}$ ratio. It is the ratio of the retention factor obtained with the Chiraldex column to the retention factor obtained with the analogous RTIL containing column. In most cases, this ratio is higher than one. It means that the retention of the same chiral molecule on the Chiraldex columns is significantly higher than on the RTIL containing columns. This is relatively surprising since the average polarity of the RTIL stationary phase is higher than the polarity of the polymer used in the Chiraldex columns to coat the capillary internal wall (see indexes in Table 3.1). It is possible that inclusion complexation with the empty CD of the commercial columns be responsible for this higher retention. Such inclusion complexation is not possible with the CDs of the RTIL stationary phase. In this case, the magnitude of the $k_{chiraldex}/k_{RTIL}$ ratio would be an indication of the magnitude of the inclusion energy for the molecules and the CD-CSP, that is the value of the stability constants of the solute-CD complex (Figure 3.1). Camphene, norbornene and fenchon have $k_{chiraldex}/k_{RTIL}$ ratio higher than 3. They also have structural similarities that make them candidates for tight inclusion complexation with the CD cavity. The chlorine atom of 3-chloro-2-norbornanone may hinder such inclusion complexation with the permethylated CD ($k_{chiraldex}/k_{RTIL}$ ratio equal to 1.1, Figure 3.1 bottom) and not with the dimethylated CD ($k_{chiraldex}/k_{RTIL}$ ratio equal to 2.7, Figure 3.1 top).
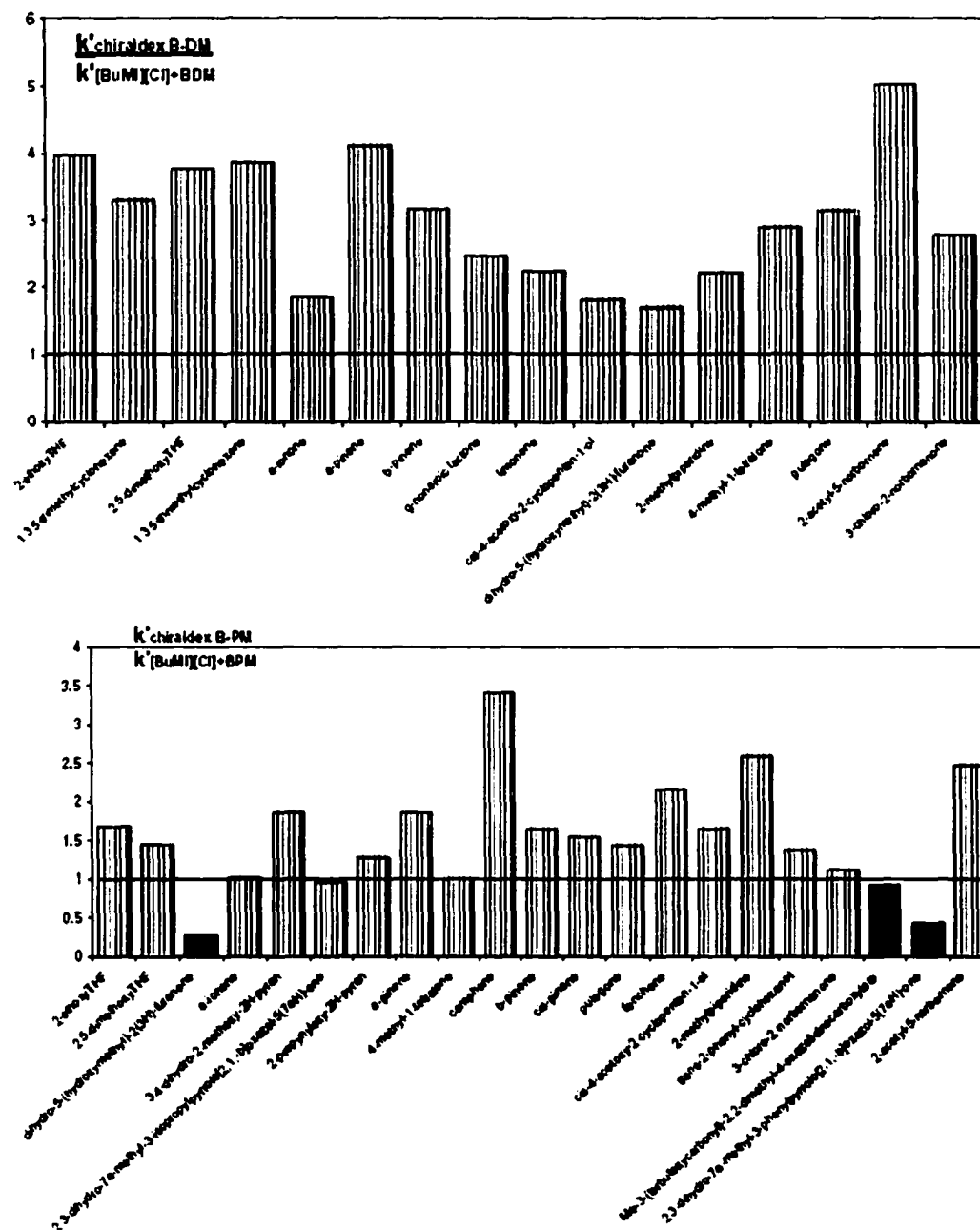
Figure 3.1. Diagram of the ratio of the retention factors of the commercial column over that of the RTIL column. Top: BDM chiral selector; bottom: BPM chiral selector. Black bars: the retention factors are higher on the RTIL column. Lined bars: the retention factors are higher on the commercial column. Data are given in Tables 3.2 and 3.3.

It should be pointed out that the use of the $k_{chiraldex}/k_{RTIL}$ ratio to estimate the complexation capability of a chiral molecule with a CD selector should be done only if the chiral molecule is fully derivatized. A polar or proton donor or acceptor group in it would increase the retention by the RTIL "solvent". The retention by the polysiloxane of the commercial Chiraldex column would be normal and the $k_{chiraldex}/k_{RTIL}$ ratio would be biased. It shows that [BuMI][Cl] is an RTIL that can be a useful solvent for GC stationary phases provided that all the polar proton donor or acceptor functionalities of the analyzed solutes are completely derivatized in very weak hydrogen donor or acceptor esters or amides substituents. Since such derivations render the analytes more volatile, this restriction may not be a problem in most practical cases.

3.3.4. Peak Efficiency

Figure 3.2 shows the chromatograms of α-ionone at 100 °C on the commercial Chiraldex B-PM 20m column (left) and on the 10m column containing the BPM CD dissolved in [BuMI][Cl] (right). This case was selected because the retention factors were similar on the two columns($21<k<23$). As discussed, the enantiomer separation is better achieved with the commercial column. The selectivity and resolution factor obtained with the commercial column are superior to the corresponding values obtained with the RTIL containing column (Figure 3.2 and 3.3). However, the peak efficiencies were different. As listed in Tables 3.2 and 3.3, the peak efficiencies obtained with the RTIL containing columns were most often superior to the one obtained with the corresponding commercial columns. For α-ionone (Figure 3.2), the efficiencies obtained with the RTIL column (~12000 plates) were 50% higher than the corresponding efficiency obtained with the commercial column (~8000 plates). It is recalled that the RTIL columns are 10 m long, two times shorter than the commercial Chiraldex columns. It means that the efficiencies obtained with the RTIL containing columns are significantly higher than the ones obtained with the commercial columns.

Figure 3.3 is a plot of the efficiency ratio (RTIL over commercial column) versus the column temperature. The first observation is that the BDM containing RTIL column (triangle) seems to produce the highest efficiency, up to 25 times higher than that obtained with the corresponding commercial column (1,3,5-trimethylcyclohexene, Table 3.3). The BDM containing RTIL produces efficiencies commonly 700% higher than the corresponding values obtained with the BDM commercial column. The difference is lower with the BPM column (squares in Figure 3.3). If we take in account the difference in column lengths, most compounds still show a better efficiency with the RTIL BPM column. The three compounds
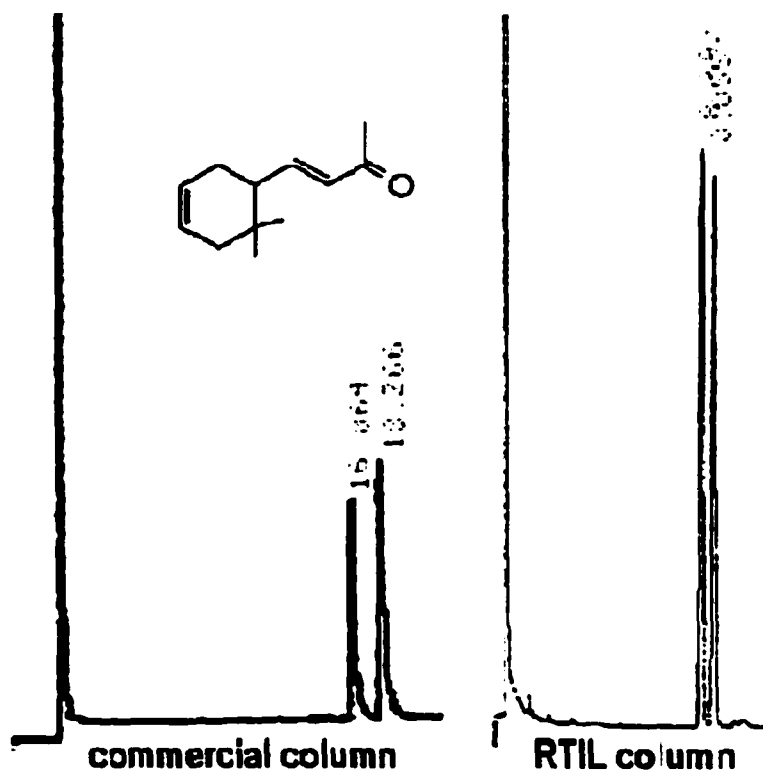
Figure 3.2. Chromatogram of α-ionone on the commercial BPM column (left) and the RTIL containing BPM column (left). Experimental conditions: 100 °C isotherm, helium carrier gas, 0.07 MPa (10 psi) inlet pressure, gas average velocity = 44 cm/s, FID detection. Commercial column: Chiraldex B-PM, 20 m, 250 μm i.d., 0.25 μm film thickness, dead time 46 s; RTIL column: [BuMI][Cl] with 26.4% BPM CD, 10 m, 250 μm i.d., 0.25 μm film thickness, dead time 23 s.
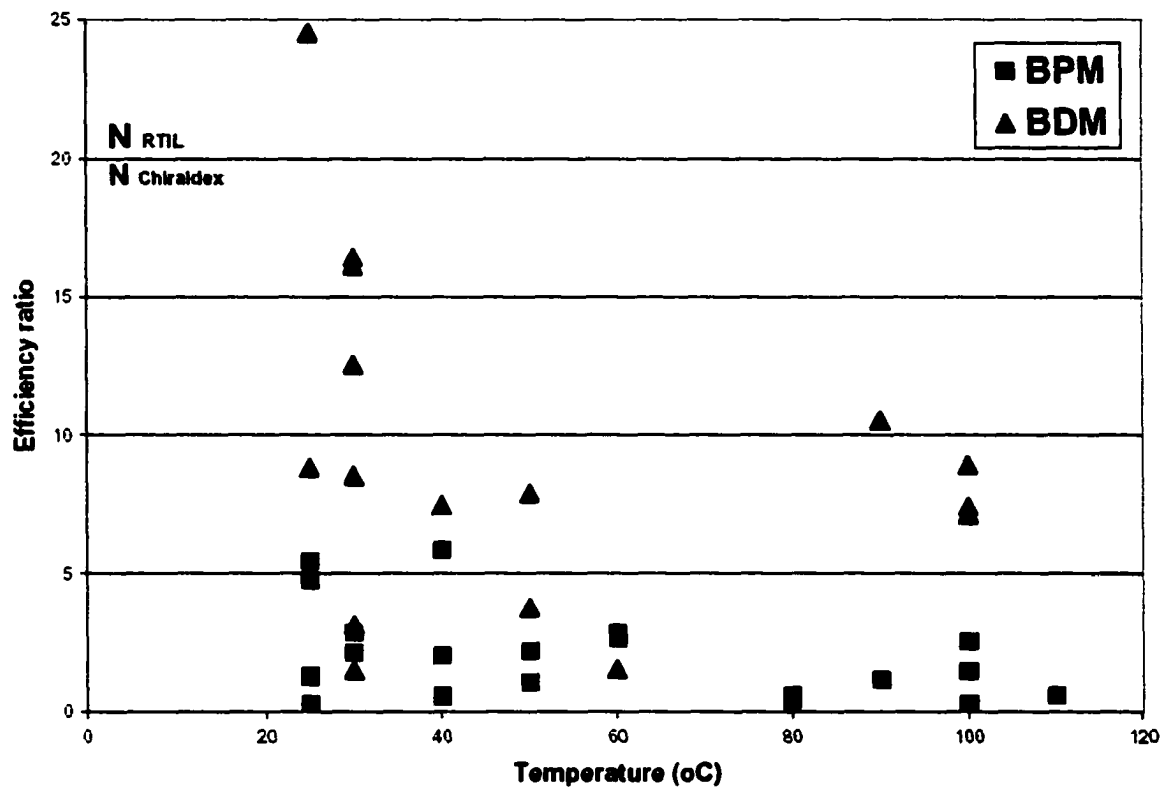
Figure 3.3. Plot of the ratio of the peak efficiencies obtained with RTIL containing columns over that obtained with the commercial columns versus the column temperature. Squares: BPM columns; Triangles: BDM columns. Data are given in Table 3.2 and 3.3.

that had a longer retention factor with the RTIL column (black bars in Figure 3.1) also had a lower efficiency compared to the commercial column. Efficiencies should be compared for similar retention factors. We propose two explanations to this efficiency difference. The first one is that the efficiencies on the RTIL containing CSP are greater because no inclusion complex formation with the analyte is possible. Although inclusion complexation gives greater enantioselectivity for some compounds, it also tends to result in poorer mass transfer and lower efficiencies [8]. The second explanation could be that the observed efficiency difference is due to a viscosity difference between the [BuMI][Cl] ionic liquid and the polymer used in the commercial column to dissolve the CD chiral selectors. Figure 3.3 shows that the efficiency enhancement decreases when the working temperature increases. Inclusion complexation is reduced at elevated temperature. Also, the viscosity decreases when the temperature increases. But the viscosity of the commercial polymer could decrease more rapidly than that of the RTIL.

3.3.5. Use of RTILs as Solvents for GC Stationary Phase

In conclusion, this work establishes that the [BuMI][Cl] RTIL is a useful solvent for GC stationary phases. It is able to dissolve a large amount of a chiral selector (more than 25% *w/w*) without intervening too much in the retention process of the derivatized analytes. It has a good viscosity producing a good kinetics in the solute-stationary phase exchange process and consequently, producing sharp peaks. Unfortunately, the chiral selectors studied, methylated CDs, were able to form inclusion complexes with small aromatic molecules and especially [BuMI][Cl]. The complexation of the CD cavity by the RTIL hindered this inclusion mechanism for the separation of the analyte enantiomers. Consequently, it turned out that the CD-RTIL capillary columns were only able to separate enantiomers by external adsorption. This allows one to examine the inclusion complex formation and independent contributions to enantioselective GC involving CD-based CSPs. RTIL should be able to work well as GC stationary phase solvents with other molecules not able to make inclusion complexation.

REFERENCES

1. Sun, J.; Forsyth, M.; MacFarlane, M.J. *J. Phys. Chem. B*, **1998**, *102*, 8858.

2. Seddon, K.R. *Kinetics and Catalysis*, **1996**, *37*, 693.

3. Bonhote, P.; Dias, A.P.; Papageorgiou, N.; Kalyanasundaram, K.; Grätzel, M. *Inorg. Chem.*, **1996**, *35*, 1168.

4. Dickinson, V.E.; Williams, M.E.; Hendrickson, S.M.; Masui, H.; Murray, R.W. *J. Am. Chem. Soc.*, **1999**, *121*, 613.

5. Armstrong, D.W.; He, L.; Liu, Y.S. *Anal. Chem.*, **1999**, *71*, 3873.

6. Berthod, A.; Wang, X.; Gahm, K.; Armstrong, D.W. *Geochem. Cosmochem. Acta*, **1998**, *62*, 1619.

7. Armstrong, D.W.; Li, W.Y.; Pitha, J. *Anal. Chem.*, **1990**, *62*, 214.

8. Berthod, A.; Li, W.Y.; Armstrong, D.W. *Anal. Chem.*, **1992**, *64*, 873.

9. ASTEC, *Chiraldex Handbook, A Guide to Using Cyclodextrin Bonded Phases for Chiral Separations by Capillary Gas Chromatography* **1999** and associated CD-ROM.

10. Berthod, A.; Zhou, E.Y.; Le, K.; Armstrong, D.W. *Anal. Chem.*, **1995**, *67*, 849.

11. Rundlett, K.L.; Armstrong, D.W. *J. Chromatogr. A*, **1996**, *721*, 173.

CHAPTER 4

IONIC LIQUIDS AS MATRICES FOR MATRIX-ASSISTED LASER DESORPTION/IONIZATION MASS SPECTROMETRY

A paper published in Analytical Chemistry[1]

Daniel W. Armstrong, Li-Kang Zhang, Lingfeng He, and Michael L. Gross

ABSTRACT

Room-temperature ionic liquids are useful as solvents for organic synthesis, electrochemical studies, and separations. We wished to examine whether their high solubalizing power, negligible vapor pressure, and broad liquid temperature range are advantageous if they are used as matrixes for UV-MALDI. Several different ionic matrixes were synthesized and tested, using peptides, proteins, and poly(ethylene glycol) (PEG-2000). All ionic liquids tested have excellent solubilizing properties and vacuum stability compared to other commonly used liquid and solid matrixes. However, they varied widely in their ability to produce analyte gas-phase ions. Certain ionic matrixes, however, produce homogeneous solutions of greater vacuum stability, higher ion peak intensity, and equivalent or lower detection limits than currently used solid matrixes. Clearly, ionic liquids and their more amorphous solid analogues merit further investigation as MALDI matrixes.

4.1. INTRODUCTION

The development of mass spectrometric instruments and techniques for the determination of high molecular weight compounds has been a tremendous success [1-8]. In particular, the soft ionization techniques of electrospray ionization (ESI) and matrix-assisted laser desorption/ionization mass spectrometry (MALDI-MS) have increased the applicability to both large biological and synthetic molecules [9-30]. MALDI's success is due in large part to the development of a number of effective matrixes and an increased understanding of their role and use [9-30], reflecting the earlier development of matrixes for fast atom bombardment [31]. The general properties of effective matrixes for MALDI are well known: they must dissolve (liquid matrix) or cocrystallize (solid matrix) with the sample, strongly absorb the laser light, remain in the condensed phase under high-vacuum conditions, stifle both chemical and thermal degradation of the sample, and promote the ionization of the sample via any of a number of mechanisms [12,14,19,22,23]. Although most MALDI matrixes are simple components consisting of small, polar, organic molecules, others are mixtures of different components, to produce the most beneficial effects (vide supra) [9-30]. It is well known that a matrix that is optimal for one type of sample (proteins or peptides) may not be as effective for other types of samples (e.g., synthetic polymers or RNA and DNA fragments). Hence, a variety of different matrixes have been developed for a wide range of samples and approaches.

Although both solids and liquids have been used as MALDI matrixes, solid matrixes are more widely utilized. They have the advantages of having low vapor pressure and in being simple, single-component systems with indigenous UV chromophores. Unfortunately, the analytes cannot be dispersed throughout the solid matrix in a homogeneous manner. Both the solute and impurities segregate in the matrix, resulting in a considerable degree of heterogeneity and poor reproducibility. Conversely, liquid matrixes produce more homogeneous solutions and better shot-to-shot reproducibility. Their inherent volatility, however, results in a dynamic, changing, uncontrolled matrix. In addition, liquid matrixes usually do not contain the desired UV chromophore. Consequently, other components must be added to make up for this deficiency. An ideal matrix for MALDI may be an UV-absorbing liquid that has little or no vapor pressure and promotes ionization as well or better than do the current solid matrixes.

Room-temperature ionic liquids (RTILs) and other low-melting-point analogues, have many of the properties thought to be beneficial for MALDI matrixes. RTILs are analogous to high-temperature melts of ions [32]. RTILs are good solvents for a variety of organic,

inorganic, and polymeric substances [33-36]. They have good thermal stability and a liquid range of 300 °C in some cases[37]. The viscosity of RTILs can vary appreciably, but importantly for mass spectral applications, they have very low vapor pressures. RTILs are also relatively easy to prepare from inexpensive substances.

RTILs have been used as novel solvent systems for organic synthesis [38-43] and for electrochemical studies [44]. Most recently, we have used RTILs as stationary phases in gas chromatography (GC) [35-36]. The low volatility of RTILs and their ability to solubilize complex organic molecules proved to be beneficial. These same properties are important for their use in mass spectrometry; yet, to our knowledge, no report has appeared on the use of room-temperature ionic liquids or solids as matrixes for MALDI.

4.2. EXPERIMENTAL SECTION

4.2.1. Materials.

1-Methylimidazole, chlorobutane, 3-chloro-1-propanol, hexafluorophosphoric acid, sodium tetrafluoroborate, 2-sulfobenzoic acid cyclic anhydride, poly(ethylene glycol) methyl ether (MePEG, average M_n ~350), p-tosyl chloride, anthraquinone-2-sulfonic acid (sodium salt monohydrate), α-cyano-4-hydroxycinnamic acid (CHCA), sinapinic acid (SA), 3,5-dimethyl-4-hydroxycinnamic acid, trifluoroacetic acid (TFA), aniline, ammonium hydroxide, ethanolamine, ethylamine, butylamine, N,N-diethylamine, N,N-diethylaniline, N,N-diethylmethylamine, N,N-dimethylamine, pyridine, tributylamine, triethylamine, tripropylamine, poly(ethylene glycol) (PEG, average M_n ~2000), and silver nitrate were purchased from Aldrich (Milwaukee, WI). All HPLC grade organic solvents were obtained from Fisher (St. Louis, MO). Bradykinin, human insulin, and horse skeletal apomyoglobin were ordered from Sigma (St. Louis, MO). 2-(2-Benzotriazolyl)-p-cresol (BTAC) was purchased from TCI America, Inc. (Portland, OR). All of these chemicals were used without further purification.

4.2.2. Methods.

4.2.2.1. *Synthesis of Organic Salts.*

Room-temperature ionic liquids, 1-butyl-3-methylimidazolium chloride ([BuMIm][Cl]), 1-butyl-3-methylimidazolium hexafluorophosphate ([BuMIm][PF$_6$]), 1-

butyl-3-methylimidazolium tetrafluoroborate ([BuMIm][BF$_4$]) and 1-(1-hydroxypropyl)-3-methylimidazolium chloride, were prepared according to a previously published procedure [35]. The synthesis of polyether-tailed 2-sulfobenzoic acid ([MePEG-BzSO$_3^-$][H$^+$]), polyether-tailed triethylammonium tosylate ([MePEG-Et$_3$N$^+$][tosylate$^-$]), and polyether-tailed trieylammonium anthraquinone-2-sulfonate ([MePEG-Et$_3$N$^+$][AQSO$_3^-$]) also was reported previously [44,45]. To obtain 1-butyl-3-methylimidazolium α-cyano-4-hydroxycinnamate, the same procedure as in the synthesis of [MePEG-Et$_3$N$^+$][AQSO$_3^-$] was used [45]. Briefly, 1.2 g of AgNO$_3$ (0.7 mmol) was added to a warm methanolic solution of CHCA. After being stirred for ~1 h, the solution was slowly cooled to room temperature and then to 0 °C in an ice bath, precipitating the silver salt. This insoluble salt was added to a 30-mL methanolic solution of [BuMIm][Cl] or 1-(1-hydroxypropyl)-3-methylimidazolium chloride (0.6 mmol). The mixture was heated to boiling with stirring for 30 min, then cooled to 0 °C, and filtered to remove precipitate. Flash evaporation gave the final product. Organic salts of CHCA and SA were prepared by dissolving ~0.5 g of acid in 15 mL of methanol. After equimolar base was added, the mixture was sonicated for 5 min, then filtered, and flash-evaporated to remove solvent. All products were placed in a vacuum oven at room temperature for 12 h to remove residual solvent.

4.2.2.2. *Sample Preparation for FAB and MALDI-TOF Analysis.*

The molecular weights of all organic salts were confirmed by both FAB and MALDI-TOF. The liquid matrix for FAB was a mixture of 3-nitrobenzyl alcohol/glycerol/TFA (1:1:1, v/v/v). Samples were dissolved in the matrix at a concentration of ~1 μg/μL. In MALDI studies of organic salts, they were used as self-matrixes to obtain their own MALDI mass spectra because derivatives of CHCA and SA can absorb UV strongly at 337 nm. Otherwise, the MALDI matrix was BTAC. In this case, BTAC and organic salts were dissolved in a mixture of acetonitrile/water (2:1, v/v, 0.1% TFA) at a concentration of 0.5 and 0.01 M, respectively. Samples were prepared by vortexing 2 μL of matrix solution and 2 μL of salt solution and then applying 1 μL of the mixture to the MALDI plate.

In the case of organic salts tested as MALDI matrixes, all organic salts were dissolved in the mixture of acetonitrile/water (2:1, v/v, 0.1% TFA) at a concentration range from 0.4 to 0.7 M. If this concentration exceeded the solubility of the salt, a saturated solution was used. Bradykinin (fw 1059.6), human insulin (fw 5807.6), horse skeletal apomyoglobin (fw 16952.6), and PEG 2000 were chosen as test analytes. Peptides and proteins were dissolved in deionized water at a concentration of 10 μM, while PEG 2000 was dissolved in the mixture of acetonitrile/water (2:1 v/v, 0.1% TFA) at 1 mM. Samples were

prepared by first vortexing 4 μL of matrix solution and 4 μL of test analyte solution for 1 min and then spotting 1 μL of mixture solution on a stainless steel plate. Evaporation of volatile solvent from the sample plate was assisted by a stream of air. Some of the organic salt matrixes that were synthesized were liquids, and others were solids. Several of the low-melting-point solid salts were evaluated as well. The homogeneity of analytes in "poorly crystalline" solids seemed to exceed that of highly crystalline solid matrixes. The matrix-to-analyte molar ratios were 50,000:1 for peptides and protein, and 500:1 for PEG polymer. Note that the higher molar ratios for the proteins are partly a consequence of the high molecular weight of these analytes relative to the low molecular weight of the matrix. For the purpose of comparison, CHCA and SA also were tested under the same conditions as the organic salts. Table 4.1 lists the ionic matrixes that had good solubilizing capabilities and good vacuum stability but did not adequately promote analyte-gas-phase ion formation.

4.2.2.3. Mass Spectrometry.
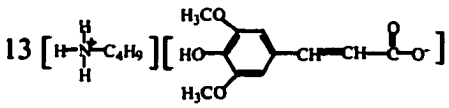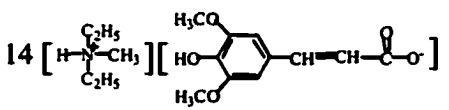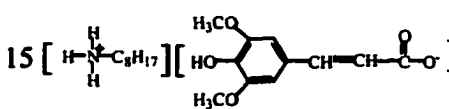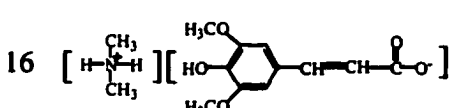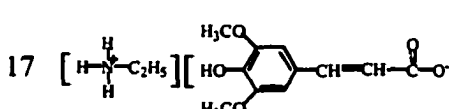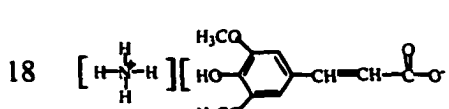
Low-resolution, fast-atom bombardment (FAB) mass spectra for all the liquid matrixes were obtained by using a VG ZAB-SE, a reverse geometry (BE) two-sector, double-focusing mass spectrometer. Sample ionization was performed by FAB using a xenon beam (of an energy of 8 DeV). The instrument was operated at an accelerating voltage of 8 kV and a mass resolving power of 1000.

A Voyager-RP Biospectrometry workstation time-of-flight mass spectrometer (PerSeptive Biosystems, Framingham, MA) was used in reflector or linear mode. The laser source was a nitrogen laser (337-nm, 3-ns pulse), with a variable intensity up to ~200 μJ on an arbitrary scale from 0 to 1000. Positive- and negative-ion modes were used to obtain mass spectra of all organic salts, but only positive-ion mode was used to test these organic salts as MALDI matrixes. A vertical flight tube of 1.2 m was operated with an acceleration voltage of 20 kV and a center guide wire held at 10 V. A delay time (between the laser pulse and extraction of ions into the mass analyzer) of 200 ns was used. This results in narrower ion arrival time distributions and, therefore, higher mass resolution. A MALDI mass spectrum consisted of the average ion signal acquired from 18 to 60 shots. When the uniformity of a sample spot and the ability to produce ions over the entire surface was evaluated, the spot was evenly divided into nine parts. One measurement was randomly performed on each part (Figure 4.1). A relative standard deviation (RSD) of signal from a sample was calculated from these nine measurements.

Table 4.1. Ionic liquids (and solids) that were tested for MALDI-MS, but failed to produce MS signals for the test analytes: Bradykinin (monoisotopic MW 1060.55) and polyethlyene glycol(PEG-2000)[a]

Matrix Number	Structures of ionic liquids	State (25 °C)	Molecular weight	Signal of analytes
1	[H₃C–N⊕N–CH₂CH₂CH₂CH₃][Cl⁻]	Solid	174.4 (138.9+35.5)	None
2	[H₃C–N⊕N–CH₂CH₂CH₂CH₃][PF₆⁻]	Liquid	283.7 (138.9+144.8)	None
3	[H₃C–N⊕N–CH₂CH₂CH₂CH₃][BF₄⁻]	Liquid	225.8 (138.9+86.8)	None
4	[C₂H₅–N⁺(C₂H₅)–(CH₂CH₂O)₇–CH₃][benzenesulfonate⁻]	Liquid	595.1 (424.3+170.8)	None
5	homophthalic anhydride with (CH₂CH₂O)₇–CH₃ and SO₃⁻ H⁺	Liquid	524.59 (1.0+523.6)	None
6	[C₂H₅–N⁺(C₂H₅)–(CH₂CH₂O)₇–CH₃][anthraquinone sulfonate⁻]	Liquid	711.3 (424.3+287.0)	None
7	[H₃C–N⊕N–CH₂CH₂CH₂CH₃][HO–C₆H₄–CH=C(COO⁻)–C≡N]	Liquid	326.7 (138.9+187.8)	None
8	[H₃C–N⊕N–CH₂CH₂CH₂OH][Cl⁻]	Liquid	176.4 (140.9+35.5)	None
9	[H₃C–N⊕N–CH₂CH₂CH₂OH][HO–C₆H₄–CH=C(COO⁻)–C≡N]	Liquid	328.7 (140.9+187.8)	None
10	[H₃C–N⊕N–CH₂CH₂CH₂OH][HO,HO–C₆H₃–CH=CH(COO⁻)]	Solid	319.6 (140.9+178.7)	None
11	[C₄H₉–N⁺(C₄H₉)–C₄H₉(C₄H₉)][HO–C₆H₄–CH=C(COO⁻)–C≡N]	Solid	430.7 (242.5+188.2)	None
12	[H₃C–N⊕N–H][H₃CO,HO,H₃CO–C₆H₂–CH=CH–C(O)–O⁻]	Solid	306.3 (83.1+223.2)	None

Table 4.1. (Continued)

Matrix Number	Structures of ionic liquids	State (25 °C)	Molecular weight	Signal of analytes
13		Solid	297.3 (74.1+223.2)	None
14		Liquid	311.4 (88.2+223.2)	None
15		Solid	353.5 (130.3+223.2)	None
16		Solid	269.3 (46.1+138.1)	None
17		Solid	269.3 (46.1+138.1)	None
18		Solid	241.2 (18.0+223.2)	None

a All of these organic salts were analyzed by MALDI-MS to determine their molecular weights (matrix used was BTAC).
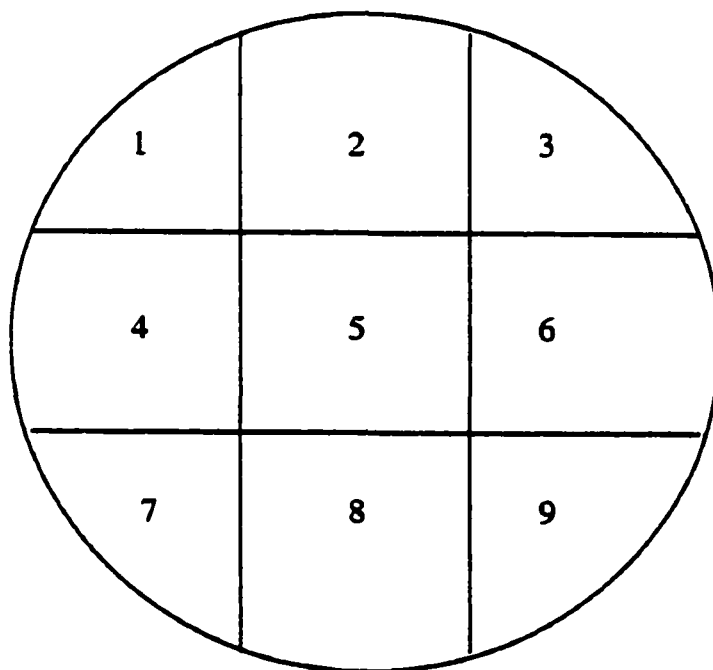
Figure 4.1. Schematic of the nine-part grid used to sample different parts of the sample / matrix spot.

4.3. RESULTS AND DISCUSSION

Most effective liquid matrixes used in UV MALDI are actually liquid mixtures of a low-volatility solvent and an UV-absorbing organic compound (usually a weak acid) [12,14,19,20]. Typically, much higher laser intensities are needed to produce results comparable to those found for analogous solid matrixes. In a vacuum, volatilization of the liquid matrix occurs, making reproducibility tenuous, but matrix longevity is sometimes sufficient to produce qualitative results [12-20]. Clearly, a matrix that combines the best (most useful) properties of both liquid and solid matrixes, and has the shortcomings of neither, would be beneficial. Further, an ideal liquid matrix for MALDI would be a single-component system capable of forming homogeneous solutions with all analytes of interest and, at the same time, having the absorptivity, low volatility, and ion-promoting capabilities of the best solid matrixes. This possibility may be realized for the first time using the concept of ionic liquids and related low-melting-point ionic solids.

All of the ionic liquids used as matrixes in this study easily dissolved the biological solutes and polymers of interest, forming smooth, uniform spots on the stainless steel sample plate (Figure 4.2). This is in contrast to the traditional solid matrixes that show cracking, flaking, crystallization, and numerous unconformities (Figure 4.2). Furthermore, the ionic matrixes persisted in high-vacuum conditions longer than the commonly used solid matrixes SA and CHCA. This was found to be a great advantage when doing a large number of samples or repeat analysis on a single sample plate.

Although all of the evaluated ionic matrixes showed good dissolution (of analytes) and vacuum properties, they varied tremendously in their ability to promote ionization of peptides, proteins, and synthetic polymers (relevant results are summarized in Tables 4.2 and 4.3). One thing that is eminently clear from these studies is that the matrix must have available protons to promote ionization. More conventional RTILs such as the 1-butyl-3-methylimidazolium chloride, tetrafluoroborate, or hexafluorophosphate salts produced no MALDI signals (compounds 1-3, Table 4.1). Likewise, polyether-based ionic liquids and the tetrabutylammonium salt of α-cyano-4-hydroxycinnamic acid (the free acid of which is a well-known solid matrix) produce no MALDI signals for any of the solutes tested (compounds 4-18, Table 4.1). However, ionic liquids (and solids) in which the cationic moiety contained an acidic proton often produced the desired gas-phase ions. The type and nature of the protonated amine portion of the matrix appears to have influence on the intensity of the $[M + H]^+$ signal (Tables 4.2 and 4.3). There does not appear, however, to be any consistent relationship between the pK_a of the matrix and signal intensity.

A)
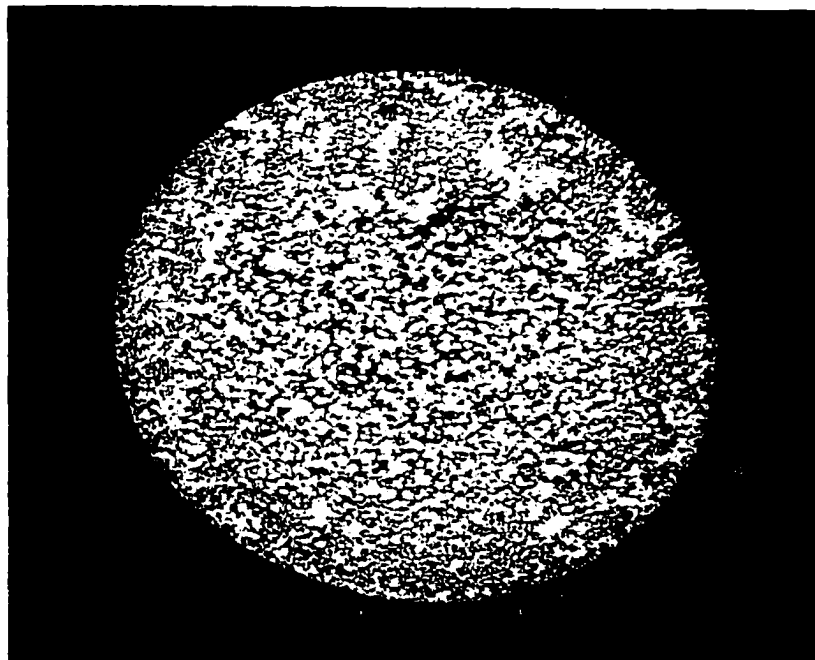
B)
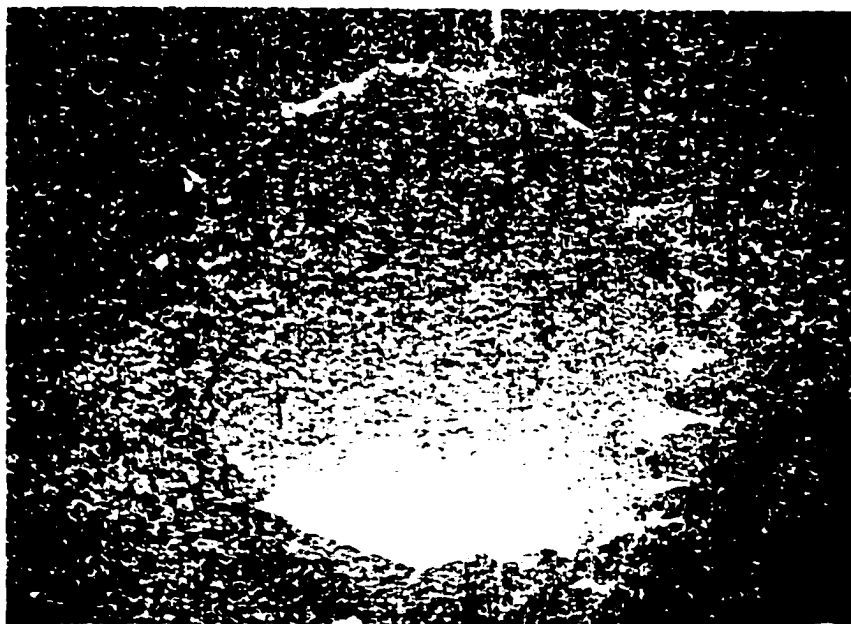
Figure 4.2. Photographs of A) the solid CHCA matrix showing cracks, crystals, and numerous incongruities, and B) the ionic matrix of organic salt [1-methylimidazolium] [CHCA], a transparent film or droplet. Note that the imperfections of the steel plate can be seen through this clear matrix.

Table 4.2. CHCA and its organic salts used as matrices for MALDI-MS. Test analytes are PEG (MW ~2,000, 1 μM), Bradykinin (monoisotopic MW 1060.55, 10 μM) and human insulin (monoisotopic MW 5808.6, 10 μM); laser wavelength 337 nm

Matrix Number	Structure of organic salts	State of film	pk$_a$ of cation	Intensity of M+H⁺ signal [a]		
				PEG 2,000	Bradykinin	Human isulin
19	HO—⟨⟩—CH=C(COOH)—C≡N	Solid	~3.0	40,000	40,000	24,000
	[C₂H₅—N⁺H—C₂H₅, C₂H₅][HO—⟨⟩—CH=C(COO⁻)—C≡N]	Liquid	10.78 (18 °C)	40,000	50,000	8,000
	[C₃H₇—N⁺H—C₃H₇, C₃H₇][HO—⟨⟩—CH=C(COO⁻)—C≡N]	Liquid	10.65	20,000	57,000	-
	[C₄H₉—N⁺H—C₄H₉, C₄H₉][HO—⟨⟩—CH=C(COO⁻)—C≡N]	Liquid	10.89	24,000	53,000	11,000
	[⟨⟩—N⁺H—C₂H₅, C₂H₅][HO—⟨⟩—CH=C(COO⁻)—C≡N]	Liquid	6.61 (22 °C)	37,000	52,000	7,000
	[C₂H₅—N⁺H—CH₃, C₂H₅][HO—⟨⟩—CH=C(COO⁻)—C≡N]	Liquid	10.35 (25 °C)	22,000	56,000	-
	[CH₃—N⁺H—H, CH₃][HO—⟨⟩—CH=C(COO⁻)—C≡N]	Solid	10.73 (25 °C)	34,000	45,000	5,000
	[C₂H₅—N⁺H—H, C₂H₅][HO—⟨⟩—CH=C(COO⁻)—C≡N]	Solid	11.09 (20 °C)	25,000	50,000	15,000
	[C₄H₉—N⁺H—H, H][HO—⟨⟩—CH=C(COO⁻)—C≡N]	Liquid	10.78 (20 °C)	26,000	55,000	16,000
2	[H—N⁺H—H, H][HO—⟨⟩—CH=C(COO⁻)—C≡N]	Solid	9.25 (25 °C)	25,000	27,000	-
	[H₃C—N⁺⟨⟩—H][HO—⟨⟩—CH=C(COO⁻)—C≡N]	Liquid	6.9.5 (25 °C)	23,000	61,000	7,000
	[C₂H₅—N⁺H—H, H][HO—⟨⟩—CH=C(COO⁻)—C≡N]	Solid	10.70 (25 °C)	25,000	56,000	-
	[HOH₂CH₂C—N⁺H—H, H][HO—⟨⟩—CH=C(COO⁻)—C≡N]	Solid	9.50 (25 °C)	26,000	50,000	-
32	[⟨N⟩H][HO—⟨⟩—C(H)=C(COO⁻)—CN]	Solid	5.25 (25 °C)	52,000	45,000	64,000
	[⟨33⟩—N⁺H—H, H][HO—⟨⟩—CH=C(COO⁻)—C≡N]	Solid	4.60 (25 °C)	50,000	62,000	34,000

[a] The numbers represent the signal intensity (i.e., number of counts) for the MH⁺ species. Small adjustments in the laser power (i.e., <± 10%) used for desorption from different matrixes, were made until an optimum signal was observed (see Results and Discussion). If the space is left blank (-), then no signal was detected.

Table 4.3. Sinapinic acid and its organic salts used as matrices for MALDI-MS. Test analytes are Bradykinin (monoisotopic MW 1060.55, 10 μM), human insulin (monoisotopic MW 5808.6, 10 μM) and horse skeletal apomyoglobin (monoisotopic MW 16952.56, 10 μM); laser wavelength 337 nm.

Matrix Number	Structure of organic salts	State of film	pk_a of cation	Intensity of M+H$^+$ signal		
				Bradykinin	Human isulin	Apomyoglobin
34		Solid	~4.4	12,000	43,000	28,000
		Liquid	10.78 (18 °C)	50,000	-	-
		Solid	5.25 (25 °C)	-	32,000	27,000
		Liquid	10.89 (25 °C)	65,000	25,000	53,000
		Solid	6.61 (22 °C)	57,000	10,000	7,000

[a] The numbers represent the signal intensity (i.e., number of counts) for the MH$^+$ species. Small adjustments in the laser power (i.e., <±10%), used for desorption from different matrixes, were made until an optimum signal was observed (see Results and Discussion). If the space is left blank (-), then no signal was detected.

In every case, an ionic matrix could be found that out-performed the analogous solid matrix (of α-cyano-4-hydroxycinnamic acid or sinapinic acid) in its ability to promote ion formation at comparable laser intensities. Figure 4.3 illustrates this fact for proteins (i.e., human insulin and horse apomyoglobin). Note that the aprotic ionic liquid (or solid) matrixes, shown on the left side of Figure 4.3 (i.e., Figure 4.3A and D), produced no discernible mass spectral signals. The conventional solid acid matrixes (middle spectra B and E in Figure 4.3) produced acceptable mass spectral responses, whereas desorption from optimized ionic matrixes produced the most intense spectra under comparable conditions (right-side spectra C and F in Figure 4.3). Different absorptivities and varying matrix/analyte interactions for different MALDI matrixes make it difficult to compare spectra obtained with the different matrixes. To obviate these difficulties, we made small adjustments in the laser power used for desorption until an optimum signal was observed for the test substance in a particular matrix. All spectra compared in Figures 4.3 and 4.4 were taken under those optimized conditions. We suggest the signal broadening in Figure 4.3F is caused by desorption of various metal-ion adducts that arise from contaminant metal salts in the matrix. In addition, the spectra obtained by desorption from conventional solid matrixes (CHCA and SA) could be obtained only after several attempts to find appropriate "hot spots" that gave acceptable signals. This search procedure was not necessary when the fluid ionic matrixes were used. This will be discussed in more detail subsequently.

Optimized ionic matrixes also worked well for MALDI determination of poly(ethylene glycol) (Figure 4.4). Once again, aprotic ionic liquids (or solids) produced no significant mass spectral signal (Figure 4.4C). Protic ionic liquid matrixes did give mass spectral signals more intense (Figure 4.4B) or less intense (Figure 4.4D) than that achieved when the CHCA solid matrix was used, depending on the nature of the matrix cation. Note that the dominant mass peaks in these spectra are the Na^+-cationized sample molecules. The smaller adjacent peaks represent the K^+-cationized species.

Others described previously the possible advantages of liquid matrixes for MALDI (e.g., a more homogeneous mixture of analyte and matrix, improved shot-to-shot reproducibility, more laser shots per spot because of diffusion and sample flow, allowing direct interfacing with liquid separation techniques, etc.) [12,14,19,20]. To quantify some of these "advantages", a comparison was made of MALDI mass spectral results using an ionic matrix versus the analogous solid CHCA matrix. All conditions, except for the matrix type, were identical. Bradykinin (MW 1060.2) was used as the test analyte. Each circular sample spot was divided approximately into nine area parts with a grid as shown in Figure 4.1. One MALDI mass spectral determination was done at the middle of each of the nine grid sections
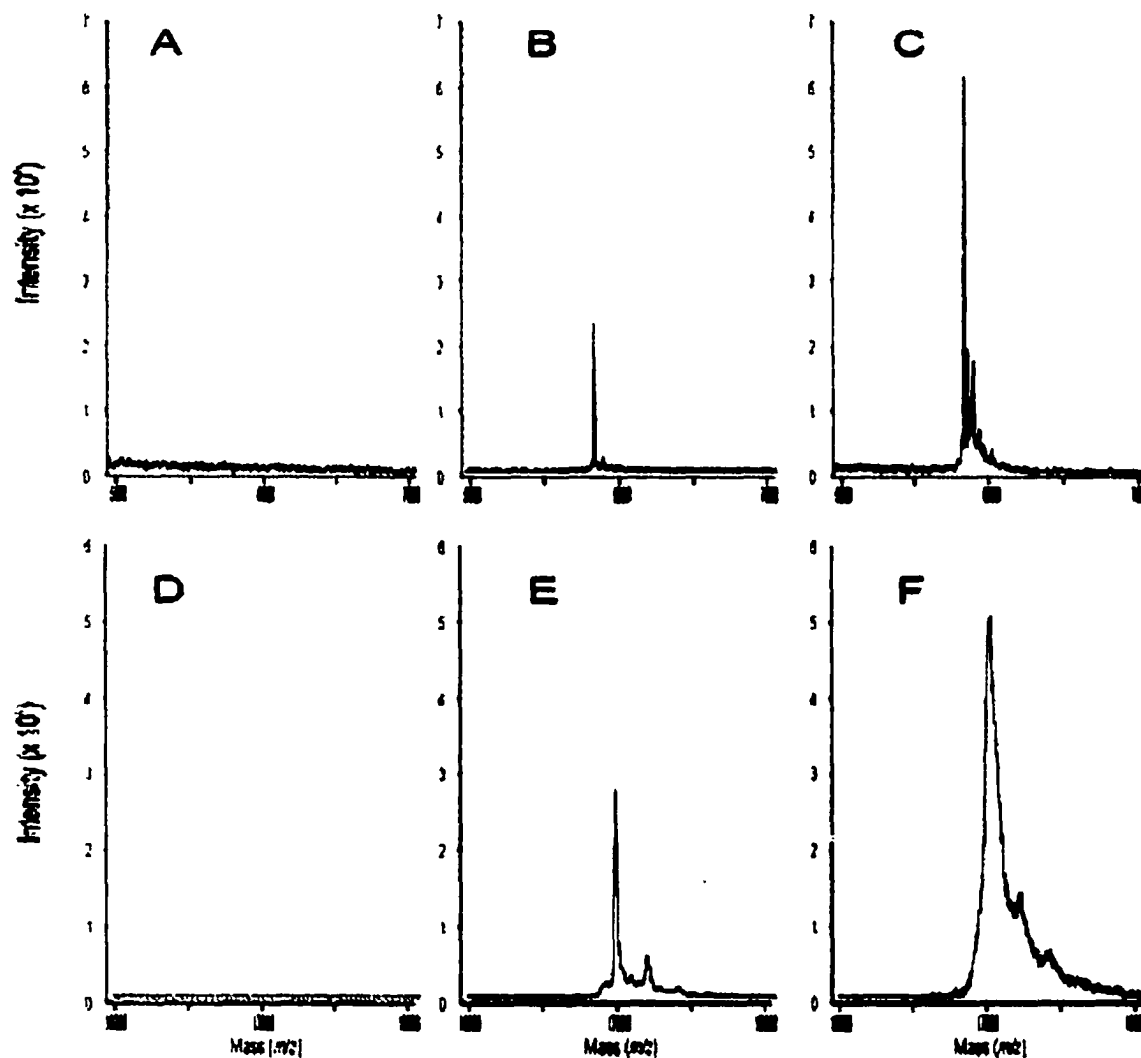
Figure 4.3. MALDI mass spectra of insulin in a matrix of (A) ionic liquid 2, (B) CHCA, (C) ionic liquid 32; and apomyglobin in a matrix of (D) ionic liquid 2, (E) SA, and (F) ionic liquid 37. The structures of the ionic liquid matrixes are given in Tables 4.1-4.3. See Experimental Section and Tables 4.2 and 4.3 for experimental details.
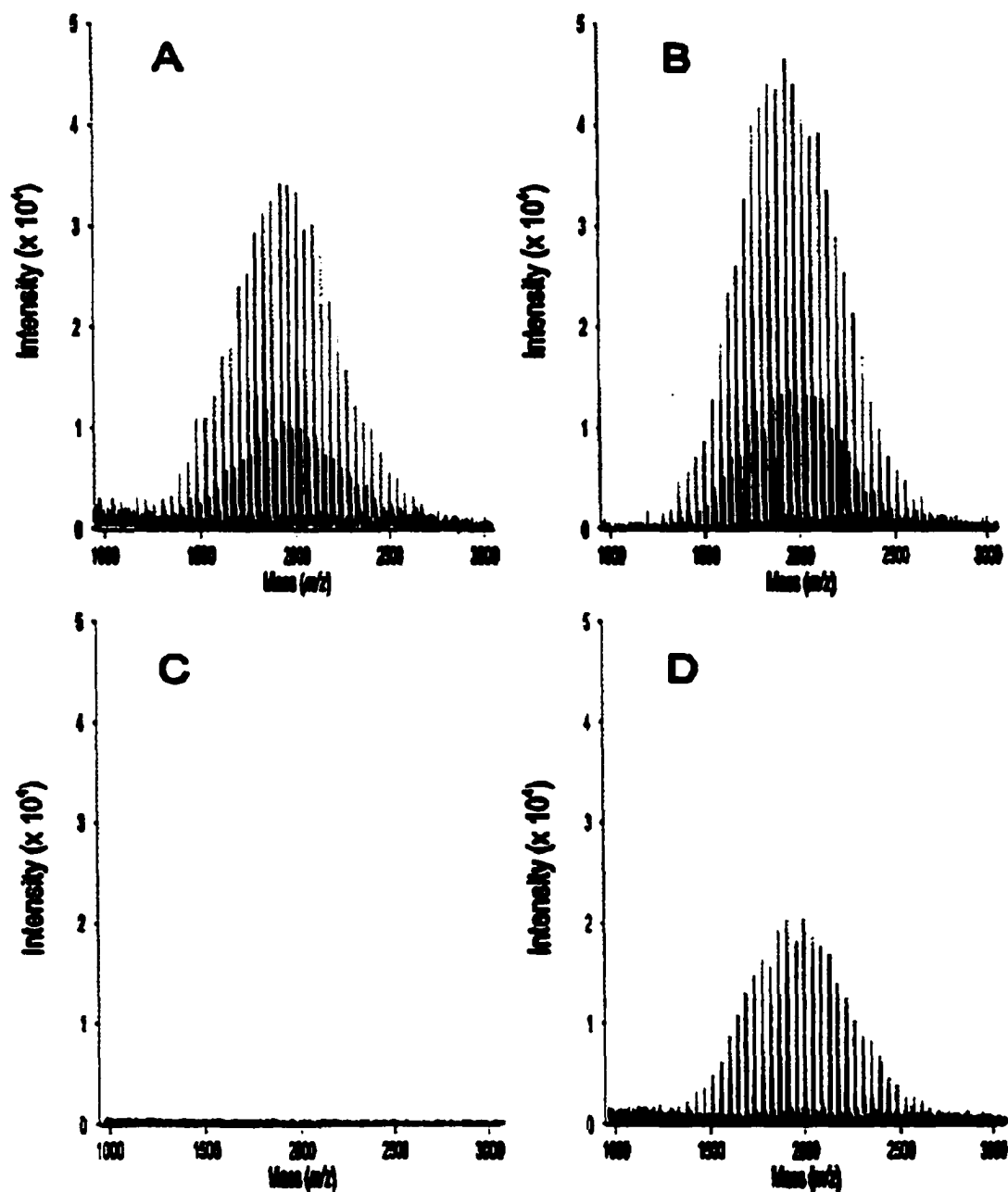
Figure 4. MALDI mass spectra of PEG-2000 in matrixes consisting of (A) CHCA, (B) ionic liquid 32, (C) ionic liquid 2, and (D) ionic liquid 22. See Experimental Section for further details.

(see 1 and 2 in Table 4.4). As can be seen, there is a huge discrepancy in the results. The ionic liquid matrix, because it was fairly homogeneous, produced a relatively narrow range of analyte ion signal intensities. Its use also gave the highest average ion intensity and a relative standard deviation of ~16%. Of course, the problem with the solid matrix (2 in Table 4.4) is that a random selection of sampling points within a solid matrix spot often produces no signal. Indeed, at least half the points examined produced no signal. Consequently, the average signal intensity is always low, and the relative standard deviation is high (150%). However, the results summarized in 2 of Table 4.4 do not reflect the way that MALDI is done with solid matrixes. Typically, an analyst will test several points within the sample matrix spot to find a point that yields the highest sample signal. Thus, we also decided to use this approach in each of the nine grid locations for the solid CHCA matrix (Figure 4.1). Only the highest intensity result was used from each of the nine grid locations in 3 and 4 of Table 4.3. Note that these results are for experiments where the initial solutions spotted on the sample plate are sonicated (3) or not sonicated (4). These solid matrix results are more consistent. There is a higher average signal intensity and smaller RSD. The reproducibility and homogeneity are still significantly less than those obtained by using the ionic liquid matrix, even though no "hot spot search" was done in that case (Table 4.4).

The detection limits for peptides and proteins in ionic liquid matrixes appear to be comparable to, or better than, those found in the analogous solid matrixes. This is shown in Table 5. Using a solid CHCA matrix, we detected bradykinin only at concentrations greater than 10 fmol/μL (Table 4.5). With ionic liquid matrix 23, the detection limit is more than 3 orders of magnitude less (1 amol/μL). Further, the detection limit can vary with the type of ionic liquid (see matrix 33 vs. matrix 23 in Table 4.5). In the case of insulin, the detection limit with the solid matrix SA (100 fmol/μL) was identical to that with the ionic matrixes (Table 4.5).

4.4. CONCLUSION

Optimally conceived and utilized ionic liquids and solids may make the most useful MALDI matrixes. With ionic matrixes, it is possible to combine the beneficial qualities of liquid and solid matrixes. Ionic liquids produce a much more homogeneous sample solution (as do all liquid matrixes) yet have greater vacuum stability than most solid matrixes. In many (most) cases, an ionic matrix can be found that produces greater spectral peak intensities and lower limits of detection than comparable solid matrixes. Most ionic liquids readily dissolve biological oligomers, proteins, and polymers. However, ionic liquids can

Table 4.5. Detection limits for bradykinin and insulin in different solid and ionic liquid matrixes.

Analyte	Matrix [a]	Concentration of analyte in matrix [b]						
		10 pmol/µL	1 pmol/µL	100fmol/µL	10 fmol/µL	1 fmol/µL	100 amol/µL	1 amol/µL
Bradykinin	CHCA	40000	17000	7000	-	-	-	-
Bradykinin	33	60000	20000	4000	6000	6000	-	-
Bradykinin	23	53000	12000	8000	15000	10000	7000	10000
Bradykinin	SA	53000	12000	0	-	-	-	-
Bradykinin	36	30000	15000	0	-	-	-	-
Bradykinin	37	35000	4000	0	-	-	-	-

[a] CHCA, α-cyano-4-hydrocinnamic acid; SA, sinapinic acid. Structures for matrixes 50, 9, 15, and 23 are given in Table 4.2. [b] The numbers represent the signal intensity (i.e., number of counts) for the MH^+ species. Small adjustments in laser power (i.e., $<\pm5\%$) used for desorption from different matrixes were made until an optimum signal was obtained (see Results and Discussion). If the space under the concentration is left blank (-), then no signal was detected.

vary tremendously in their ability to promote analyte ionization. Both the cationic and anionic portion of the ionic matrix must be chosen with a consideration for the special requirements of UV-MALDI. The ionic matrix must have significant absorbance at the desired wavelength, but also available protons. Most conventional ionic liquids that lack these properties are ineffective as MALDI matrixes.

ACKNOWLEDGMENT

REFERENCES

1. Macfarlane, R. D.; Torgerson, D. F. *Science* **1976**, *191*, 920-923.

2. Armstrong, D. W.; Sequin, R.; McNeal, C. J.; Macfarlane, R. D.; Fendler, J. H. *J. Am. Chem. Soc.* **1978**, *100*, 4605-4606.

3. Benninghoven, A.; Sichtermann, W. K. *Anal. Chem.* **1978**, *50*, 1180-1184.

4. Barber, M.; Bordoli, R. S.; Sedgwick, R. S.; Tyler, A. N. *J. Chem. Soc., Chem. Commun.* **1981**, 325-327.

5. Blakely, C. R.; Carmody, J. J.; Vestal, M. L. *Anal. Chem.* **1980**, *52*, 1636-1641.

6. Whitehouse, C. M.; Dreyer, R. N.; Yamashita, M.; Fenn, J. B. *Anal. Chem.* **1985**, *57*, 675-679.

7. Cotter, R. J. *Anal. Chim. Acta* **1987**, *195*, 45-59.

8. Hillenkamp, F.; Karas, M.; Beavis, R. C.; Chait, B. T. *Anal. Chem.* **1991**, *63*, 1193A-1203A.

9. Karas, M.; Hillenkamp, F. *Anal. Chem.* **1988**, *60*, 2299-2301.

10. Beavis, R. C.; Chait, B. T. *Rapid Commun. Mass Spectrom.* **1989**, *3*, 432-435.

11. Beavis, R. C.; Chait, B. T. *Anal. Chem.* **1990**, *62*, 1836-1840.

12. Dominic Chan, T. W.; Colburn, A. W.; Derrick, P. T. *Org. Mass Spectrom.* **1992**, *27*, 53-56.

13. Fitzgerald, M. C.; Parr, G. R.; Smith, L. M. *Anal. Chem.* **1993**, *65*, 3204-3211.

14. Cornett, D. S.; Duncan, M. A.; Amster, I. J. *Anal. Chem.* **1993**, *65*, 5, 2608-2613.

15. Huberty, M. C.; Vath, J. E.; Yu, W.; Martin, S. A. *Anal. Chem.* **1993**, *65*, 2791-2800.

16. Juhasz, P.; Biemann, K. *Proc. Natl. Acad. Sci. U.S.A.* **1994**, *91*, 4333-4337.

17. Beeson, M. D.; Murray, K. K.; Russell, D. H. *Anal. Chem.* **1995**, *67*, 1981-1986.

18. Cohen, S. L.; Chait, B. T. *Anal. Chem.* **1996**, *68*, 31-37.

19. Williams, J. B.; Gusev, A. I.; Hercules, D. M. *Macromolecules* **1996**, *29*, 8144-8150.

20. Dale, M. J.; Knockenmuss, R.; Zenobi, R. *Anal. Chem.* **1996**, *68*, 3321-3329.

21. Gimon-Kinsel, M.; Preston-Schaffter, L. M.; Kinsel, G. R.; Russell, D. H. *J. Am. Chem. Soc.* **1997**, *119*, 2534-2540.

22. Caldwell, K. L.; Murray, K. K. *Appl. Surf. Sci.* **1998**, 127-129, 242-247.

23. Zenobi, R.; Knockenmuss, R. *Mass Spectrom. Rev.* **1998**, *17*, 337-366.

24. Limback, P. A. *Spectroscopy* **1998**, *13*, 16-27

25. Williams, T. L., Fenselau, C. *Eur. Mass Spectrom.* **1998**, *4*, 379-383

26. Asara, J. M.; Allison, J. *J. Am. Soc. Mass Spectrom.* **1999**, *10*, 35-44.

27. Kirpekar, F.; Berkenkamp, S.; Hillenkamp, F. *Anal. Chem.* **1999**, *71*, 2334-2339.

28. Sporns, P.; Wang, J. *Food Res. Int.* **1998**, *31*, 181-189.

29. Ring, S., Rudich, Y. *Rapid Commun. Mass Spectrom.* **2000**, *14*, 515-519

30. Zhang, L.-K.; Gross, M. L. *J. Am. Soc. Mass Spectrom.* **2000**, *11*, 854-865.

31. De Pauw, E., Agnello, A., Derwa, F. *Mass Spectrom. Rev.* **1991**, *10*, 283-301

32. Osteryoung, R. A. *NATO ASI Ser., Ser. C* **1987**, *202*, 329 (*Molten Salt Chemistry: An Introduction and Selected Application*; Mamantov, G., Marassi, R., Eds.).

33. Wilkes, J. S.; Levisky, J. A.; Wilson, R. A.; Hussey, C. L. *Inorg. Chem.* **1982**, *21*, 1263-1264.

34. Huddleston, J. G.; Willauer, H. D.; Swatloski, R. P.; Visser, A. E.; Rogers, R. D. *Chem. Commun.* **1998**, 1765-1766.

35. Armstrong, D. W.; He, L.; Liu, Y.-S. *Anal. Chem.* **1999**, *71*, 3873-3876.

36. Berthod, A.; He, L.; Armstrong, D. W. *Chromatographia* **2000**, *53*, 63-68.

37. Freemantle, M. *Chem. Eng. News* **1999**, (Jan. 4), 23.

38. Wilkes, J. S.; Zaworotko, M. J. *J. Chem. Soc., Chem. Commun.* **1992**, 965-967

39. Chauvin, Y.; Oliver-Bourbigou, H. *CHEMTECH* **1995**, *25* (9), *26-30*.

40. Suarez, P. A. Z.; Dullius, J. E. L.; Einloft, S.; DeSouza, R. F.; Dupont, J. *Polyhedron* **1996**, *15*, 1217-1219.

41. Adams, C. J.; Earle, M. J.; Roberts, G.; Seddon, K. R. *Chem. Commun.* **1998**, 2097-2098.

42. Earle, M. J.; McCormac, P. B.; Seddon, K. R. *Chem. Commun.* **1998**, 2245-2246.

43. Dyson, P. J.; Ellis, D. J.; Parker, D. G.; Welton, T. *Chem. Commun.* **1999**, 25-26.

44. Dickinson, V. E.; Williams, M. E.; Hendrickson, S. M.; Masui, H.; Murray, R. W. *J. Am. Chem. Soc.* **1999**, *121*, 613-616.

45. Long, J. W.; Kim, I. K.; Murray, R. W. *J. Am. Chem. Soc.* **1997**, *119*, 11510-11515.

PART TWO

DETERMINATION OF CELL VIABILITY USING CAPILLARY ELECTROPHORESIS COUPLED WITH LASER-INDUCED FLUORESCENCE DETECTION

CHAPTER 5

GENERAL INTRODUCTION AND LITERATURE REVIEW

The assessment of cell viability is important in many industries. Applications include detection and enumeration of food spoilage organisms, evaluation of inactivation treatments, quality control of starter cultures for beer, wine, and yogurt production, biodegradation, production of antibiotics, evaluation of sperm quality for artificial insemination, and numerous others [1-7]. The determination of cell viability is much more complex than one might imagine. Indeed, it is an issue that is subject to considerable debate. This is clearly reflected by the fact that an almost endless list of terms is used to describe inactive cells such as dead, moribund, starved, dormant, resting, quiescent, viable but non-culturable, injured, sublethally damaged, stressed, inhibited, resuscitable, living, active, vigorous, vital, and so on. A profound discussion concerning the proper use of these terms can be found in a recent review [2].

The definition of viability is neither simple nor straightforward. For prokaryotes, Postgate gave a practical definition, namely, that viability is the property possessed by that portion of a bacterial population capable of multiplication when provided with optimal conditions for growth [3]. The optimal conditions, such as the composition of medium, atmosphere, temperature, pH, etc., however, are ambiguous and not known for a majority of microorganisms in natural environments such as soil or seawater and varies significantly with individual populations [4]. Later, Breeuwer *et al.* gave a more general definition that cells are considered to be viable if they are capable of performing all cell functions necessary for survival under specific conditions [1]. The properties that viable cells exhibit include: (i) intact cytoplasmic (plasma) membrane which acts as a barrier between the cytoplasm and the extracellular environment; (ii) DNA transcription and RNA translation; (iii) generation of energy for maintenance of cell metabolism, biosysthesis of protein, nucleic acid, polysaccharides, and other cell components; (iv) growth and reproduction. All methods implemented to assess the viability of cells are rooted from these properties, and summarized in Table 5.1.

5.1. Viability Assessment of Cells

Viability assays are used to enumerate live and dead cells in a population. The viability is usually determined by the ratio of the living cell number to the total cell number in a sample, whether alive or dead. It is a common practice to obtain the total cell count with

Table 5.1. Criteria and methods for the assessment of viability of cells

Criterion	Method	Analysis time	Comments
Reproduction	Plate count method	2-5 days	High sensitivity
Cell morphology (cell elongation)	Inhibition of cell division by nalidixic acid or other antibiotics	6 hours	Only for antibiotic-sensitive bacteria, microscopic analysis elongated cells
Membrane integrity	Dye exclusion methods, e.g., methylene blue labeling, influx DNA probes	30 min	Viable cells with an intact cytoplasmic membrane will not be stained
Respiration	Reduction tetrazolium dyes in cells with an active electron transfer chain	1-4 hours	Accumulation of insoluble formazan products. Not applicable for fermentative microorganisms
Metabolic activity	Radiolabeling method and microautoradiography	4-6 hours	Only metabolically active cells incorporate radioactively labeled substrate (such as $[^3H]$glucose, $[^3H]$acetate).
Enzyme activity	Fluorescein diacetate method (esterase activity)	30 min	Fluorescein is accumulated in intact cells
Membrane potential (negative inside)	Distribution of Rhodamine 123, carboxycyanine dyes, and oxonols	1 hour	Potential dependent uptake or exclusion of dyes
pH gradient	Intracellular pH measurement using, e.g., fluorescein derivatives	1 hour	Viable cell maintain pH gradient

a number of counting chambers or electronic counters. For example, a Petroff-Hausser counting chamber is often used for counting bacteria; hemocytomers, originally designed for counting blood cells, are used for enumerating larger eucaryotic microorganisms. Using the counting chambers is easy, fast, inexpensive, and also provides information about the size and morphology of microorganisms. These devices, however, are only suitable for evaluating small numbers of cells. Electronic counters, such as the Coulter Counter, are capable of analyzing a large number of cells, and are extremely useful in dealing with larger cells (> ~2 μm) such as protozoa, algae, nonfilmentous yeasts, red blood cells, and white blood cells. Unfortunately, the Coulter Counter cannot give accurate results with bacteria because of interference by small debris particles, the formation of filaments, and other problems. Moreover, it is difficult or impossible to distinguish living cells from dead cells in all counting chambers and electronic counters [8].

The total number of viable cells present in a microbial population can be determined by the viable count. Conventionally, the ability of cells to reproduce is considered as the benchmark method for determination of viability, and since the turn of the last century the plate count method was widely employed to obtain a "total viable count" in many situations. In most plate counting procedures, a diluted sample of a microorganism is spread over a solid surface (such as agar). Each cell or group of cells develops into a distinct colony. The original number of viable cells in the sample can be easily calculated from the number of colonies formed and the sample dilution.

Although the plate count method is simple and sensitive, it is inherently an indirect enumeration approach and has come under increasing criticism for many reasons. One of the main reasons is the existence of a "viable but unculturable" state, in which bacterial cells retain all physiological functions except the ability to grow on media normally used for their cultivation. Consequently, large discrepancies have been constantly reported between results of plate counts and total direct microscopic counts [9]. As an example, *Klebsiella aerogenes* was found that, if maintained under starvation condition (i.e., in nonnutrient buffer) before culture, only 20% of the treated population could be recovered from the stress and form colonies after 24 hours incubation, while 80 % of the population were unculturable but remained intact and responsive to mild changes in medium composition and concentration [10]. In natural environments such as soil and seawater, this category of microorganisms is, unfortunately, vast [4]. Additionally, plate counts are deficient in that no single medium will culture all bacteria in a sample, whether terrestrial or aquatic [11]. Moreover, clumping of cells and inhibition by neighboring cells also can lead to inaccurate counts.

All methods of indirect enumeration, i.e., those requiring culture, were considered to be inherently selective and therefore deficient [12]. Therefore, direct count methods are preferable. In an effect to overcome the problems associated with plate count methods, a number of direct counting procedures, based on the properties of viable cells, have been developed (see Table 5.1) [4,5,13-19]. For example, radiolabeling techniques were used to obtain viable counts making use of the cellular metabolic activity of viable cells [15-17]. In this methods, cells are suspended in a solution containing an radioactively labeled substrate. Only cells that are metabolically active are able to incorporate the substrate and are detected on photographic film or enumerated with a scintillation counter. Radiolabeling methods can be used either alone or in combination with other methods such as fluorescent labeling [17].

A unique method developed by Kogure, et al., was found useful in directly counting the viable bacteria present in seawater [18,19]. In this method, nalidixic acid, a specific inhibitor of DNA synthesis, is used to prevent cell division in gram-negative bacteria by inhibiting DNA replication and cross-wall formation. Since other cellular synthetic pathways continue to function, viable cells will demonstrate active metabolism and form an elongated shape in the presence of nutrients. These cells are easily discriminated from dead cells under microscopy. Consequently, this direct viability count allows enumeration of viable cells which are actively growing as well as dormant cells which are physiologically responsive, thus effectively overcoming the problem of underestimation of viable cells by plate counts. It should be noted that nalidixic acid is operative only against susceptible gram-negative bacteria; some gram-negative bacteria are resistant to the antibiotic, potentially causing underestimation of viable population. In this case, other antibiotics with similar function have been used to expand the usefulness of this method [1].

Although the above mentioned, time-honored direct count methods achieved some success, many of them are expensive, inconvenient to use, or are only useful for a narrow range of cells. More universal and efficient methods are needed for both the academic and industrial fields in which microorganisms and other cells are involved. Fluorescence labeling approaches represent such a direction and are becoming currently the most widely employed methods for the assessment of cell viability in a population. The importance of these methods is clearly reflected in Table 5.1.

5.2. Fluorescence Labeling

Fluorescence labeling techniques have many advantages such as high sensitivity (i.e., a very small amount of fluorogenic probe molecules is needed), high time resolution ($\sim 10^{-8}$ s), and the potential to distinguish vigorous, frail, or injured cells, in addition to differentiating live and dead ones. Numerous fluorescent probes have been developed and are commercially available [20]. The applications of these dyes are summarized in Table 5.2 and some of their structures are given in Figure 5.1. The use of fluorescent probes to estimate cell viability is based on the criteria of living organisms outlined in Table 5.1.

The integrity of the cell membrane is a criterion that is often employed to discriminate between living and dead cells. Since dead cells have compromised membranes, membrane-impermeant nucleic acid stains such as propidium iodide (PI), ethidium bromide (EB), PO-PRO-3, and SYTO Green easily diffuse into the cytoplasm and label the dead cells by intercalating with their DNA. These fluorescent probes for dead cell counting are often used in combination with membrane-permeant DNA counterstains such as 4',6-diamidino-2-phenylindole (DAPI), SYBR-14, Hoechst 33342, SYTO series, etc. Following excitation, both groups of dyes produce fluorescence at different wavelength, therefore, living and dead cells can be distinguished and enumerated using flow cytometry or an array of imaging techniques. An important advantage of the DNA-specific fluorochromes is that their fluorescence increases significantly only when they are bound to their target molecules, so they produce an extremely low background signal. Different types of cells may require different dyes or combinations of dyes. For example, the LIVE/DEAD BacLight Bacterial Viability Kit from Molecular Probes, containing PI and SYTO 9, is a proven tool for assessing viability of bacteria; FUN-1 [2-chloro-4-(2,3-dihydro-3-methyl-(benzo-1,3-thiazol-2-yl)-methylidene)-1-phenyl-quinolinium iodide] is useful for analyzing yeast with microscope, and the LIVE/DEAD Sperm Viability Kit, containing PI and SYBR-14, is recommended for analyzing the viability of sperm in different species [20].

Acridine orange (AO), also a membrane-permeant nucleic acid stain, has been used to differentiate between both living and dead cells [21]. This application is based on the observation that AO can react with both double-stranded and single-stranded nucleic acid polymers, and resulting complexes fluoresce green and red-orange, respectively. Since living cells have active metabolism and contain higher amounts of RNA than dead cells, therefore, living cells show high RNA/DNA ratio, while dead cells demonstrate low RNA/DNA ratio. Thus, it may be valid to correlate red fluorescence with active cells and green fluorescence with inactive cells. However, the metachromatic property of AO is influenced by many

Table 5.2. Some frequently used dyes for estimating cell viability by flow cytometry and fluorescence microscopy

Dye	Target / mode of action
4',6-Diamidino-2-phenylindole (DAPI) Propidium iodide Ethidium homodimer SYTO series	Nucleic acid and membrane integrity
SYBR-14 Hoechst 33342 Hoechst 33258	Mammalian sperm DNA/ membrane integrity
FUN-1	Nucleic acid / production of cylindrical intravacuolar structures (CIVS) in yeast
Acridine orange	Nucleic acids
Hydroethidine	Oxidation to ethidium bromide and subsequent DNA binding
Fluorescenin diacetate (FDA), carboxyfluorescein diacetate (CFDA), BCECF-AM, Calcein AM	Esterase activity and membrane integrity
Dihexyloxacarbocyanine, rhodamine 123, oxonol (DiBaC$_4$ (3))	Transmembrane electrochemical potential
Fluorescein, cF, BCECF, BCECF-AMs, pyranine, cSNARF-1, and SNARFs	Intracellular pH gradient / enzymatic activity
Chemichrome Y Fungolite	Fungal enzymatic and membrane integrity
Fluorescein di-β-D-galactopyanoside	β-Galactosidase activity and membrane integrity
5-Cyano-2,3-ditolyl tetrazolium chloride (CTC), 2-(p-iodophenyl)-3-(p-nitrophenyl)-5-phenyl tetrazolium chloride (INT)	Respiratory chain activity
Mithramycin	Cell elongation (incubation with nalidixic acid and yeast extract, followed by staining)
Calcafluor white	Cell-wall chitin (regardless of metabolic state)
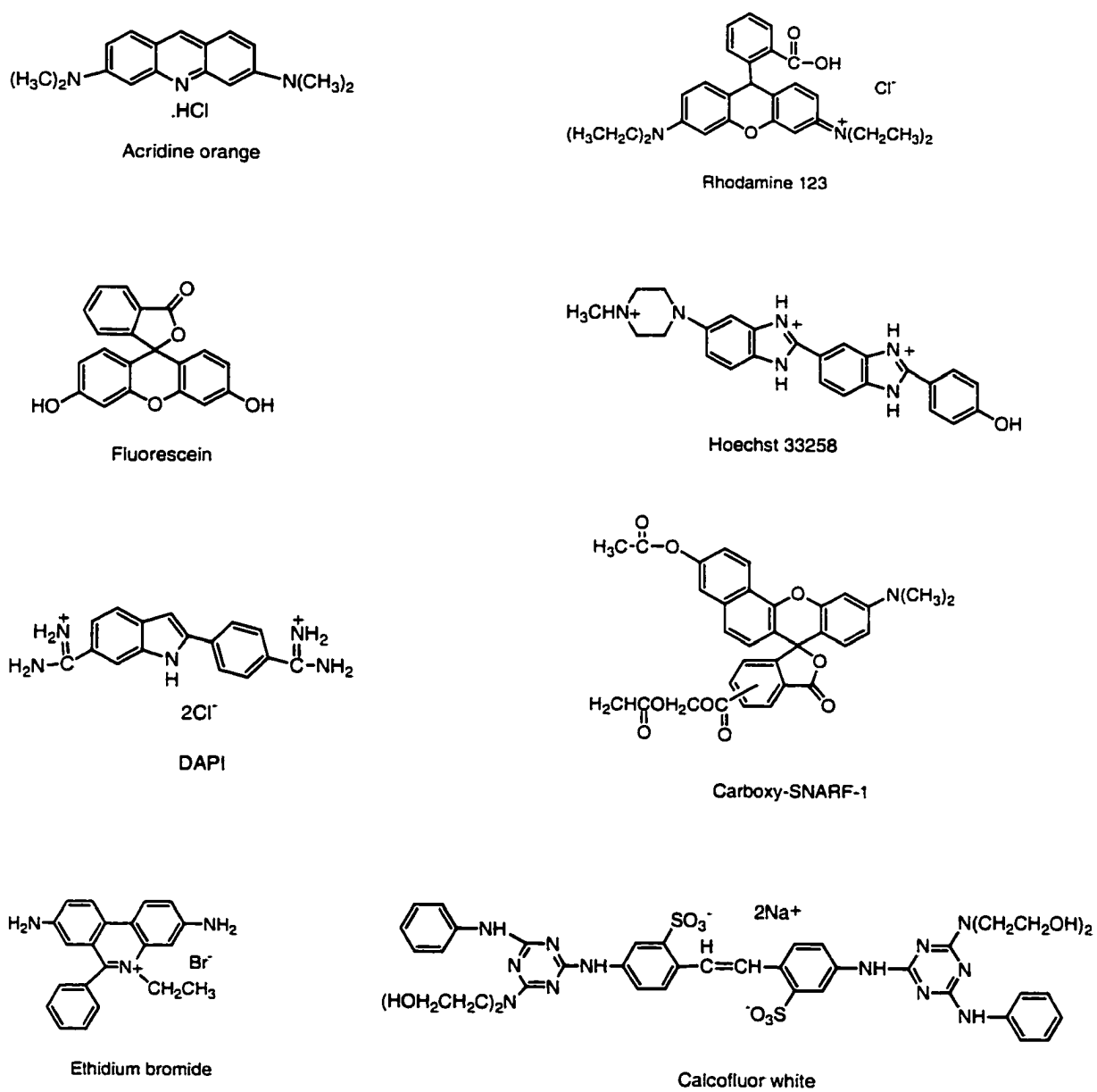
Figure 5.1. Structures of some common fluorescent dyes used in cell viability determination.

factors, such as pH of dye solution, incubation time, and AO concentration. Accordingly, AO was not recommended by some for the applications to cell viability measurement [22].

Fluorescein derivatives, such as diacetate (FDA), carboxyfluorecein (cF), calcein AM, 2',7'-Bis(2-carboxyethyl) 5(6)-carboxyfluorescein (BCECF) and its acetoxymethyl esters (BCECF-AMs), are fluorogenic esterase substrates and membrane permeable. Some of these dyes are also used to measure the intracellular pH, as will be discussed later. Upon being taken up by cells, these molecules will be cleaved by intracellular esterases to yield green fluorescent products (fluorochromes). Only cells which have an intact membrane and esterase activity are able to accumulate the fluorescent products. Therefore, these dyes can be used to count viable fungi, bacteria, mycobacteria, and mammalian cells. Propidium iodide is frequently applied as a counterstain to count the dead cells [23,24].

Tetrazolium dyes represent another class of fluorogenic dyes which target the respiration of viable bacteria. They act as electron acceptors and can be reduced by viable cells to their respective formazan products. For example, non-fluorescent redox 2-(p-iodophenyl)-3-(p-nitrophenyl)-5-phenyl tetrazolium chloride (INT) is reduced to fluorescent 2-(p-iodophenyl)-3-(p-nitrophenyl)-5-phenyl tetrazolium chloride-formazan, which is deposited as optically dense, dark red, intracellular aggregates. Tetrazolium reduction can be used to estimate the viability of bacteria cultures [25]. Counterstaining with DAPI for determination of the total count is commonly performed. Formazan deposition may be enhanced by the addition of substrates such as succinate, glucose, and intermediate electron carriers such as phenazine methasulfate [26,27]. It is worth noting that tetrazolium dyes also can be reduced by extracellular inorganic phosphate, at concentrations above 10 mM [27]. Futhermore, some tetrazolium dyes such as 5-cyano-2,3-ditolyl tetrazolium chloride (CTC) have toxic effects on bacteria from natural water samples resulting in an underestimation of the fraction of viable cells [28].

Membrane potential ($\Delta\Psi$) is a sign of living cells. The existence of a membrane potential across eukaryotic cell membranes typically is a consequence of K^+, Na^+, and Cl^- concentration gradients that are maintained by active transport processes. The potential ranges from ~10 to 90 mV for mammalian cells, with the cell interior negative with respect to the exterior. In microorganisms, the membrane potential (100 to 200 mV) is normally generated by energy metabolism, namely the extrusion of H^+ ions by the H^+ATPase or the electron transfer chain. It is believed that only viable cells can maintain a membrane potential. Theoretically, the potential can be estimated from the distribution of lipophilic cationic molecules between cells and the suspending medium according to the Nernst

equation [29]. Fluorescent molecules, which are used to measure membrane potential, include the cationic or zwitterionic styryl dyes, the cationic carbocyanines and rhodamines, the anionic oxonols and hybrid oxonols, and merocyanine 540. Among them, positively charged rhodamine 123 and carbocyanines such as 3,3-dihexyloxacarbocyanine iodide (DiOC$_6$(3)), and the negatively charged bis-(1,3-dibutylbarbituric acid)-trimethine oxonol (DiBAC$_4$(3)) have been used to assess cell viability [1,30]. Cells that have a membrane potential intracellularly accumulate the cationic dyes; anionic dyes are excluded or at least confined to the outer lipoprotein layer of the cytoplasmic membrane unless the membrane potential is collapsed by damage or cell death. Since the fluorescent response of these dyes varies with the magnitude of the membrane potential, viable and dead cells are easily differentiated by their fluorescence characteristics.

Another important parameter associated with cell viability is intracellular pH (pH$_i$). Cells may use this pH gradient as a driving force for various energy-requiring processes such as the uptake of amino acids and sugars, the rotation of flagella, and the synthesis of ATP. Intracellular pH is generally between ~6.8 and 7.4 in the cytosol and ~4.5 and 6.0 in the cell's acidic organelles. Specifically, pH$_i$ in microorganisms exhibits a wide range of values that may vary from 5.6 to 9 [31]. Various studies suggest that the pH$_i$ may provide a good indication of cell viability. For example, it was found that S.cerevisiae cells are capable of maintaining a pH gradient when incubated at low pH (pH 3), whereas non-proliferative cells cannot [32]. Fluorescent probes that have been exploited to measure the pH$_i$ include fluorescein, 5-(and 6-)-carboxyfluorescein (cF), BCECF and its acetoxymethyl esters (BCECF-AMs), pyranine. carboxyseminaphthofluoresceins (cSNARF-1) and carboxysemi-naphthorhodafluors (SNARFs). Their fluorescence intensity is pH-dependant, since the ionization states of the function groups of these fluorescent probes, which are directly relative to the fluorescence of dyes, are affected by the intracellular pH of cells. To quantitatively measure pH, it is essential to match the indicator's pK$_a$ to the pH of the experimental system. Based on their fluorescent property, it is possible to count the living and dead cells, and estimate the cell viability in a population [32].

5.3. Detection Systems Coupled with Fluorescence Labeling Methods

The availability of numerous fluorescent probes provides a vast opportunity for researchers to study the vital functions and status of cells. Microscopes have, since the seventeenth century, been used to examine cells and tissue sections. Fluorescent vital staining makes it convenient to analyze individual cells, both living and dead, under a fluorescence microscope, which is fitted with an appropriate lamp and filters so that the fluorescence of

the cells can be excited and observed. Incident or epi-illumination fluorescence microscopy, often called epifluorescence microscopy, is the most commonly used type of microscopy, since objects may be viewed on opaque surfaces. A microscope can also be equipped with a camera or photodetector, which will then record the fluorescence images of cells in the field of view. The application of epifluorescence microscopy in the assessment of cell viability has been reviewed by Ploem [33]. When a small number of cells are studied, the methods using fluorescence microscopy often give accurate results. These procedures, however, are laborious and time-consuming due to the reason that they are difficult to automate, and it is generally not practical to analyze more than a few hundred cells for a given sample using these methods, when the viability of large amount of cells must be evaluated.

Flow cytometry (FCM) is a technique for making rapid measurements on particles or cells. Since its debut in early 1970s, FCM, associated with the availability of a wide range of fluorescent probes, has been found to be a powerful tool for directly estimating cellular parameters such as nucleic acid content, enzyme activity, calcium flux, membrane potential and intracellular pH [34]. Recently, it has been demonstrated that FCM can be used for the determination of cell viability because it allows rapid analysis of thousands of individual cells in a cell population [34-40]. Figure 5.2 is a diagram illustrating the operational principle and central components of a typical flow cytometry with cell sorting function. Samples are suspended in an aqueous buffer solution and then carried within a fast-flowing fluid stream, called the sheath fluid. The sheath fluid provides the supporting vehicle for directing cells or particles through the laser beam, and usually buffer of a composition that is appropriate to the types of particles being analyzed. For leukocytes or other mammalian cells, phosphate-buffered saline solution is commonly used. Other cells or other particles may have other preferences.

The important feature of flow cytometric analysis is that measurements are made separately on each particle within the suspension in turn and not just as average values for the whole population. As particles pass through the light beam three parameters are measured: forward angle light scatter (FSC), side angle light scatter and fluorescence at selected wavelengths. Light scattering is related approximately to cell mass, structure, surface properties and optical density of the internal medium. Fluorescence is measured to detect either autofluorescence or, more commonly, fluorescent dye labels. As outlined earlier, a variety of fluorescent dyes have been used to estimate the vital status of a cell. Many of these fluorescent dyes and reagents are easily coupled with flow cytometry and often used in combination to produce multiple correlated measures. For example, it is now commonplace in microbiology to assess the viability of bacteria using the combination of nucleic stains PI/
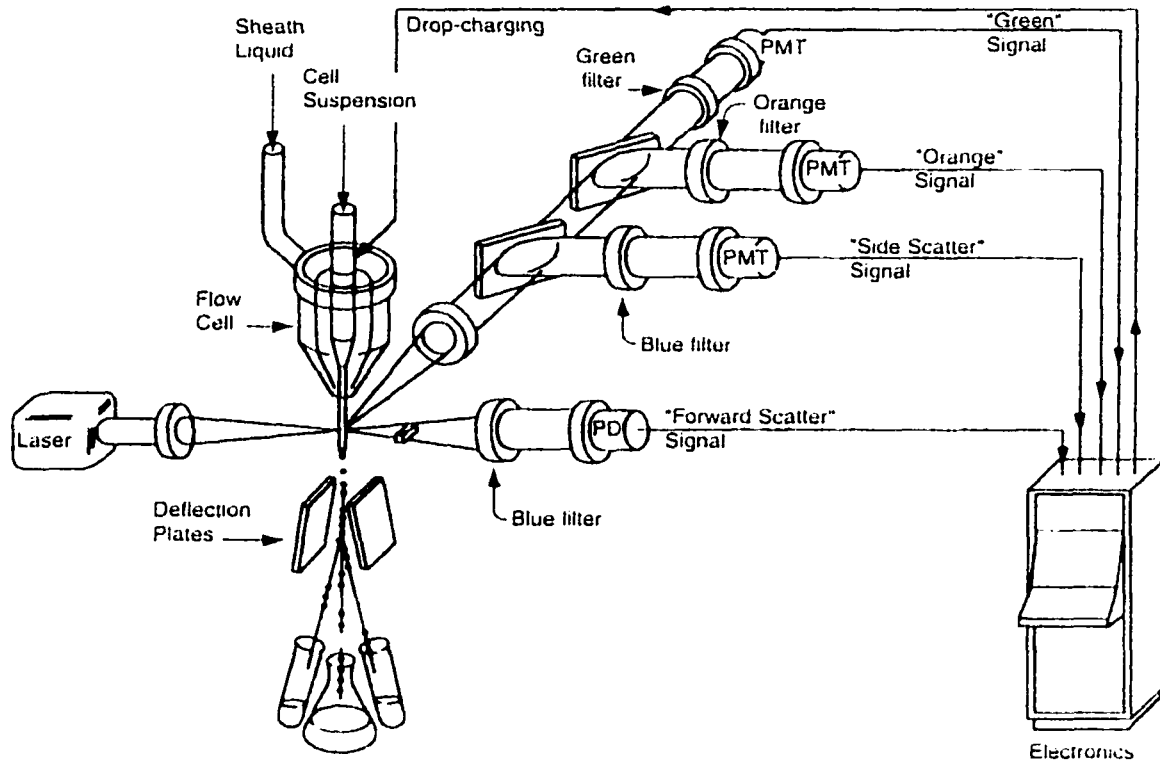
Figure 5.2. Components of a typical flow cytometer with sorting function. This configuration allows the simultaneous measurement of three parameters: forward angle light scatter (FSC), side angle light scatter (SSC) and fluorescence at selected wavelengths. The drop charging, the deflection, and the drops moving into separate test tubes apply only to sorting cytometers and not to benchtop instruments. Adapted from Becton Dickinson Immunocytometry Systems.

SYTO-9 [37]. In this case, dead cells labeled by PI fluoresce red and living cells labeled by SYTO-9 brightly fluoresce green, both dead and living cells in a population are easily differentiated and enumerated with a flow cytometer, thus estimating their viability. Cell sorting flow cytometers are capable of physically selecting (sorting) different cell types, individually, from the bulk population.

Although the use of flow cytometry is becoming widespread, unfortunately, flow cytometers are not simple instruments (see Figure 5.2). As with all sophisticated measuring devices, in addition to possessing a basic knowledge of the underlying principles of operation, it is important to have intensive training and experience so that the significance and accuracy of the results can be assessed. Other disadvantages include lack of ability to differentiate sperm cells from contaminating bacteria or other particles of similar size, and highly expensive instrumentation. All these factors restrict the accessibility of this method. Therefore, a more affordable, accurate and operationally simple method is needed.

5.4. Capillary Electrophoresis

Capillary electrophoresis (CE) is well-known for its high efficiency, high selectivity, high-throughput screening ability, and its simplicity in nature and operation. It has been used to great advantage in the analysis of small molecules, ions, and macromolecules. In recent years, CE has shown increasing potential for the separation and characterization of charged colloidal particles and biological vesicles or cells [41-51]. Recently, Armstrong and co-workers demonstrated that microorganisms could be separated in a manner with extremely high apparent peak efficiencies ($\sim 10^6$-10^{10} theoretical plates per meter) [41-45]. Later, Shintani et al. achieved separations of S. enteritidis from other bacteria using a similar CE method, but with a different polymer [51]. These new developments of CE have made it possible to separate, identify, and quantitate microorganisms in a single run [41-43, 49].

Fluorescence labeling techniques have been used in CE analysis since its inception. The second part of dissertation will attempt to exam the usefulness of CE for the determination of cell viability, when combined with laser induced fluorescence (LIF) detection. Chapter 7 will focus on the separation and simultaneous determination of the viability of bacteria and yeast using CE-LIF techniques, while Chapter 8 will extend the application of CE-LIF to the evaluation of the potency of animal sperm cells.

6.4.1. Basis for Electrophoretic Separations

Electrophoresis is the migration of ions or charged particles in solution under the influence of an electric field. Capillary electrophoresis is actually a miniaturized format of traditional electrophoresis. One key feature of CE is the overall simplicity of the instrumentation. A schematic of a typical CE instrument is shown in Figure 5.3. Experiments are carried out in a buffer-filled fused-silica capillary that is typically 10 to 100 μm in inner diameter and 40 to 100 cm in length. Both ends of the capillary are immersed in running buffer reservoirs that also hold two platinum electrodes. The solution content of the reservoirs is identical to that within the capillary. The sample can be introduced into one end of the tubing by applying a hydrodynamic height, an electrical field or external pressure. A DC electric field, generally 100-500 V/cm, is applied between the two electrodes throughout the experiments. Optical detection can be made at the opposite end, directly through the capillary wall.

Electrophoretic separations are achieved as a result of the unequal rate of migration of different solutes under the influence of the externally applied electric field. The migration velocity v of a charged particle, in centimeters per second, in an electric field is determined by the external field strength E (V/cm) and the electrophoretic mobility μ (cm^2/Vs) of the particle. That is

$$v = \mu E \qquad (5.1)$$

The electric field is simply a function of the applied voltage and capillary length. The electrophoretic mobility, μ, for a given ion and medium, is a constant which is characteristic of the ion. It is defined as the steady-state velocity per unit field strength, or, from Eq. (5.2),

$$\mu = q / f \qquad (5.2)$$

where q = the net charge of an ion and f = the transitional friction coefficient. For a spherical particle, f is governed by Stoke's Law as

$$f = 6\pi\eta r \qquad (5.3)$$

where η = the viscosity of the surrounding medium and r = the radius of an ion. From equation (5.2), it is clear that the differences in the electrophoretic mobility of ions can arise
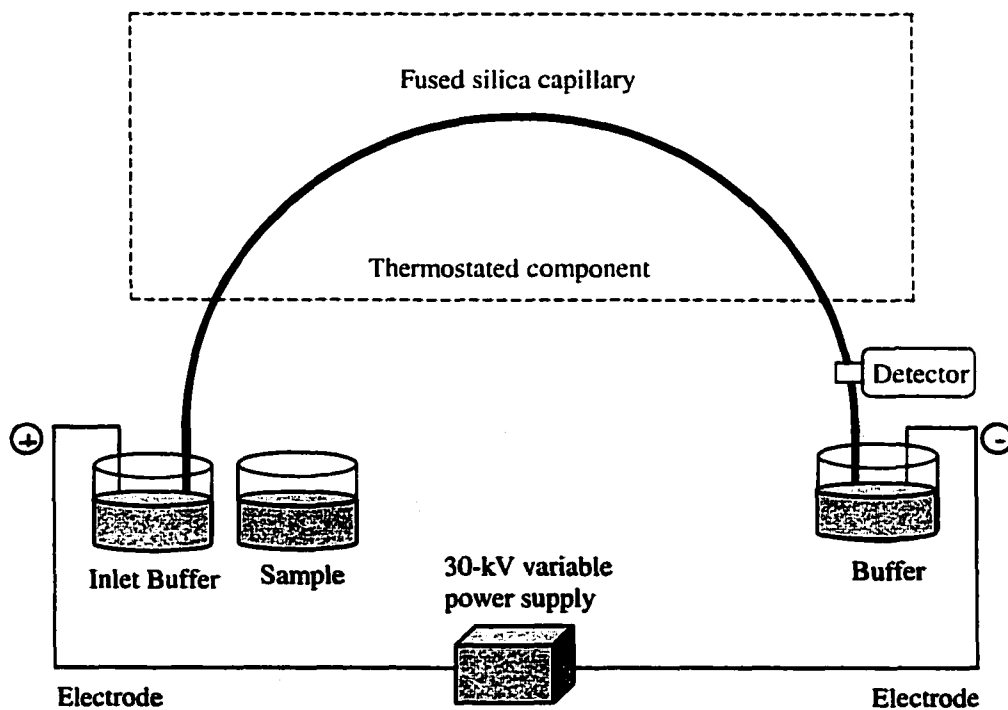
Figure 5.3. Basic schematic of a typical capillary electrophoresis instrument.

as a result of differences in frictional properties, i.e., size or shape, or as a result of differences in the net charge on the ion. These differences in the properties of ions constitute the basis for the selectivity in CE separations.

A fundamental constituent of CE operation is the existence of electroosmotic, or electroendosmotic flow (EOF). EOF is the bulk flow of liquid in the capillary, and is a consequence of the surface charge, known as the zeta potential (ζ), on the interior capillary wall. The magnitude of the EOF is generally greater than the electrophoretic migration velocities of the individual charged species, therefore the EOF effectively becomes the driving force of CE and carries all solutes towards the detector. EOF controls the migration time of solutes by superposition of its flow with the solute mobility, but it does not affect selectivity. In the presence of EOF, the measured mobility of an ion is called the apparent mobility, μ_{app}, and is the sum of the effective mobility of the ion, μ_{eff}, and the mobility of EOF, μ_{EOF}. Thus,

$$\mu_{app} = \mu_{eff} + \mu_{EOF} \tag{5.4}$$

Both μ_{app} and μ_{EOF} can be experimentally measured, and are determined by Eq. 5.5 and 5.6, respectively.

$$\mu_{app} = L_d L_t / t V \tag{5.5}$$

$$\mu_{app} = L_d L_t / t_{neutral} V \tag{5.6}$$

where L_d is the length of capillary from injection to the detector, L_t is the total length of the capillary from end to end, V is the voltage applied between the two ends, t is the time required for an ion to migrate from the injection end to the detector, and $t_{neutral}$ is the migration time of a neutral marker, which can produce signal (UV absorption or fluorescence) on the detector. Based on equation 6.4-6.6, μ_{eff}, can be easily calculated as

$$\mu_{eff} = \mu_{app} - \mu_{EOF} = L_d L_t / V (1/t - 1/t_{neutral}) \tag{5.7}$$

6.4.2. Charge at Cell Surfaces

Nearly all particles in suspension exhibit a surface charge independent of their chemical nature. They acquire their surface charge either by adsorption (e.g., solid particles, air bubbles, oil droplets) or by the ionization of surface charged groups; in some systems

both these mechanisms may be operative [52]. The net charge on the cell surfaces of almost all microorganisms as well as eukaryotic cells are negative (anionic) at physiological pH as demonstrated by particle electrophoresis and interaction with cationic molecules [53]. The negative charges are mainly due to the ionization of phosphate, carboxylate, and, less commonly, sulfate groups of various polymers on cell walls. The surface charge density and composition of the cell surface polymers are influenced mainly by the cell type, and also by other several factors, such as growth stage and growth conditions [45].

An electrical double layer is formed (as a result of the build-up of counterions near the cell surface) which maintains the charge balance. The widely accepted structure of the electrical double layer is illustrated in Figure 5.4. The space above the cell surface can be roughly divided into two regions, namely, the Stern layer and the diffuse layer (Figure 5.4A). In the Stern layer the ions from surrounding solution closely contact with the cell surface, due to specific chemical adsorption or localized electrostatic interaction. Across this layer (~0.5 nm thick), there is a linear drop in potential (ψ) (Figure 5.4B). In the diffuse region, thermal agitation permits free movement of ions and the distribution of ions is not uniform. The potential decreases exponentially across this region (Figure 5.4B). The ζ-potential is the electrokinetic potential expressed at the outer perimeter of the Stern layer, the plane of shear at which the phases move relative to one another on the application of an electric field. It must be noted that the ζ-potential is different from the Nernst potential which exists between the bulk of a solid particle and the bulk of solution, and it is different from the membrane potential across a selectively permeable membrane separating electrolyte solutions of different concentration. The migration of a cell in a solution does not depend on the true surface charge of the cell, expressed as a sum of all the ionized function groups and absorbed ions, but the zeta potential as described by the Smoluchowki equation (Eq.5.8).

$$\mu = \epsilon\zeta / \eta = \epsilon_r\epsilon_0\zeta / \eta \qquad (5.8)$$

where ϵ = the permittivity (or dielectric constant) of the suspension medium, ϵ_r = the permittivity of vacuum, and ϵ_0 = the relative permittivity of the suspension medium. The Smoluchowki equation is valid for a spherical particle or cylindrical particle.

Many experimental conditions, such as the ionic strength of the running buffer, the type of buffer system, pH, and composition of buffer solution, etc., have important effects on the ζ-potentials at the surfaces of both cells and inner capillary wall. Therefore, it is important to carefully control these conditions in order to obtain successful CE separations.

Only under certain specific conditions will the differences in charge characteristics of different cells allow them to be separated from each other using CE [42,47,49,51].
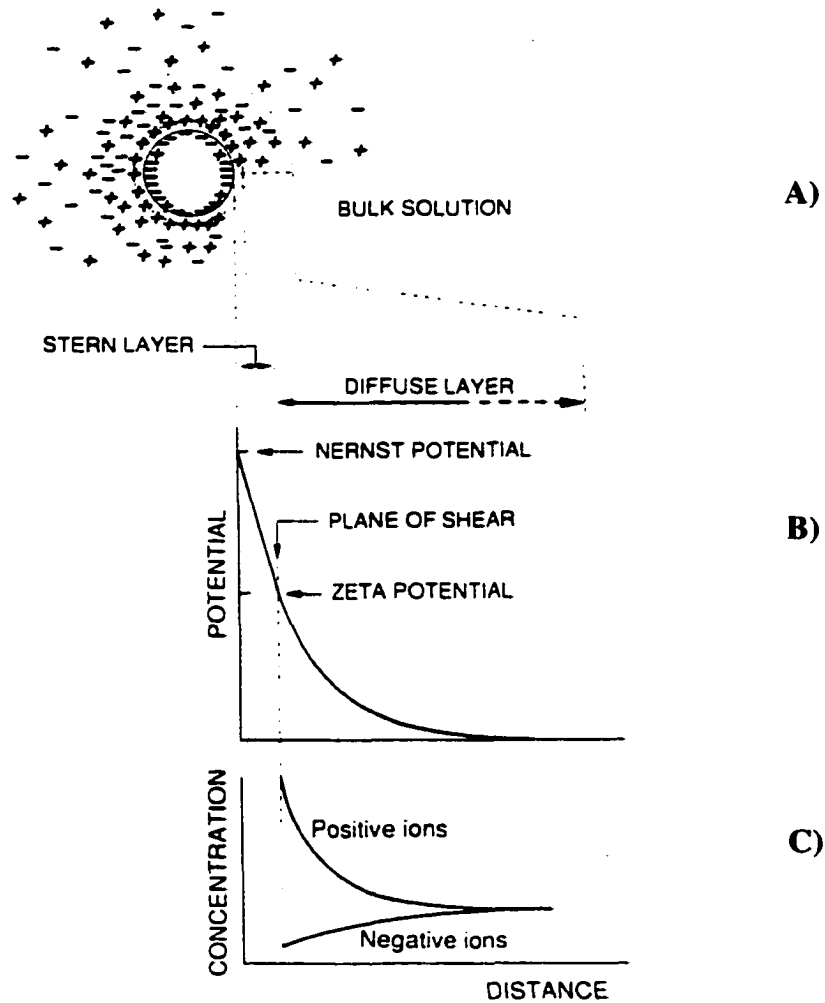
Figure 5.4. Possible structure of the double layer on a solid-electrolyte interface (A). B) shows the variation of the potential across the Stern layer in close contact with the surface and the diffuse layer extending into the liquid phase; C) shows the variation of the concentration of cations and anions across the diffuse layer. Taken from ref. 52.

REFERENCES

1. Breeuwer, P.; Abee, T. *Intl. J. Food Microbiol.* **2000**, 55, 193-200.

2. Kell, D.B.; Kaprelyants, A.S.; Weichart, D.H.; Harwood, C.R.; Barer, M.R. *Antonie Van Leeuwenhoek*, **1998**, 73, 169-187.

3. Postgate, J.R. In: *Methods in Microbiology* (Norris, J.R.; Ribbons, D. W., eds.), vo.1. Academic Press, London, **1969**, pp. 611-628.

4. Roszak, D.B.; Colwell, R.R. Microbiol. Reviews 1987, 51, 365-379

5. McFeters, G.A.; Yu, F.P.; Pyle, B.H.; Stewart, P.S. *J. Microbiol. Methods* **1995**, 21, 1-13.

6. Lloyd, D.; Hayes, A.J. *FEMS Microbiol. Letts* **1995**, 133, 1-7.

7. Bearden, H.J.; Fuquay, J.W. *Applied Animal Reproduction*, 5th ed.; Prentice Hall: Upper Saddle River, NJ, **2000**; p 151.

8. Prescott, L.M.; Harley, J.P.; Klein, D.A., *Microbiology*, 3 rd ed., Wm. C. Brown Publishers, Dubuque, IA, **1996**, pp. 118-124.

9. Francisco, D.E.; Mah, R.A.; Rabin, A.C. *Trans. Am. Microsc. Soc.* **1973**, 92, 416-421.

10. Calcott, P.H.; Postage, J.R. *J. Gen. Microbiol.* **1972**, 70, 115-122.

11. Seiburth, J.M. *Exp. Mar. Bio. Eol.* **1967**, 1, 98-121.

12. Collins, V.G.; Kipling, C. *J Appl. Bacteriol.* **1957**, 20, 257-264.

13. Brock, T.B.; Broack, M.L. *Nature (London)* **1966**, 209,734-736.

14. Tabor, P.S.; Neihof, R.A. *Appl. Environ. Microbiol.* **1982**, 44, 945-953.

15. Fliermans, C.B.; Schmidt, E.L. *Appl. Microbiol.* **1975**, 30, 676-684.

16. Jones, K.L.; Rhodes-Roberts, M.E. *J. Appl. Bacterol.* **1981**, 50, 247-258.

17. Meyer-Reil, L. *Appl. Environ. Microbiol.* **1978**, 36, 506-512.

18. Kogure, K.; Simidu, U.; Taga, N. *Can. J. Microbiol.* **1979**, 25, 415-420.

19. Kogure, K.; Simidu, U.; Taga, N. *Can. J. Microbiol.* **1980**, 26, 318-323.

20. Haugland, R.P. Chapter 15 in *Handbook of Fluorescent Probes and Research Chemicals*, 8th ed., Molecular Probes, Eugene, OR.

21. Korgaonkar, K.S.; and Ranade, S.S. *Can. J. Microbiol.* **1966**, 12, 185-190.

22. Hobbie, J.E.; Daley, R.J.; Jasper, S. *Appl. Environ. Microbiol.* **1977**, 33, 1225-1228.

23. Humphreys, M.J.; Allman, R.; Lloyd, D.; *Cytometry* **1994**, 15, 343-348.

24. Yamaguchi, N.; Nasu, M. *J. Appl. Microbiol.* **1997**,83,43-5.

25. Zimmerman, R.; Iturriaga, R.; Becker-Birck, J. *Appl. Environ. Microbiol.* **1978**, 36, 926-935.

26. Vistica, D.T.; Shekan, P.; Scudiero, D.C.A.; Monks, A.; Pittman, A.; Boyd, M.R. *Cancer Res.* **1991**, 51, 2510-2520.

27. Smith, J.J.; McFeters, G.A. *J. Appl. Microbiol.* **1996**, 80, 209-215.

28. Bartscht, K.; Cypionka, H.; Overmann, J. FEMS Microbiol. Ecol. 1999, 28, 249-259.

29. Shapiro, H.M. In: *Methods in Cell Biology* (Darzynkiewicz, Z.; Crissman, H.A., Eds), vo. 33, Academic Press, London, **1990**, pp. 25-35.

30. Mason, D.J.; Lopez-Amoros, R.; Allman, R.; Stark, J.M.; Lyoyd, D. *J. Applied Bacteriol.* 1995, 78, 309-315.

31. Booth, I.R. *Microbiol. Rev.* **1991**, 49, 359-378.

32. Imai, T.; Ohno, T. *Appl. Environ. Microbiol.* **1995**, 61,3604-3608.

33. Ploem, J.S. In: *Fluorescent and Luminescent Probes for Biological Activity* (Mason, W.T., Ed.), Academic Press, London, **1993**, pp1-11.

34. Gilvan, A.L. *Flow Cytometry: First Principles* (2nd ed.), Wiley-Liss, New York; Chichester, **2001**.

35. Prudencio, C.; Sansonetty, F.; Corte-Real, M. *Cytometry* **1998**, 31, 307-313.

36. Deere, D.; Shen, J.; Vesy, G.; Bell, P.; Bissinger, P.; Veal, D. *Yeast* **1998**, 14, 147-160.

37. Deere, D.; Porter, J.; Pickup, R.; Edwards, C. *J. Fish. Dis.* **1996**, 19, 459-467.

38. Garner, D.L.; Johnson, L.A.; Yue, S.T.; Roth, B.L.; Haugland, R.P. *J. Androl.* **1994**, 16, 620-629.

39. Garner, D.L.; Johnson, L.A. *Biol. Reprod.* **1995**, 53, 276-284.

40. Donoghue, A.M.; Garner, D.L.; Donoghue, D.J.; Johnson, L.A. *Poult. Sci.* **1995**, 1191-1200.

41. Armstrong, D.W.; Schneiderheinze, J.M.; Kullman, J.P.; He, L. *FEMS Microbiol. Lett.* **2001**, 194, 33-37.

42. Armstrong, D.W.; Schulte, G.; Schneiderheinze, J.M.; Westenberg, D.J. *Anal.Chem.* **1999**, *71*, 5465-5469.

43. Armstrong, D.W.; Schneiderheinze, J.M. *Anal. Chem.* **2000**, 72, 4474-4476.

44. Schneiderheinze, J.M.; Armstrong, D.W.; Schulte, G.; Westenberg, D.J. *FEMS Microbiol. Lett.* **2000**, *189*, 39-44.

45. Torimura, M.; Ito, S.; Kano, K.; Ikeda, T.; Esaka, Y.; Ueda, T. *J. Chromatogr. B*, **1999**, 721, 31-37.

46. Radko, S. P.; Chrambach, A. *J. Chromatogr. B*, **1999**, 722, 1-10.

47. Kenndler, E.; Blass, D. *Trends in Anal. Chem.* **2001**, 20, 543-551.

48. Van Der Mei, H.C.; Busscher, H. J. *Appl. Environ. Microbiol.* **2001**, 67, 491-494.

49. Ebersole, R.C.; McCormick, R.M. *Bio/Technology* **1993**, 11, 1278-1282.

50. Shen, Y.; Berger, S.J.; Smith, R.D. *Anal. Chem.* **2000**, 72, 4603-4607.

51. Shitani, T.; Yamada, K.; Torimura, M. *FEMS Microbiol. Lett.* **2002**, 210, 245-249.

52. James, A.M. In: *Microbial Cell Surface Analysis* (Mozes, N.; Handley, P.S.; Busscher, H.j.; Rouxhet, P.G., Eds), VCH Publishers, New York, **1991**, Chapter 9, pp. 221-261.

53. Hancock, I.C. In: *Microbial Cell Surface Analysis* (Mozes, N.; Handley, P.S.; Busscher, H.j.; Rouxhet, P.G., Eds), VCH Publishers, New York, **1991**, Chapter 2, pp. 21-59.

CHAPTER 6

DETERMINATION OF CELL VIABILITY IN SINGLE OR MIXED SAMPLES USING CAPILLARY ELECTROPHORESIS LASER-INDUCED FLUORESCENCE MICROFLUIDIC SYSTEMS

Daniel W. Armstrong and Lingfeng He

ABSTRACT

The advent of high-efficiency microbial separations will have a profound effect on both chemistry and microbiology. For the first time, it appears that it may be possible to obtain qualitative and quantitative information on microbial systems with the accuracy, precision, speed, and throughput that currently is found for chemical systems. Recently it was suggested that an analytical separations-based approach for determining the viability of cells would be advantageous. The feasibility of such an approach is demonstrated using CE-LIF of two bacteria and yeast. The analytical procedures and figures of merit are outlined. High-throughput analyses and evaluation of microorganisms now appear to be possible.

6.1. INTRODUCTION

Modern instrumentation for chemical analysis has been used by many research groups to examine microorganisms [1-9]. Most often, the goal was to identify or otherwise characterize a microorganism. These efforts have been met with varying degrees of success. It is not surprising that positive instrumental responses occur since microorganisms consist of a great variety of chemical compounds. However, using these instrumental responses to identify or characterize microbes with a high degree of certainty has been problematic. When the molecular components are used to identify a cell, at least three problems must be overcome: (i) each cell usually contains a tremendous number and variety of compounds, (ii) many (most) of the compounds in different cells are similar (sometimes identical), and (iii) the differences in the type and proportion of compounds that do exist in various cells are often no more than the variation found in a single cell type at different times during its life/growth cycle or due to environmental factors. Of course, the main exception to this is that each species has a characteristic DNA sequence that always can be used to identify it [4]. That type of experiment takes us out of the realm of simple, rapid, and general instrumentation methods for direct cell analysis, however.

Approaches for the analysis and characterization of intact microorganisms using electrokinetic-based separations, appear to have promise [10-15]. Most colloidal particles have a surface charge that originates from the ionization of surface molecules, the adsorption of ions from solution, or both. Early on it was recognized that colloidal size particles would move in a direct current electric field. Microorganisms such as bacteria, viruses, and fungi are no different. They have membranes and cell walls containing protein, lipopolysaccharides, lipid molecules, teichoic acid, etc., which give them a characteristic charge. This charge can vary with pH, solution composition, ionic strength, and even temperature. Formerly, zone electrophoresis was utilized to determine the surface charge and help characterize microorganisms [16,17]. Reports on the capillary electrophoresis of cells include the similar movement of a virus and bacteria with the CE-EOF [18,19] and the broadband separation of bacteria/bacterial aggregates from one another [20,21]. Recently, rapid, high-efficiency separations for bacteria [10,13-15], fungi [10,13], and viruses [11,12], have been reported. Capillary isoelectric focusing also has been shown to be an effective approach for analyzing microbes [10,22,23]. It was demonstrated that microorganisms could be easily separated, identified, and quantitated in the same high-efficiency manner that we do molecules [10]. This was shown for single microorganisms and mixtures. Analyses can be done in complex matrixes including various consumer products [15] and biological fluids [13]. Most recently, it has been pointed out that, under appropriate conditions, cell viability

(i.e., percent live and percent dead cells) also can be determined in a CE or microfluidic experiment [15]. In this work, we examine the use of CE to evaluate cell viability, and determine the analytical figures of merit for this process.

6.2. EXPERIMENTAL SECTION

6.2.1. Materials

Tris(hydroxymethyl)aminomethane (TRIS), boric acid, disodium ethylenediamine-tetraacetate (EDTA), and poly(ethylene) oxide (PEO; Mn = 600 000) were purchased from Aldrich (Milwaukee, WI). Yeast extract, peptone, and nutrient broth were obtained from Difco Laboratories (Franklin Lakes, NJ). Dextrose was a product of J.T. Baker Chemical Co. (Phillipsburg, NJ). LIVE/DEAD BacLight Bacterial Viability kit and LIVE/DEAD Yeast Viability kit were purchased from Molecular Probes, Inc. (Eugene, OR). A LIVE/DEAD BacLight Bacterial Viability kit consists of SYTO 9 green fluorescent nucleic acid stain (3.34 mM) and red fluorescent nucleic acid stain, propidium iodide (20 mM). Both were dissolved separately in methyl sulfoxide (DMSO). The LIVE/DEAD Yeast Viability kit contains FUN-1 stain (10 mM), which was dissolved in DMSO. The structures of these fluorescent dyes/probes are shown in Figure 6.1. All reagents were directly used without further purification.

Band-pass filters, 505 ± 10, 510 ± 10, 610 ± 10, and 670 ± 10 nm, were obtained from Edmund Industrial Optics (Barrington, NJ). The 510 ± 15 and 630 ± 15 nm band-pass filters and 600-nm long-pass filters were purchased from Omega Optical, Inc. (Brattleboro, VT). The 520 ± 20-nm band-pass filter and 663-nm long-pass filters were obtained from Beckman Coulter, Inc. (Fullerton, CA).

6.2.2. Methods

6.2.2.1. *Capillary Electrophoresis.*

A stock buffer solution containing 4.5 mM Tris, 4.5 mM boric acid, and 0.1 mM EDTA (TBE buffer) was prepared by dissolving the appropriate amount of each reagent in filtered deionized water yielding a buffer of pH 8.4. This buffer solution was then diluted 8-fold with deionized water. A 0.2-g sample of PEO was added to 40 mL of this diluted buffer
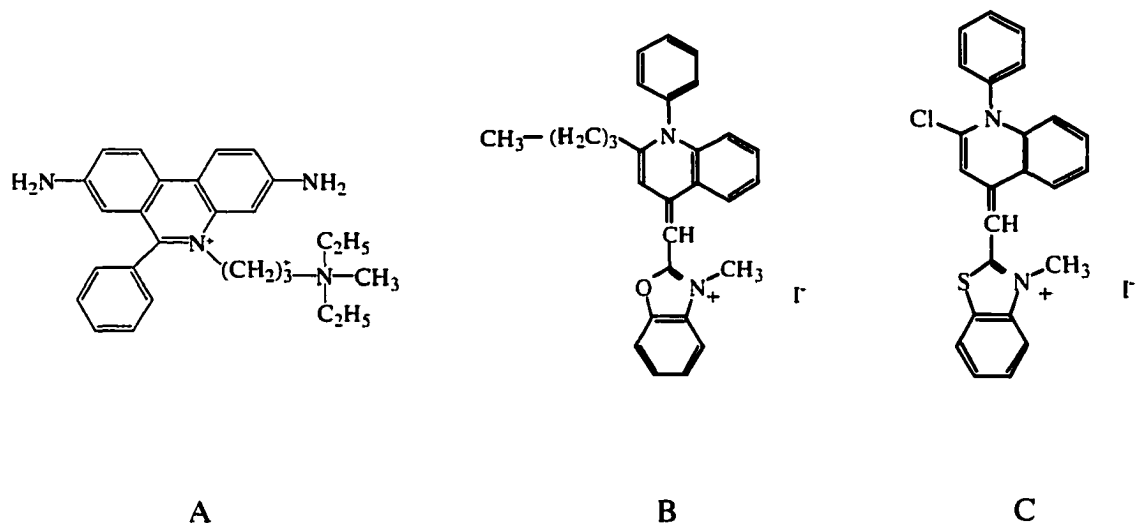
Figure 6.1. Structure of the fluorescent "probe molecules" used in this viability study. (A) propidium iodide, (B) SYTO 9, and (C) FUN-1. The structure for SYTO 9 was deduced from the data in refs 36 and 37. Note that there are resonance structures for both (B) and (C) in which the 1-phenylquinoline group is the charged quaternary amine (rather than the oxazol or oxathiazol group).

solution and the resultant mixture stirred overnight at room temperature to give a polymer solution with a concentration of 0.5%. The CE running buffer solution was prepared by diluting the stock polymer solution with diluted TBE buffer solution to a final polymer concentration of 0.025%. As indicated previously, the dilute solution of PEO has a dramatic effect on the separation of colloidal size microorganisms [10]. It greatly increases their migration times and enhances efficiency. Comparable separations can sometimes be achieved without PEO by doing capillary isoelectric focusing with a coated capillary [10,22,23]. The mechanism of the CE/PEO/microorganism separation currently is under investigation.

The CE separations were performed on a Beckman Coulter P/ACE MDQ capillary electrophoresis system equipped with a 488-nm laser-induced fluorescence (LIF) detector. Untreated fused-silica capillary with a 100-m i.d. was purchased from Polymicro Technologies, Inc. (Phoenix, AZ). The capillary used for the separations was 30 cm in length (20 cm to detection window). When a capillary was first used, it was rinsed for 0.5 min with water, 5 min with 1 N NaOH, and 0.5 min with water. Five preliminary runs should be made in order to obtain highly reproducible electropherograms. Prior to each injection, the capillary was washed for 0.5 min with water, 0.2 min with 1 N NaOH, and 0.5 min with water, followed by 2 min with running buffer. The running buffer was changed between each run. Separations were performed at 15 kV and a temperature of 25 °C. The green and red fluorescent light was monitored simultaneously with a LIF detector, which was equipped with a proper green light filter and red light filter. Data were collected by P/ACE system MDQ software.

6.2.2.2. Microorganisms.

Milk-free *acidophilus* distributed by Schiff Products, Inc. (Salt Lake City, UT) and Solaray brand BabyLife manufactured by Nutraceutical Corp. for Solaray, Inc. (Park City, UT) are dietary supplements containing *Lactobacillus acidophilus* and *Bifidobacterium infantis*, respectively. Both were purchased from a local nutrition store. *Saccharomyces cerevisiae* (baker's yeast), purchased as freeze-dried cells from Wal-Mart, was a product of Hodgson Mill, Inc. (Effingham, IL). Fresh cultures of *L. acidophilus*, *B. infantis*, and yeast were grown in-house. The cells from the Schiff tablet and BabyLife powder were allowed to grow in nutrient broth at 37 °C on a shaker at 600 rpm for 16-20 h. The starting culture of baker's yeast was transferred from solid agar to YPD medium (10 g of yeast extract, 20 g of peptone, and 20 g of dextrose/L) and grown at 30 °C on a shaker at 300 rpm for 12-15 h. Samples from cultures were obtained by removing 4-6 mL of the liquid culture and pelleting the cells in a centrifuge (Fisher model 228, Pittsburgh, PA) at 3400 rpm. The supernatant was

decanted, and the cells were washed with 3-4 mL of CE running buffer and pelleted again. After another wash, the cells were dispersed in CE running buffer. The cell concentration was determined from the optical density of the solution at 670 nm with an UV/visible spectrophotometer (model U-2000, Hitachi Instruments, Inc.). The *L. acidophilus* suspension was adjusted to ~0.250 OD_{670} (~3 × 10^7 cells/mL), B. infantis suspension to ~0.350 OD_{670} (~4.0 × 10^7 cells/mL), and baker's yeast suspension to ~1.00 OD_{670} (~10^7 cells/mL). The viabilities of fresh cultures of three microbes were checked with flow cytometry (Beckman Coulter Epics XL-MCL), which showed that over 90% of the cells of fresh cultures in solution were live. Dead cells of *L. acidophilus* and *B. infantis* were obtained by suspending cells in acetone at -20 °C overnight (~10 h), then washing twice with running buffer to remove residue acetone, and resuspending in running buffer.

6.2.2.3. *Fixation of S. cerevisiae.*

To find the proper fixation method for baker's yeast cells, five different approaches were evaluated: (a) the yeast culture in YPD media solution was fixed at 80 °C for 5 min and then cooled and stored immediately in an ice bath until use; (b) the yeast culture was suspended in HPLC grade acetone (Fisher Scientific Co., Hanover Park, IL) and stored at -20 °C overnight; (c) after washing the yeast with distilled water and removing the water, the yeast culture was stored at 80 °C overnight; (d) the yeast culture was suspended in distilled water and stored at 80 °C overnight; (e) the yeast culture was dispersed in 40% formaldehyde, which was diluted from methanol-free 16% formaldehyde solution (Polysciences, Inc., Warrington, PA), and stored at room temperature overnight. After being fixed, the baker's yeast samples were washed and resuspended in CE running buffer. The cell concentrations were adjusted to ~2.6 × 10^6 cells/mL. A 4-mL suspension was stained using 1 μL of 20 mM propidium iodide and incubated in the dark for 40 min. The fluorescence intensity of the solution was measured with a LS 50B luminescence spectrometer (Perkin-Elmer Instruments, Inc., Norwalk, CT). A formaldehyde-fixed yeast sample that was not stained with propidium iodide was used as a blank.

6.2.2.4. *Saturation of L. acidophilus Cells with Green and Red Dyes.*

The 3.0-mL aliquots of fixed *L. acidophilus* cell suspension (~10^7 cells/mL) were stained with ` different amounts of green or red dyes. Solutions were incubated in the dark for 15 min. Generally, SYTO 9 stain labels all bacteria in a population, i.e., those with intact membranes and those with damaged membranes. In contrast, propidium iodide only penetrates bacteria with damaged membranes. It quenches the green fluorescence of SYTO 9

and replaces it with its own red fluorescence. Thus, live bacteria with intact cell membranes stain fluoresce green, whereas dead bacteria with compromised membranes stain fluoresce red. Samples were injected for 10 s at 0.5 psi and measured 3-6 times. A 520-nm band-pass filter and 663-nm long-pass filter were the green light filter and red light filter, respectively, unless noted otherwise. Both of these dyes bind to the nucleic acid material (RNA, DNA) in cells. Their fluorescence is enhanced upon binding.

6.2.2.5. Evaluation of Filters.

L. acidophilus was the microorganism used to evaluate different combinations of green light and red light filters. Fifty microliters of stock L. acidophilus suspension was diluted to 3.0 *m*L with running buffer and then stained with 0.5 μL of SYTO 9 green dye or propidium iodide red dye. Solutions were incubated in the dark for 15 min. The red light filter was fixed at the 663-nm long-pass filter, while the green filters were studied. In this case, *L. acidophilus* cells were only stained with SYTO 9 green dye. When the red light filters were evaluated, the 520-nm band-pass filter was the green light filter. In this case, killed cells were used and only stained with propidium iodide. Samples were injected for 10 s at 0.5 psi. Each filter combination was measure up to 8 times.

6.2.2.6. Separation of Mixtures of Microorganisms.

The Schiff tablets, BabyLife powder, and freeze-dried baker's yeast were used to make up the microbial mixture. All three samples were suspended in the CE running buffer with proper cell concentrations. Fifty microliters of each microorganism solution was diluted to 3.0 *m*L with CE running buffer and stained separately with a 1-μL mixture of green and red dyes (1:1, v/v). Solutions of Schiff tablets and BabyLife powder were incubated in the dark for 15 min while baker's yeast suspension was incubated in the dark for 40 min and then mixed together right before injection. The mixture was injected for 10 s at 0.5 psi. A 520-nm band-pass filter and 663-nm long-pass filter were used to monitor the green light and red light, respectively. The viability of individual microorganism solutions also was measured with flow cytometry.

6.2.2.7. Calibration Curves of Microorganisms.

To achieve various proportions of live/dead cells for each microbe, six different proportions of fresh and properly fixed cell suspensions with a total volume of 50 μL were mixed and diluted to 3.0 *m*L. Therefore, the ratios of live/dead cells in solution were 0:100,

20:80, 40:60, 60:40, 80:20, and 100:0. All cells were stained with 1 μL of a mixture of green and red dyes (1:1, v/v). In a separate experiment, yeast cells were labeled with 1 μL of FUN-1 stain. After the FUN-1 stain was added to the yeast solution, the sample was mixed thoroughly and incubated at 30 °C in the dark for 30 min. When loaded with FUN-1 stain, dead yeast cells exhibit extremely bright, diffuse, green-yellow fluorescence, while metabolically active cells were marked with distinct orange-red fluorescence when observed under the fluorescence microscope. Each sample was injected for 10 s at 0.5 psi and measured 3-6 times. A 520-nm band-pass filter and 663-nm long-pass filter were the green light filter and red light filter, respectively. The calibration curves were obtained by plotting ratios of green to red fluorescent intensities versus the ratios of live to dead cells that were prepared.

6.2.2.8. *Flow Cytometry.*

Before flow cytometry measurement, samples used for CE analysis were diluted 100 times, then stained with 1 μL mixture of SYTO 9 and propidium iodide (1:1, v/v) from the LIVE/DEAD Bacterial Viability kit, following the same staining procedures as that for CE. Quantitative data on the fluorescent stained microorganism suspensions were collected with an Epics XL-MCL (Beckman-Coulter Corp., Miami, FL). Epics XL-MCL uses an air-cooled argon ion laser emitting at 488 nm. Gates were set for the side and forward light scatter perimeters so that only those cells possessing the light scatter characteristics were analyzed for fluorescence intensity. The green fluorescence that passed through a 525-nm band-pass filter was collected as the log of green fluorescence. The red fluorescence was collected through 675-nm band-pass filter as a log function. Compensation (15%) was used to minimize spillover of green fluorescence into the 675-nm red channel. The generated data were then analyzed for the relative fluorescence of the log red and log green using Beckman-Coulter System V version 3.0 program.

6.3. RESULTS AND DISCUSSION

The determination of cell viability (i.e., the percent live vs. percent dead cells in a sample) is a very important, albeit often labor-intensive process. Some techniques can be fairly subjective, and others have quantitative limitations. Direct animal testing of pathogens is a case in point [24]. If the animal comes down with the pathogen-caused disease, then it can be assumed that there were living cells in the sample and vice versa. For many years, the benchmark technique for the determination of cell viability has been the plate count method

[25,26]. In this case, a well-dispersed, diluted sample of cells is spread over a solid agar surface. Ideally, each microorganism or group of microorganisms develops into a distinct colony that can be counted. Despite being slow and labor intensive, only the viable microorganisms in a sample can be estimated [24,25]. Radiochemical techniques, such as ^{51}Cr-release assays [27,28] have fallen out of favor for several reasons including cost and hazard concerns. The use of selective colorimetric or fluorescent dyes for viability studies has grown tremendously [25,26,29-31]. Specific dyes can selectively associate with or be excluded from live and/or dead cells. For example, trypan blue stains nonviable cells with compromised membranes but does not stain viable cells [32,33]. There are a variety of fluorescent nucleic acid and membrane-based dyes. They can be used alone or in specific combinations to help assess cell viability [25-32]. After the chosen staining procedure is completed, the individual cells must be counted via microscopy [33,34] or with an instrument such as a flow cytometer [35]. There are errors, advantages, and disadvantages associated with virtually every staining and counting procedure [23-35]. A fluorescence microscope (which can be as expensive as a high-end CE instrument) can be used in a labor-intensive procedure, requiring extensive manual manipulation and optimal dilutions of each sample. Problems can include nonuniform distribution of cells, cell adhesion to surfaces, ambiguous staining of some cells, overlapping cells, and so on. The flow cytometer tends to be the most expensive instrument used for viability studies. After pretreatment, the cells are evaluated one at a time. The cells are usually categorized as viable, nonviable, or ambiguous. The boundaries for each of these categories are not always straightforward [35]. We have found that CE with LIF detection offers advantages of speed, sensitivity, efficiency, automation, and overall effectiveness for determining cell viability. This approach is now possible because of recent advances in high-efficiency microbial separations [10-15].

Both the chemical properties and biological disposition of the dye/stain/probe molecule must be considered if it is to be properly utilized to produce optimum results. Typically, the stain/dye/probe molecules used in microbial studies will selectively associate either with the membrane or nucleic acids or various organelles within the cell [25-34]. Some molecules are taken up by both live and dead cells. Other molecules, such as trypan blue, ethidium bromide, and propidium iodide, are excluded from live cells and only stain dead cells with compromised membranes. We have evaluated two different dye combinations for the CE determination of microbial viability. SYTO 9 is an unsymmetrical cyanine dye that acts as a nucleic acid stain for both live and dead cells (Figure 6.1). Its green fluorescence is enhanced ~1000 times upon nucleic acid binding. Propidium iodide (Figure 6.1) is a red fluorescent nucleic acid dye that is excluded from live cells. Upon binding with DNA, its fluorescence is enhanced ~40-fold. In addition, it quenches fluorescence from SYTO 9.

FUN-1 is another unsymmetrical cyanine dye used mainly for yeast and fungi analyses. It has exceptional membrane permeability (for both live and dead cells). It gives the fungi's cytoplasm a diffuse green fluorescence. However, living cells process this dye into distinct compact vacuolar structures which then exhibit red fluorescence. This process takes ~30 min in live cells and is accompanied by a corresponding decrease of the original green fluorescence. Obviously this process cannot occur in dead cells that maintain a green fluorescence.

The fluorescence spectra of nucleic acid-bound SYTO 9, propidium iodide, and the free and vacuolar FUN-1 are shown in Figure 6.2. It is clear from these spectra that although each dye or dye form produces a distinct green or red fluorescence, there is some spectral overlap that must be accounted for. The monitoring wavelength for both the green and red emissions must be selected to maximize the overall signal, while minimizing the spectral overlap. From the data in Table 6.1, it appears that either the 510 ± 15- or 520-nm band-pass filter offers the best performance for monitoring the green fluorescent light (i.e., highest intensity and lowest spectral overlap). Also, it is apparent from these results that the light intensity from the green fluorescent dye is greater than that from the red fluorescent, and it has less spectral overlap (Table 6.1).

The best choice of filter for the red light is not as straightforward. The 670-nm filter gives essentially no spectral overlap, but the intensity of the red light that passes is below practical limits (Table 6.2). The optimal choices appear to be the 630-nm band-pass filter or the 663-nm long-pass filter. Each has different beneficial properties. The 630-nm filter detects more of the fluorescence from the red dye, and there is acceptable spectral overlap from the green dye (Figure 6.2). Conversely, the 663-nm long-pass filter shows the least spectral overlap for the green fluorescent dye, while maintaining a signal for the red dye.

There is a basic conceptual and practical difference in determining cell viability using fluorescent probes in CE-LIF versus microscopy [33,34] or flow cytometry [35]. In the latter methods, each individual cell is counted. It does not really matter how much of the fluorescent dye is incorporated into the various cells, as long as (1) there is sufficient dye to stain all of the cells present and (2) each cell has at least enough dye to discern a red or green fluorescence (or whatever color is being monitored). In CE-LIF, the total luminescence is measured and it must be proportional to the number of cells present. Thus, all cells must be saturated with the dye to an extent that the addition of more dye will not alter their fluorescence. As can be seen from Figure 6.3, this amounts to ≥ 1 μM green fluorescent dye for 10^7 cells/mL and ≥ 7 μM red fluorescent dye for 10^7 cells/mL. These concentrations are
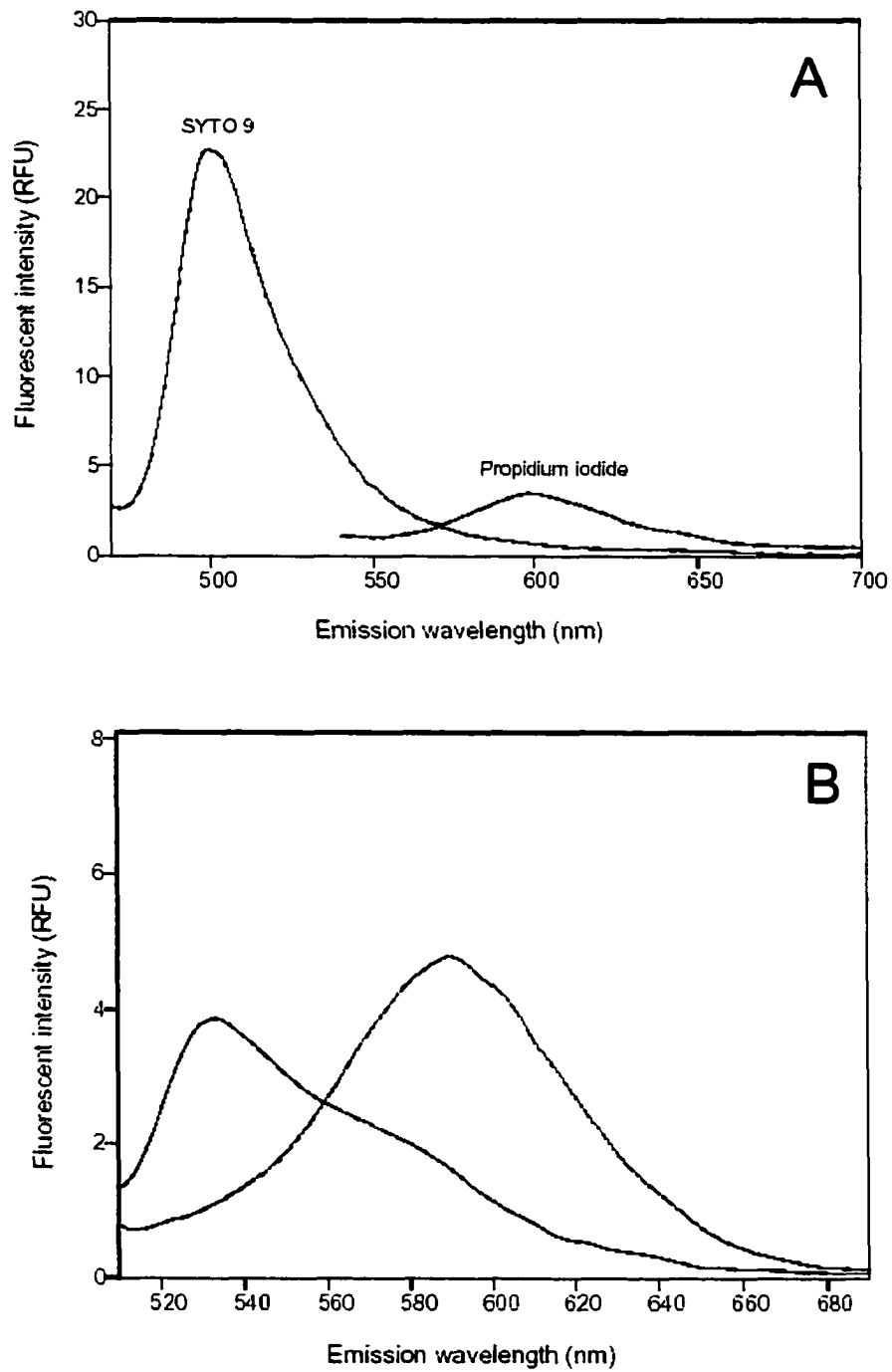
Figure 6.2. Fluorescence spectra of (A) propidium iodide (λ_{max}, 600 nm) and SYTO 9 (λ_{max}, 514 nm) and (B) cytoplasmic FUN-1 (λ_{max}, 538 nm) and vacuolar FUN-1 (λ_{max}, 591 nm).

Table 6.1. Data showing the spectral overlap and relative intensities (of red and green fluorescent light) using different green-light filters and a single red-light long pass filter (663 nm). Two types of experiments were done: (A) for samples stained only with green fluorescent dye [a] and (B) for samples stained only with the red fluorescent dye [b] (see Experimental Section).

	Type of filters (green light)			
	505 ± 10 nm band pass	510 ± 10 nm band pass	510 ± 15 nm band pass	520 ± 20 nm band pass
(A)For green stained samples only [a] Green/Red light ratio of intensities (% of red signal from the green dye)	34.5 (2.9%)	38.2 (2.6%)	110.9 (0.9%)	128.0 (0.8%)
(B)For red dyed samples only [b] Red/Green light ratio of intensities (% of green signal from the red dye)	4.4 (22.9%)	3.3 (30.3%)	5.6 (17.9%)	8.7 (11.5%)

[a] The green fluorescent stain is SYTO 9 (see Experimental Section). The percent RSD was ± 17% for n = 5. [b] The red fluorescent stain is propidium iodide (see Experimental Section). The percent RSD was ± 24% for n = 5.

Table 6.2. Data showing the spectral overlap and relative intensities (of red and green fluorescent light) using different red-light filters and a single green-light band pass filter (520 ± 20 nm). Two types of experiments were done: (A) for samples stained only with green fluorescent dye [a] and (B) for samples stained only with the red fluorescent dye [b] (see Experimental Section).

	Type of filters (red light)					
	600 nm long pass	610 ± 10 nm band pass	630 ± 15 nm band pass	650 ± 10 nm band pass	663 nm long pass	670 ± 10 nm band pass
(A)For green stained samples only [a] Green/Red light ratio of intensities (% of red signal from the green dye)	0.9 (111.1%)	7.0 (14.3%)	11.5 (8.7%)	56.7 (1.8%)	128.0 (0.8%)	37046 (0.00%)
(B)For red dyed samples only [b] Red/Green light ratio of intensities (% of green signal from the red dye)	1.7 (58.8%)	14.0 (7.1%)	55.7 (1.8%)	4.0 (25.0%)	8.7 (11.5%)	0 (-)

[a] The green fluorescent stain is SYTO 9 (see Experimental Section). The percent RSD was ± 13% for n = 5. [b] The red fluorescent stain is propidium iodide (see Experimental Section). The percent RSD was ± 28% for n = 5.
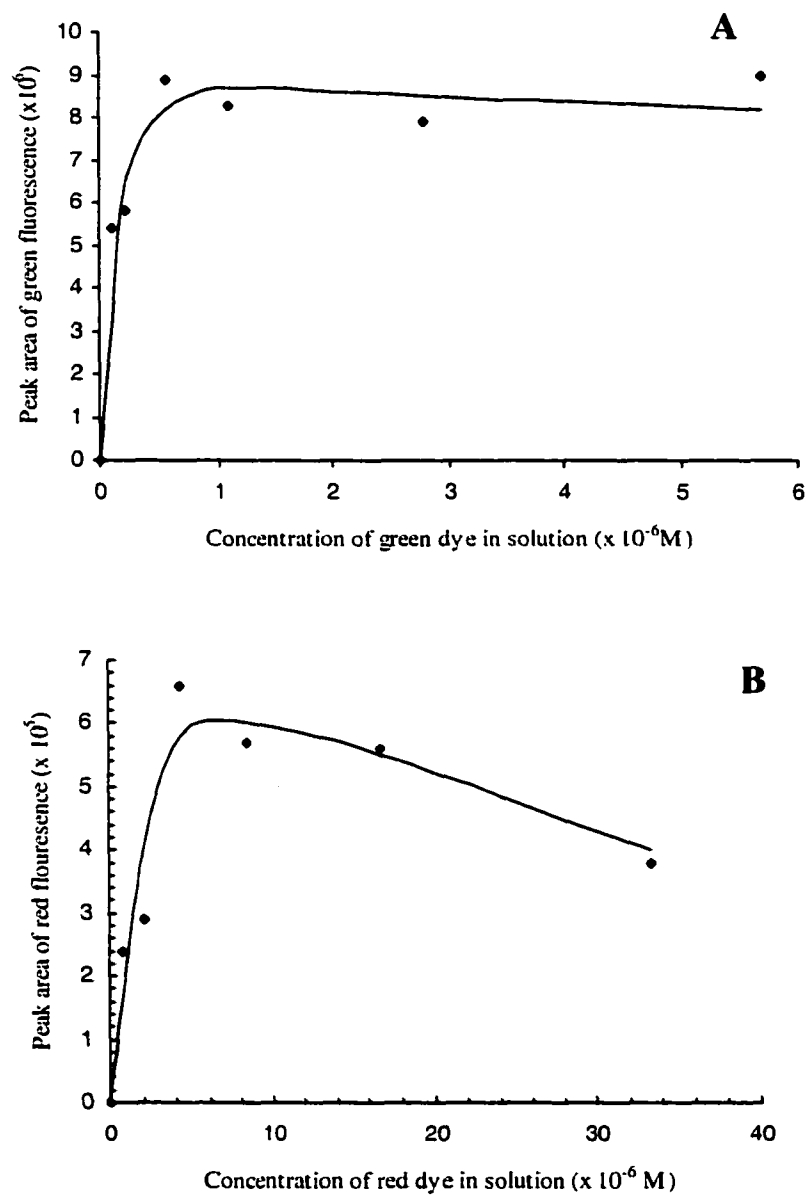
Figure 6.3. Microbe (L. acidophilus) saturation curves for (A) SYTO 9 green fluorescent dye and (B) propidium iodide red fluorescent dye. The cell concentration was 10^7 cells/mL. The decreasing fluorescence intensity for propidium iodide (B) is an artifact due to an inner filter effect from the excess dye in cells.

somewhat higher than those used when cells are stained for microscopy. Once the dye concentrations are properly optimized, the CE, CIEF, or microfluidic separation can be accomplished as previously outlined [10,13-15]. However, simultaneous LIF detection of the red fluorescent light (>663 nm) and the green fluorescent light (520 nm) is done as shown in Figure 6.4.

Both the correction for spectral overlap and the viability determination are accomplished using a standard curve that plots the ratio of the green/red signal versus the percentage of live cells (Figure 6.5). It is imperative that the standard curves be accurate and representative of the unknown cells to be measured. Specifically, standard dead or fixed cells must be obtained that absorb the dye in the same way and amounts as the cells from the unknown sample that have died naturally. This requires specific fixing procedures to produce the stained dead cells (see Experimental Section). The optimum fixing procedure for one type of cell may not be appropriate for another.

Yeast cells are a case in point. Cells that have been fixed by different procedures absorb different amounts of propidium iodide. This is clearly shown in Figure 6.6. The fixing procedure of Figure 6.6a produced dead cells with a membrane permeability similar to the nonviable yeast cells in natural or unknown samples. These "standard" fixed yeast cells were used to prepare the curve in Figure 6.6c. It should be noted that the SYTO 9/propidium iodide system is recommended for use with bacteria but not for yeast or fungi [35,36]. The recommended dye/stain for yeast and fungus is FUN-1 (see Figure 6.1). The spectral overlap (Figure 6.2B) and the less intense fluorescence of this system produced unacceptably high errors when used by us in a CE format. When the SYTO 9/propidium iodide system was used on yeast (with an improper fixing system, i.e., Figure 7.6b-e) the errors (RSD) in the viability determination sometimes approach 40%. However, with the proper fixing procedure (Figure 6.6a) the SYTO 9/propidium iodide system is effective for both bacteria and yeast in a CE-FID format. In our hands, the FUN-1 viability system was useful only when fluorescence microscopy was used.

Likewise, the standard live cells must be all or nearly all alive. Usually this can be achieved by using cells taken from the log-growth phase of a culture (see Experimental Section). This can only be done with proper culture, capture, and staining techniques. Once the experimental conditions have been optimized, cell viability can be rapidly and efficiently evaluated for either single-cell samples or mixtures of cells.

Using the ratio of peak areas in Figure 6.4, it was determined that the viability of
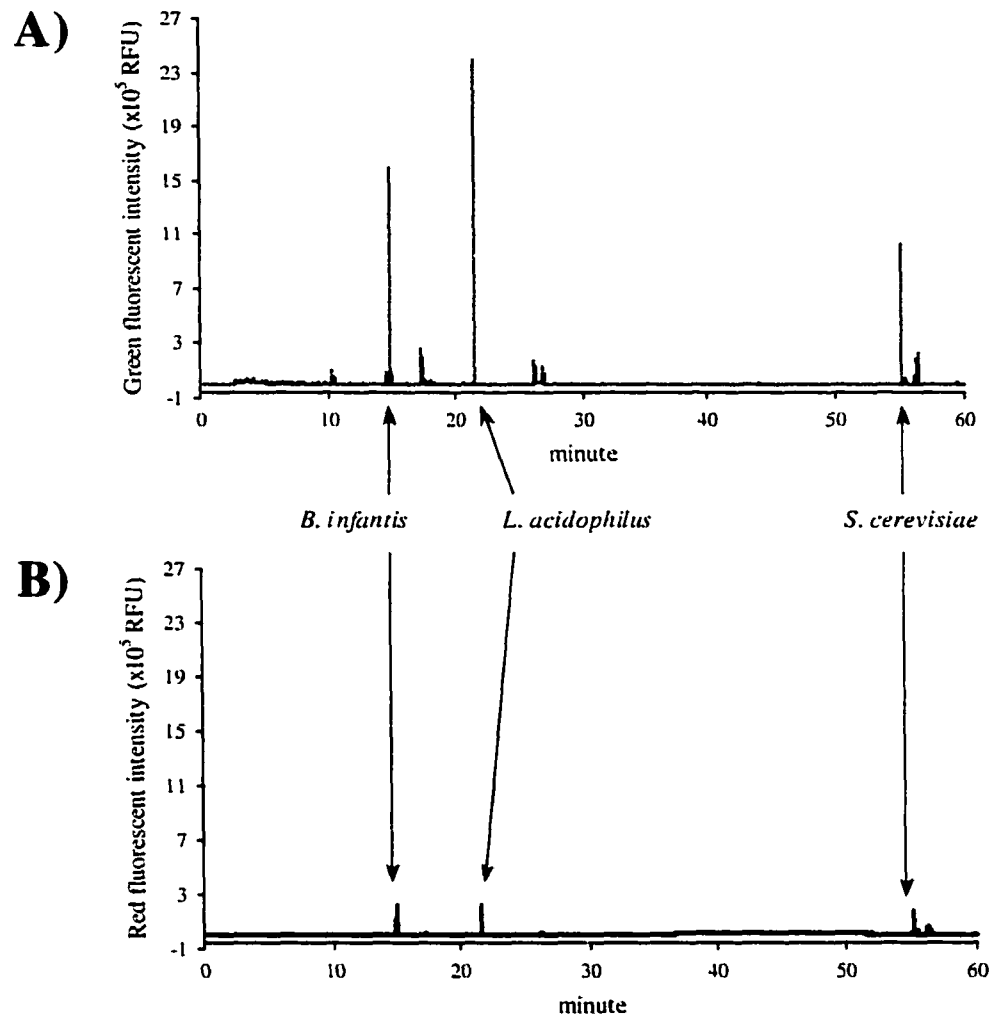
Figure 6.4. Electropherograms showing the simultaneous separation of *B. infantis*, *L. acidophilus*, and *S. cerevisiae* and detection of (A) live (green fluorescence curve, top electropherogram) and (B) dead (red fluorescence curve, bottom electropherogram) cells.
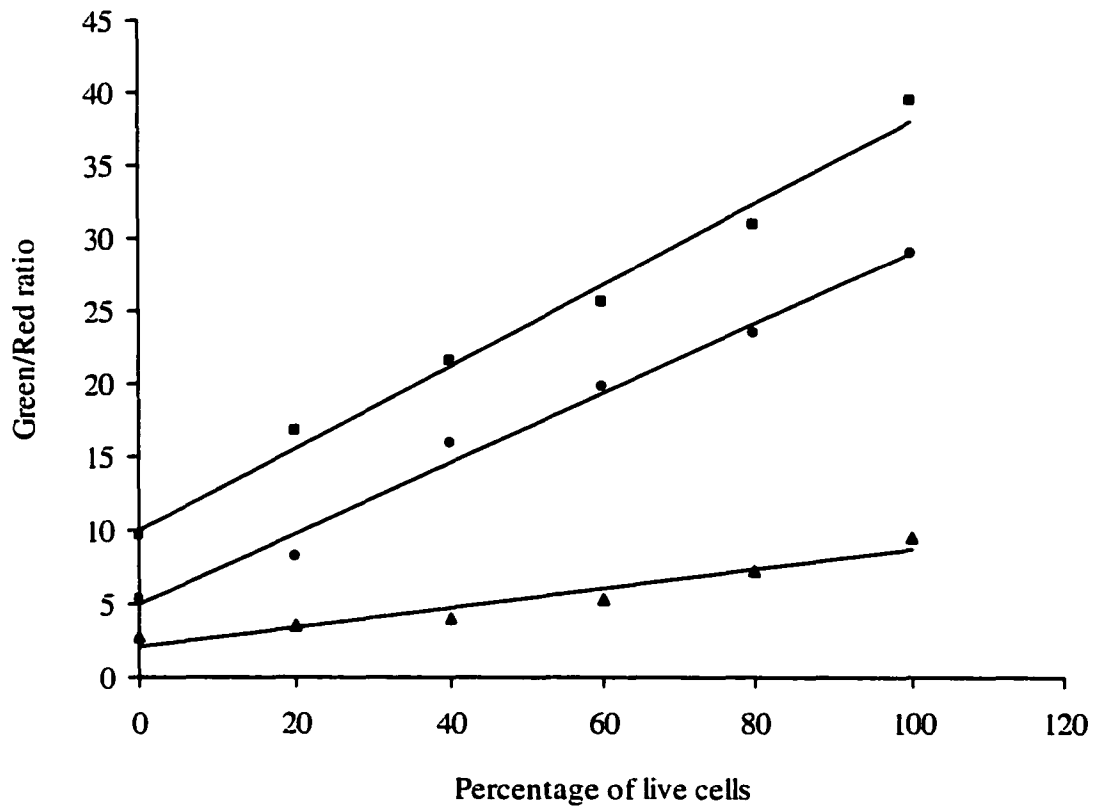
Figure 6.5. Standard viability curves for *B. infantis* (■), *L. acidophilus* (●), and *S. cerevisiae* (▲).
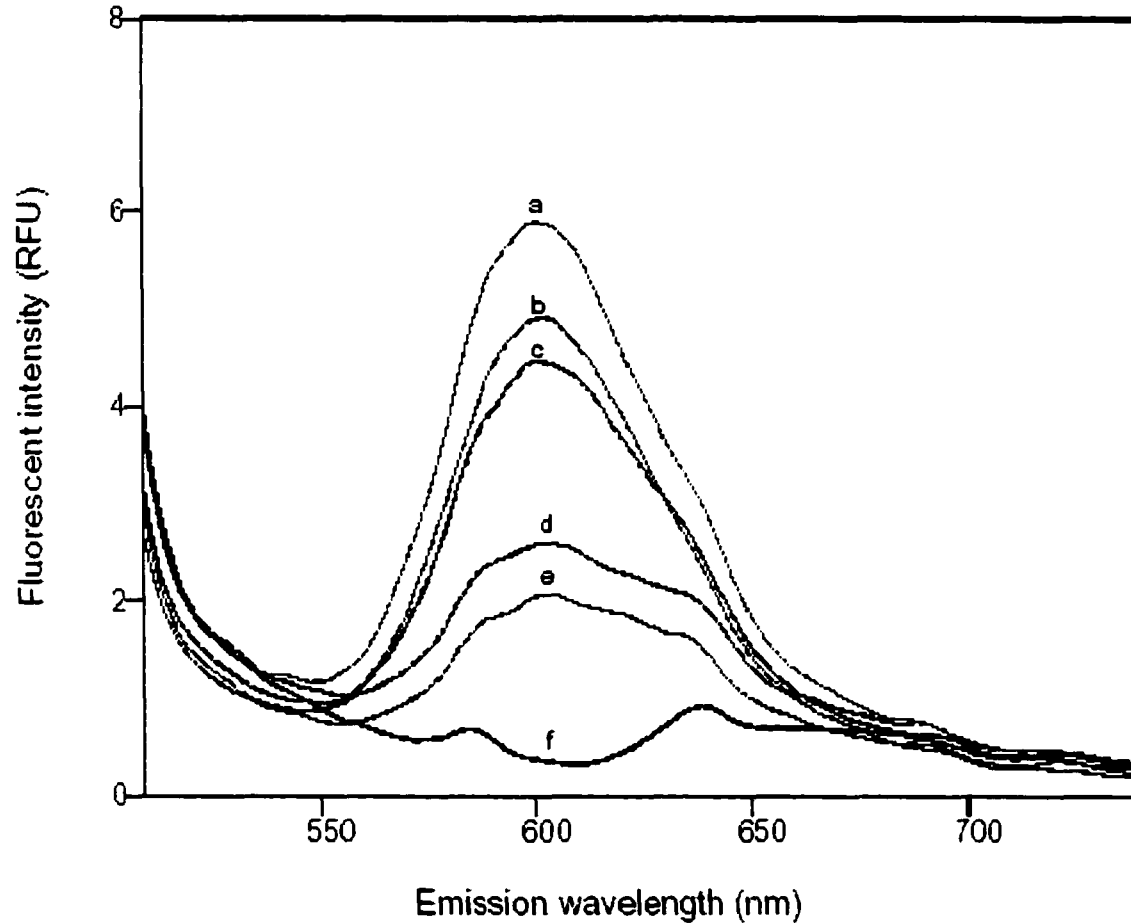
Figure 6.6. Effect of different fixation methods for baker's yeast cells on the uptake of propidium iodide. Yeast cells were fixed in the following ways: (a) at 80 °C in culture media for 5 min, and then ice-cooled; (b) by acetone at -20 °C overnight; (c) at 80 °C overnight when sample was dry; (d) at 80 °C in distilled water overnight; (e) by 4.0% formaldehyde at room temperature overnight. Fixed samples were stained by propidium iodide; (f) formaldehyde-fixed yeast sample that was not stained by propidium iodide.

L. acidophilus was 45%, the *S. cerevisiae* was 43%, and the *B. infantis* was <2%. The error in these determinations (RSD, n = 5) was 14, 10, and 16%, respectively. The CE-LIF viability numbers were checked using flow cytometry and were found to be the same within the experimental error of these methods (see Experimental Section).

The CE-LIF procedure is linear for solutions containing up to 2.4×10^8 cells/mL. At the lower end of the concentration range, a single cell is easily detected. However, to obtain an accurate viability measurement, a representative sample of several cells must be evaluated. Since very small volumes of solution are used in CE (typically 2-50 nL), it is possible that direct injection of a dilute solution of cells will contain too few or even no cells. Consequently, the concentration of cells should be greater than 10^6 cells/mL for direct injection. Much more dilute solutions of cells can be evaluated by first centrifuging the sample into a pellet (thereby concentrating it) and discarding the supernatant liquid. In this case, solutions containing 10^2-10^3 cells/mL often can be evaluated.

We can now separate, identify, quantitate, and determine viability of microbes all in a single run (Figure 6.3). Furthermore, this has been automated and can be performed via an autoinjection system for over 200 samples. Previously, it was possible to accomplish one of the aforementioned measurements at a time, and they were often tedious experiments [21-32]. High-throughput analyses of microbial samples now appear to be feasible.

REFERENCES

1. Shelby, D. C.; Quarles, J. M.; Warner, I. M. *Clin. Chem.* (Washington, D.C.) **1980**, 26, 1127-1132.

2. Ewetz, L.; Stranger, K. Acta Pathol., *Microbiol. Immunol. Scand.*, Sect. B **1974**, B82, 375-381.

3. Pau, C.-P.; Patonay, G. W.; Carione, G. M.; Rossi, T. M.; Wainer, I. M. *Clin. Chem.* **1986**, 32, 987-991.

4. Belgrader, P.; Benett, W.; Hardley, D.; Richards, J.; Stratton, P.; Mariella, R., Jr.; Milanovich, F. *Science* **1999**, 284, 449-450.

5. Stinson, S. C. *Chem. Eng. News* **1999**, 77 (March 29), 36-38.

6. Reiner, E.; Hicks, J. J.; Beam, R. E.; David, H. L. *Am. Rev. Respir. Dis.* **1971**, 104, 656-660.

7. Meuselaar, H. C. L.; Kistemaker, P. G. *Anal. Chem.* **1973**, 45, 587-590.

8. Simmonds, P. G. *Appl. Microbiol.* **1970**, 20, 567-572.

9. Bundy, J.; Fenselau, C. *Anal. Chem.* **1999**, 71, 1460-1463.

10. Armstrong, D. W.; Schulte, G.; Schneiderheinze, J. M.; Westenberg, D. J. *Anal. Chem.* **1999**, 71, 5465-5469.

11. Okun, V. M.; Ronacher, B.; Blaas, D.; Kenndler, E. *Anal. Chem.* **1999**, 71, 2028-2032.

12. Okun, V.; Ronacher, B.; Blaas, D.; Kenndler, E. *Anal. Chem.* **2000**, 72, 4634-4639.

13. Armstrong, D. W.; Schneiderheinze, J. *Anal. Chem.* **2000**, 72, 4474-4476.

14. Schneiderheinze, J. M.; Armstrong, D. W.; Schulte, G.; Westenberg, D. J. *FEMS Microbiol. Lett.* **2000**, 189, 39-44.

15. Armstrong, D. W.; Schneiderheinze, J. M.; Kullman, J. P.; He, L. *FEMS Microbiol Lett.* **2001**, 194, 33-37.

16. Hjerten, S. In Cell Separation Methods; Bloemendal, H., Ed.; Elsevier: Amsterdam, **1977**; pp 117-128.

17. Gullmar, B.; Hjerten, S.; Wastrom, T. *Microbios* **1988**, 55, 183-192.

18. Hjerten, S.; Elenbring, K.; Kilar, F.; Liao, J.-L.; Chen, A. T.; Seibert, C. J.; Zhu, M.-D. *J. Chromatogr.* **1987**, 403, 47-61.

19. Hjerten, S.; Kubo, K. *Electrophoresis* **1993**, 14, 390-395.

20. Pfetsch, A.; Welsch, T. Fresenius' *J. Anal. Chem.* **1997**, 359, 11198-11201.

21. Ebersole, R. C.; McCormick, R. M. *Biotechnology* **1993**, 11, 1278-1282.

22. Schnabel, V.; Groiss, F.; Blaas, D.; Kenndler, E. *Anal. Chem.* **1996**, 68, 4300-4303.

23. Shen, Y.; Berger, S. J.; Smith, R. D. *Anal. Chem.* **2000**, 72, 4603-4607.

24. Burghardt, R. C.; et al. In Principles and Methods of Toxicology, 3rd ed.; Hayes, A. W., Ed.; Raven Press: New York, **1994**, pp 1231-1258.

25. Lloyd, D.; Hayes, A. J. *FEMS Microbiol. Lett.* **1995**, 133, 1-7.

26. Breewwer, P.; Abee, T. *Int. J. Food Microbiol.* **2000**, 55, 193-200.

27. Thoma, J. A.; Thoma, G. J.; Clark, W. Cell. *Immunol.* **1978**, 40, 404-418.

28. Hillman, G. G.; Roessler, N.; Fulbright, R. S.; Pontes, J. E.; Haas, G. P. *Biotechniques* **1993**, 15, 744-749.

29. Kaneshiro, E. S.; Wyder, M. A.; Wu, Y.-P.; Cushion, M. T. *J. Microbiol. Methods* **1993**, 17, 1-16.

30. McFeters, G. A.; et al. *J. Microbial Methods* **1995**, 21, 1-13.

31. Millard, P. L.; Roth, B. L.; Kim, C. H. *Biotechnol. Int.* **1997**, 1, 291-296.

32. Sarma, K.; Ray, D.; Antony, A. *Cytotechnology* **2000**, 32, 93-95.

33. Jones, K. H.; Senft, J. A. *J. Histochem. Cytochem.* **1985**, 33, 77-79.

34. Taghi-Kilani, R.; Gyürék, L. L.; Millard, P. J.; Finch, G. R.; Belosevic, M. *Int. J. Parisitol.* **1996**, 26, 637-646.

35. Flow Cytometry: A Practical Approach, 2nd ed.; Ormerod, M. G., Ed.; IRL: Oxford, U.K., **1994**.

36. Haugland, R. P.; Yue, S. T.; Millard, P. J.; Roth, B. L. Cyclic-Substituted Unsymmetrical Cyanine Dyes. U.S. Patent 5,436,134, **1995**.

37. Millard, P. J.; Roth, B. L.; Yue, S. T.; Haughland, R. P. Fluorescent Viability Assay Using Cyclic-substituted Unsymmetrical Cyanine Dyes. U.S. Patent 5,534,416, **1996**.

CHAPTER 7

ELECTROPHORETIC BEHAVIOR AND POTENCY ASSESSMENT OF BOAR SPERM USING A CAPILLARY ELECTROPHORESIS–LASER INDUCED FLUORESCENCE (CE-LIF) SYSTEM

Lingfeng He, Rebecca J. Jepsen, Lawrence E. Evans, Daniel W. Armstrong

ABSTRACT

The viability of sperm cells can be accurately and reproducibly determined in less than ten minutes using a CE-LIF technique. This is significantly faster than most other known procedures. Furthermore, this approach is not compromised by the presence of molecular or colloidal contaminants as are other techniques including flow cytometry. The effect of pH, ionic strength, applied voltage and polymer additive was studied systematically and optimized. The reproducible focusing behavior of sperm cells in the presence of extender solution and dilute polyethylene oxide (PEO) was confirmed and utilized as an integral part of this assay.

7.1. INTRODUCTION

Artificial insemination remains the most practical and cost-effective method for genetic upgrading of cattle, in spite of major advances in other reproductive technologies in recent years [1]. This procedure allows the cattle producer to make efficient use of the ample supply of sperm available from an individual male. Among the properties of semen, viability is one of the most important parameters used to assess its quality. A variety of laboratory tests, including sperm progressive motility, acrosomal integrity, and metabolic activity, have been used to evaluate sperm viability [2]. These are time consuming procedures, and it is generally not practical to analyze more than a few hundred sperm for a given sample using these methods, thus resulting in poor precision [3].

Recently, specific staining technologies have been developed and have provided a new approach for studying the viability of cells [4,5]. Dual fluorescent staining techniques, which target sperm nucleic acid with a combination of two stains, have been demonstrated to be one of the most useful methods for determination of sperm viability, since the integrity of the sperm membranes determines whether the cell selectively includes or excludes these stains [3, 6-13]. Among all tested stain combinations, SYBR-14 / propidium iodide (PI) has been found to be most suitable for the spermatozoal viability examination [3, 8-13]. Both dyes label the same sperm nuclear material (DNA). Membrane-permeable SYBR-14 brightly stains the nuclei of living cells with green fluorescence, while membrane-impermeant PI labels dead cells with red fluorescence. By using specific nucleic acid stains, the ambiguity of stains that target separate cellular organelles is avoided. Additionally, the excitation wavelength for these dyes falls in the visible region (488 nm), thus preventing exposure of cells to UV light, which may cause damage to the integrity and function of these cells [14]. In flow cytometric analysis, the SYBR-14/PI combination has been successfully used to assess the viability of sperm from a variety of mammals, including bull [3,9-11], boar [8,10], ram, rabbit, mouse, man [10], and turkey [13]. Although flow cytometry in combination with dual fluorescent staining techniques is becoming a widely accepted method in measuring sperm viability, its disadvantages, such as complexity of sample measurement and data explanation, lack of ability to differentiate sperm cells from contaminating bacteria or other particles of similar size, and highly expensive instrumentation, restrict the accessibility of this method. A more affordable, accurate and operationally simple method is needed.

Capillary electrophoresis (CE) is well-known for its high efficiency, high selectivity, high-throughput screening ability, and simplicity in nature and operation. It has been used to great advantage in the analysis of small molecules and macromolecules. In recent years, CE

has shown increasing potential for the separation and characterization of charged colloidal particles and biological vesicles or cells [15-24]. Recently, Armstrong and co-workers demonstrated that microorganisms could be separated in a manner with extremely high apparent peak efficiencies ($\sim 10^6$-10^{10} theoretical plates per meter) [15-19]. This highly effective microbial CE separation method involved the use of dilute solutions of certain hydrophilic polymers (such as polyethylene oxide) and/or capillary isoelectric focusing. Later, Shintani et al. achieved separations of *S. enteritidis* from other bacteria using a similar CE method, but with a different polymer [24]. Most recently, it was demonstrated that the separation, identification, and determination the viability of bacteria and yeast could be accomplished in a single run using capillary electrophoresis–laser induced fluorescence (CE–LIF) method, combined with dual fluorescent staining techniques [16]. The determination of cell viability was based on the observation that living and dead cells are selectively labeled by SYTO-9 and propidium iodide, respectively, and the ratio of fluorescence signal from live and dead cells can be correlated to the percentage of living or dead cells in a population [15,16].

It is known that sperm cells, like other biological cells, are charged and have been characterized using isoelectric focusing [25-28]. Several features of the highly efficient CE-LIF method make it an attractive tool for sperm characterization and potency assessment. For example, the high selectivity makes it possible to separate spermatozoa from contaminating somatic cells, cellular fragments and other colloidal particles present in seminal fluid. The high peak efficiency improves the method's sensitivity and accuracy. Its simplicity of operation and relatively affordable instrumentation make it more accessible to a wider scope of researchers. The focus of this work is to examine the usefulness of CE-LIF in studying the electrophoretic behavior of sperm, assessing sperm viability, and to develop the first CE-LIF potency assay.

7.2. EXPERIMENTAL SECTION

7.2.1. Materials.

Tris(hydroxymethyl)aminomethane (TRIS), poly(ethylene) oxide (PEO; Mn = 600,000), and coumarin 334 were purchased from Aldrich (Milwaukee, WI, USA). Citric acid monohydrate and sodium chloride were obtained from Fisher Scientific (Fair Lawn, NJ, USA). D-(-)-fructose was a product from Sigma (St. Louis, MO, USA). SYBR-14 (1mM) and propidium iodide (20 mM) were purchased from Molecular Probes, Inc. (Eugene, OR,

USA). Both were dissolved in DMSO separately. Deionized distilled water was filtered through 0.2 μm membrane (Alltech Associates, Inc., Deerfield, IL USA).

7.2.2. Methods.

7.2.2.1. Semen Samples.

Three healthy, mature crossbred boars, aged 3 to 4 years, provided the ejaculated semen for the study. All boars were housed in an environmentally controlled building under the same feeding and management conditions. Normally, semen collections were made weekly using the glove-hand technique. The information about raw boar semen, together with other farm animals, is given in Table 7.1. After the gel fraction of raw semen was removed by filtration through gauze, spermatozoa were evaluated microscopically for seminal quality (i.e., sperm motility and morphology). The head size of boar spermatozoa exhibits an asymmetric distribution between 2.6 and 5.5 μm and over 70% of sperm cells fall in the narrow range of 2.8-3.6 μm. Because of its relative large size, it is easier for sperm to precipitate to the bottom of suspensions. All sperm samples need to be well-mixed prior to analysis, however, vigorous mixing should be avoided. Sperm concentration in the gel-free portion was determined using either a Multisizer™ 2 Coulter Counter (Coulter Corporation, Inc., Hialeah, FL) or a hemocytometer, and found to be in the range of 2-10 x 10^8 sperm/ml. A semen stock solution was prepared by diluting gel-free raw semen 4-10 times with appropriate boar semen extender. Five boar semen extenders were used in this investigation. Both Beltsville Thaw Solution (BTS) and X-CELL were ordered from IMV International Corp. (Minneapolis, MN, USA), Modena from Swine Genetics International, Ltd. (Cambridge, IA, USA), MR-A from Kubus, S.A. (Madrid, Spain), and Androhep Plus from Minitube of America, Inc. (Verona, WI, USA). These commercial boar semen extenders vary by manufacturers and generally consist of glucose, sodium citrate, sodium bicarbonate and many other additives. Their complete chemical compositions are not available. The solutions of these extenders were prepared by dissolving appropriate amount of powder in filtered deionized distilled water and stored in refrigerator. Since boar spermatozoa are extremely sensitive to cold shock, all semen stock solutions were preserved at 16-19 °C all the time. Prior to CE analysis, semen stock solutions were further diluted to a sperm concentration of ~10^7/ml.

7.2.2.2. Capillary Electrophoresis.

A stock buffer solution containing 0.20 M Tris and 0.066 M citric acid was prepared

Table 7.1. General characteristics of semen from farm animals [a]

	Cattle		Sheep	Swine	Horses
	Dairy	Beef			
Volume (ml)	6	4	1	125[b]	60[b]
Sperm concentration (billion/ml)	1.2	1.0	2.0	0.2	0.15
Total sperm (billion)	7	4	3	45	0.15
Motile sperm (%)	70	65	75	60	70
Morphologically normal sperm (%)	80	80	80	60	70
pH	6.5-7.0	6.5-7.0	5.9-7.3	6.8-7.5	6.2-7.8

[a] Adapted from ref 1.
[b] Gel-free portion.

by dissolving an appropriate amount of each chemical in filtered deionized water. This stock solution was then diluted 1:200 with water yielding a buffer of pH 6.9, containing 1.0 mM Tris and 0.33 mM citric acid (diluted buffer). A 1% stock PEO polymer solution was obtained by dissolving 0.4 g PEO in above diluted buffer solution overnight with magnetic stirring. Unless stated otherwise, 1% fructose was always added to the running buffer to maintain the isotonicity.

The CE separations were performed on a Beckman Coulter P/ACE MDQ capillary electrophoresis system equipped with a 488-nm argon-ion laser-induced fluorescence (LIF) detector. Untreated fused silica capillary with 100-μm i.d. was purchased from Polymicro Technologies, Inc. (Phoenix, AZ, USA). The capillary used was 30 cm in length (20 cm to detection window). When a capillary was first used, it was rinsed for 0.5 min with water, 5 min with 1 N NaOH, and 0.5 min with water. Between runs, the capillary was washed for 0.5 min with water and 0.2 min with 1 N NaOH, followed by 5 min with running buffer. The running buffer was changed between runs. The stained semen samples were injected with a pressure of 0.5 psi for 5-15 s. The green and red fluorescent signal from samples was collected simultaneously by passing through two channels of the LIF detector. A 520-nm band-pass filter (Beckman Coulter, Inc., Fullerton, CA, USA) and 630-nm band-pass filter (Omega Optical, Inc., Brattleboro, VT, USA) were used as the green and red fluorescence filter, respectively. Data were processed using P/ACE MDQ software.

7.2.2.3. *Saturation of Boar Sperm with SYBR-14 and PI.*

The combination of membrane-permeable DNA stain, SYBR-14 and membrane-impermeant propidium iodide was utilized to assess boar sperm viability in this study. Upon briefly incubating with these dyes and exposing to 488-nm light, living sperm with intact cell membranes fluoresce bright green, while dead sperm with damaged cell membranes fluoresce red. A working solution of SYBR-14 (0.1 mM), obtained by diluting the concentrated solution (1.0 mM) 10 times with DMSO (EM SCIENCE, Gibbstown, NJ, USA), was used for staining samples. 2.0-milliliter aliquots of a boar semen suspension, with a sperm concentration of ~1.5 x 10^7/ml in BTS extender, were mixed with different amounts of SYBR-14 and incubated for 10 minutes at 36 °C. When labeled with PI, sperm cells were first killed by using freeze-thaw method (frozen for 20 minutes at –20 °C and thawed at 36 °C), and then 2-milliliter aliquots with a sperm concentration of 2.1 x 10^7/ml were added to different amounts of PI and incubated for 10 minutes at 36 °C. Samples were injected for 5 s with a pressure of 0.5 psi and approximately 5000 sperm were analyzed each time. The electrophoresis of boar semen samples was performed by applying a voltage of 10 kV. The

green or red fluorescence of each sample was measured 3-4 times and the relative standard deviation (RSD) of measurements varies between 13 and 21% (n = 4).

7.2.2.4. Effects of Experimental Conditions.

Five experimental conditions, including the pH, ionic strength, the polymer additive to the running buffer, the applied voltage and sample injection volume, were investigated for their effects on the electrophoretic mobility (μ_{eff}) and the G/R ratio of boar sperm. The G/R ratio is defined as the ratio of green fluorescence (G) from viable sperm with intact membranes (stained by SYBR-14) and red fluorescence (R) from dead sperm with compromised cell membranes (stained by PI). To avoid any variation of viability of sperm during the analysis process, only killed sperm suspensions were used as samples. 2-milliliter aliquots were stained with enough amount of SYBR-14 and PI (their ratio was fixed), and incubated at 36 °C. 0.1 N NaOH and 0.1 N HCl were used to adjust the pH of the running buffer to a desired value. The ionic strength of the running buffer was adjusted by (a) adding NaCl and keeping the concentrations of Tris and citric acid constant, i.e. 1.0 mM Tris and 0.33 mM citric acid; or (b) changing the concentrations of both Tris and citric acid, while keeping their ratio to 3:1. Coumarin 334 was used as the fluorescent electroosmotic flow (EOF) marker. The effective electrophoretic mobility (μ_{eff}) of sperm is calculated by $\mu_{eff} = \mu_{app} - \mu_{EOF}$, where μ_{app} is the apparent electrophoretic mobility of sperm measured from electropherogram, and μ_{EOF} is the electrophoretic mobility of EOF marker. Since coumarin 334 can be taken up by sperm cells because of its hydrophobicity, the migration times of EOF marker and sperm were measured separately. Both μ_{eff} and G/R value were averaged from at least 3 measurements. RSD varies between 2-11% for μ_{eff} and 3-21% for G/R ratio (n = 4).

7.2.2.5. Viability calibration curve of boar sperm.

Freshly collected boar semen diluted in BTS extender was used in this study. Over 80% of the sperm were motile with intact membranes. A viability standard curve was constructed using mixtures of the living (namely untreated with freeze-thawed method) and killed sperm prepared by mixing different portion of them: (A) 100% living / 0% killed; (B) 80% living / 20% killed; (C) 60% living / 40% killed; (D) 40% living / 60% killed; (E) 20% living / 80% killed; (F) 0% living / 100% killed. Each sample was first stained with SYBR-14 for 10 minutes and then with PI for another 10 minutes at 36 °C. In CE analysis, a solution containing 0.025% PEO, 1.0 mM Tris-0.33 mM citric acid, and 1% fructose (pH

6.9) was used as running buffer. Samples was injected for 5 sec with a pressure of 0.5 psi, and the applied voltage was 15 kV.

7.2.2.6. *Flow Cytometry.*

The viability of boar semen samples analyzed in CE was also measured with flow cytometry (Epics XL-MCL , Beckman Coulter Corp., Miami, FL, USA). To eliminate the interference of debris or other cellular particles in the sample, the side and forward light scatter parameters were gated so that only those counts possessing the light scatter characteristics of sperm analyzed for fluorescence intensity. The log of green fluorescence was obtained by collecting fluorescence signal that passed through a 525-nm band pass filter. The red fluorescence parameters were collected through 575-nm and 635-nm band pass filters, respectively, as a log function. No compensation was used in this experiment. Semen sample was diluted 1:10 with a buffer solution containing 0.2 M Tris, 0.066 M citric acid and 1% fructose. Staining procedure was the same as that used in CE analysis. At least 10,000 sperm per sample were analyzed for their fluorescence for each sample. The data were processed using Beckman Coulter System V version 3.0 program.

7.2.2.7. *CE-CCD Systems.*

Two home-built CE-CCD systems were used in this experiment. System 1 allowed us to observe the electrophoretic migration of sperm within a 10-cm detection window, and System 2, combined with a microscope, enabled us to examine the movement of individual sperm cells. The details about both systems have been reported previously [29-31]. In system 1, the capillary used had a 100-μm i.d. and 365-mm o.d with a total length of 58 cm (40 cm to detection window, 10 cm detection window, and 8 cm to the outlet end). The detection window was arranged in a vertical direction. Hydrodynamic injection (siphoning) was carried out using a 30 cm height difference between the inlet and the outlet end of the capillary. After injection, the sample plug was pushed hydrodynamically with running buffer into the 10 cm detection window. After the sample was introduced into the illuminated detection window, the height difference was removed and 22 kV voltage was applied. The running buffer consists of 0.025% PEO, 1.0 mM Tris, 0.33 mM citric acid, and 1% fructose (pH 6.9). A 520-nm band pass filter was mounted in front of the CCD camera. In system 2, a capillary with 250 μm i.d. was used. The whole capillary was filled with sample and the electric field across the capillary was 300 V/cm. In both cases, sperm cells were only stained by SYBR-14.

A new capillary was rinsed 5 min with 1N NaOH and 5 min with running buffer. Between each run the capillary was rinsed 1 min with 1N NaOH and 1 min with running buffer. The running buffer was changed after every single run. After the last run of the day the capillary was flushed 1 min with 1N NaOH, 1 min with distilled water, and finally 3 min with air. The capillary was then stored overnight.

7.3. RESULTS AND DISCUSSION

7.3.1. Electrophoretic Behavior of Boar Sperm.

Boar semen is a complex, heterogeneous mixture composed of various fluid secretions, somatic cells, cellular fragments and particulate matter in addition to the spermatozoa (Table 7.2). These co-existing particles, with sizes close to spermatozoa, will interfere with the analysis of sperm for some methods, such as flow cytometry, even though fluorescent staining improves the selectivity of these methods. This problem can be circumvented by making use of the high-selectivity and high-efficiency features of CE. Previously, we reported that CE-LIF, when coupled with dual fluorescent staining plus dual wavelength detection technique, provided an alternative way to determine the viability of bacteria and a baker's yeast [15,16]. In this method, samples were prepared by suspending microorganisms in the running buffer and a single peak was often obtained for each microbe. This sample preparation method, however, is not applicable to the analysis of sperm. If boar semen is washed and suspended in the running buffer, a cluster of peaks is commonly obtained (Figure 7.1 B and C) and more importantly the running buffer is not effective in maintaining the motility and viability of the sperm cells.

For the CE-LIF analysis of boar sperm, it is preferable to suspend the boar spermatozoa in commercial boar semen extenders and avoid any harmful treatments (such as washing, freezing or vigorously mixing). An extender is a nutrient-containing, buffered solution with the same tonicity as semen. Extender is widely used in the artificial insemination industry to increase the volume of an ejaculate, prolong the life of sperm, and protect sperm from injury during freezing and thawing. The use of extender benefits the CE-LIF analysis of boar sperm in several ways. First, extender provides an isotonic environment and a sufficient energy source, thus keeping sperm cells motile and viable. Second, extender has a higher ionic strength compared to the CE running buffer, and allows the sperm in the sample zone to experience a low electric field, avoiding any possible viability change caused by a high electric field. Finally, the extender contains components that promote the focusing

Table 7.2. Average chemical composition of semen from different species (mg/100ml)[a]

Constituent	Bull	Ram	Boar	Stallion
Fructose	530	250	13	2
Sorbitol	75	72	12	40
Glycerylphosphorycholine	350	1650	175	70
Inositol	35	12	530	30
Citric acid	720	140	130	26
Ergothionine	0	0	15	75
Plasmalogen	60	380	-	-
Sodium	230	190	650	70
Potassium	140	90	240	60
Chlorine	180	86	330	270
Calcium	44	11	5	20
Magnesium	9	8	11	3

[a] Adapted from ref.1.

Figure 7.1. Electropherograms showing EOF maker peak (A) and boar sperm peaks (B)–(E). Generally, a cluster of peaks were observed if boar semen sample was washed and suspended in running buffer: B) for green fluorescence signal and C) for red fluorescence signal. A single sharp peak for sperm was easily obtained if boar semen was suspended in boar semen extender (X-CELL): D) for green fluorescence signal and E) for red fluorescence signal. The running buffer consisted of 1 mM Tris, 0.33 mM citric acid and 1% fructose with a pH of 6.9. All samples were injected with for 10 seconds at 0.5 psi and 1.0 kV voltage was applied.

Fluorescence intensity (x 10^6 RFU)

Time (minute)

128

A

B

C

D

E
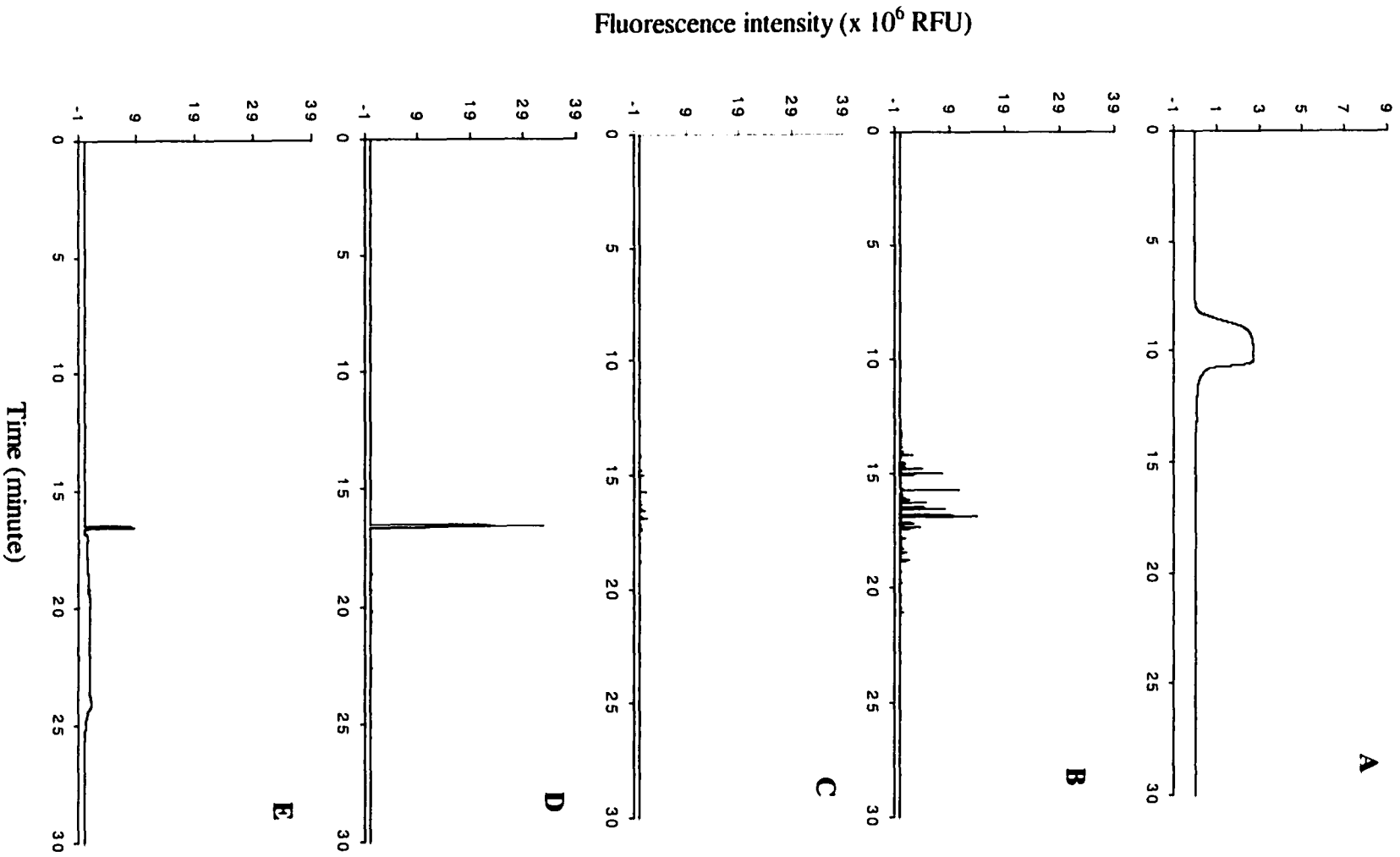
of the injected sperm into a narrow zone, even without the use of polymer in the running buffer. Microscopic observation showed that boar sperm demonstrated excellent dispersion and motility for a few days if they were suspended in extender solution. When the sample was subject to CE-LIF analysis, a reproducible single sharp peak (~16 min) was easily obtained as shown in Figure 7.1 D and E. Compare this to the broad EOF maker peak which was run under the same conditions (Figure 7.1A). The broad background peak in Figure 7.1E (from ~16-25 min) was produced by other cellular particles or the debris of sperm containing nucleic acid. These components produced strong red fluorescence and extremely weak green fluorescence, implying that they were only stained by PI. Many of these components are less dense than sperm cells and could be removed by centrifugation. Notice that the background peak can be barely seen in Figure 7.1C after the sample was washed several times with the running buffer.

It is important to note that unusually large volumes of sample often are injected in this study. An injection volume of 200-600 nL, which corresponds to an injection time of 5-15 s at 0.5 psi or 12-38% of the effective capillary length, was commonly used and such large injections had no effect on the sperm peak width. This is because of the recently discovered focusing property of certain cells undergoing electrokinetic separation in the presence of certain polymers [15-19,29,31]. In contrast, no more than 5% of the effective capillary length is filled with sample in the capillary zone electrophoresis (CZE) of molecules, otherwise, severe band broadening will occur, as illustrated in Figure 7.1A. However, further increasing the injection volume also causes problems in the CE-LIF analysis of sperm. Injection volumes large than 600 nL or injection time above 15 s at 0.5 psi always gave rise to more than one sperm peak, and resulted in significant variation of the G/R ratio measurement (see experimental section for definition).

Boar sperm have a negative μ_{eff} (eluting after the EOF peak), indicating that they are negatively charged under these experimental conditions. This is due to the dissociation of sialic acid or sulfate residues attached to the carbohydrate side chains of glycoproteins and adsorbed proteins [26]. It is well-known that a very broad peak is usually observed for microbes in normal capillary zone electrophoresis [20-23]. This broad peak may be at least partly attributed to the distribution of electrophoretic mobility reflecting the heterogeneity of microbes among a population [20, 23]. This observation is not the case for boar sperm. As can be seen in Figure 7.2, a semen sample slug (~5-cm long) was introduced into the 10-cm capillary detection window. Upon applying a voltage, the whole sample band focused into a narrow zone (<0.3 cm) within a short period (~6 min) and was carried by EOF towards the cathode [31]. The microscopic details of the focusing process is shown in Figure 7.3. The

Figure 7.2. CCD pictures showing the electrophoretic movement of sperm cells inside a 10-cm long capillary detection window at different times after 22 kV voltage was applied. Notice that the sample slug had a sharp front and a dim rear before a voltage was applied. This sharp front was caused by a small air bubble, which constrained the diffusion of sperm during the process of pushing sample slug to the detection window. In this case, air bubble had no effects on the focusing process of sperm. Boar semen was diluted with BTS extender to a sperm concentration of 1.2×10^7 /ml. See experimental section for other conditions.
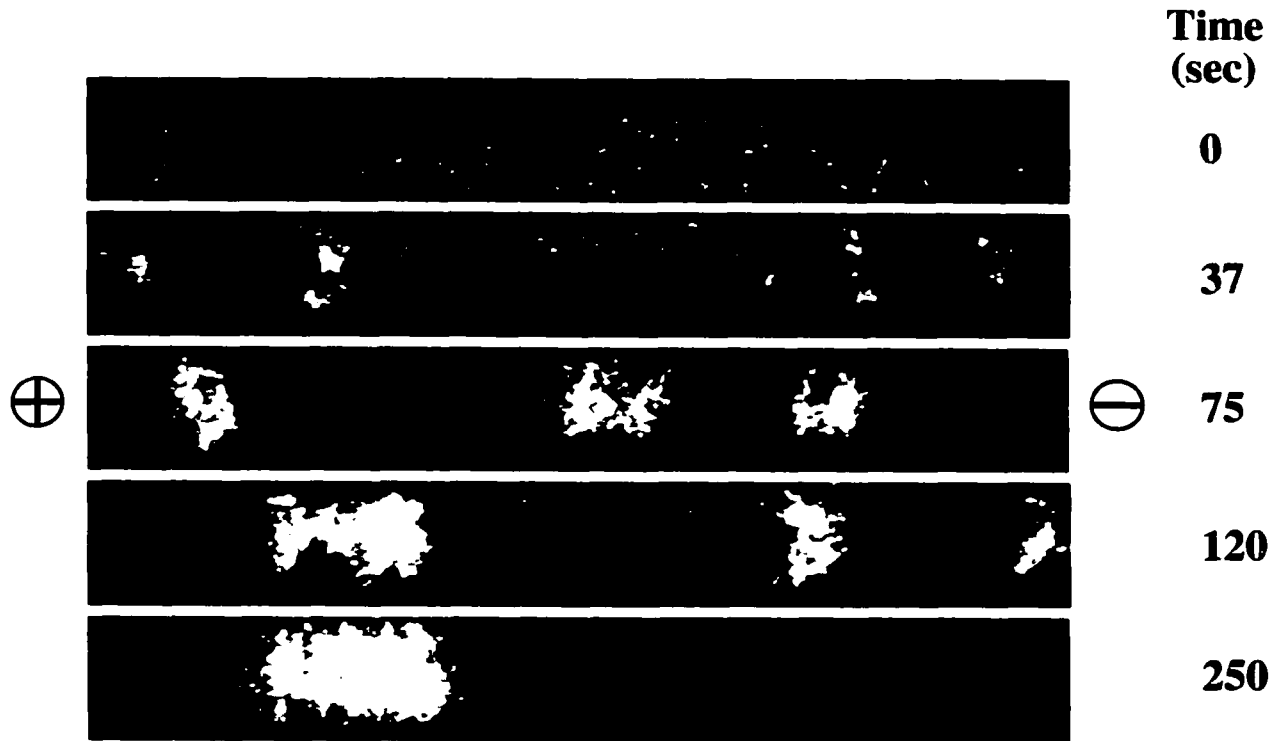
Figure 7.3. CCD pictures showing the detail of the aggregation process of sperm in the home-built CE-CCD system 2 (see experimental section). This system allows individual sperm cells to be seen clearly. In the beginning, the whole capillary was filled with boar semen sample. After a voltage (300 V/cm) was applied, sperm cells collided with each other to form aggregates. In the later time, much larger, brighter, and more compact sperm aggregates appeared in the detection window. The dimension of the each frame is 0.25 mm x 2 mm.

aggregation observed can be explained as the consequence of a combination of effects, including the differential electrophoretic mobility of sperm [31], a weak interaction between sperm cells, and the electroosmotic withdrawal of fluid between closely spaced particles in an electric field [31,32]. The randomly distributed orientations of cells give them different migration velocities in an electric field [33]. This differential migration, together with the other two factors, result in collision and aggregation of sperm cells. The aggregation efficiency depends on many variables, including the surface potential of cells, the relative size ratio of cells, the zeta potential ratio of cells, and the ionic strength of solution [31,32]. Since larger aggregates have a greater chance of colliding with other isolated cells or with other aggregates, eventually, all microbes will collide to form a single larger aggregate. Therefore, the resulting sharp peak no longer represents the distribution of electrophoretic mobilities of individual sperm cells, but rather reflects the shape and size of the formed sperm agglomerate. The measured μ_{eff} of the sperm peak characterizes the electrophoretic property of the sperm aggregate.

7.3.2. Saturation of Boar Sperm with SYBR-14 and PI.

The viability determination of sperm using CE-LIF is based on the G/R ratio, which can be correlated to the viability of sperm in a semen sample using a standard curve. For an accurate determination, it is essential that all binding sites in the sperm cells must be saturated with dye to an extent that the addition of more dye will not change their fluorescence. The data in Figure 7.4 show that the minimum amounts of dyes to saturate 10^7 sperm are 0.1 nmol for SYBR-14 and 25 nmol for PI. It should be noted that these dye amounts are higher than those used in fluorescence microscopic procedures [34].

7.3.3. Effects of Experimental Conditions.

When using the CE-LIF method to assess the viability of sperm, it is essential to control the experimental conditions, since sperm cells are very sensitive to changes in their environment. This part of the study examines the effect of pH, ionic strength, polymer additive to the running buffer, and the applied voltage on the electrophoretic mobility and the G/R ratio of the sperm peak. It should be noted that the effect of these variables is not always as predictable as it is for the CE of molecules.

7.3.4. Effect of pH.

Sperm cells have been the subject of extensive physico-chemical studies [25-28,35,
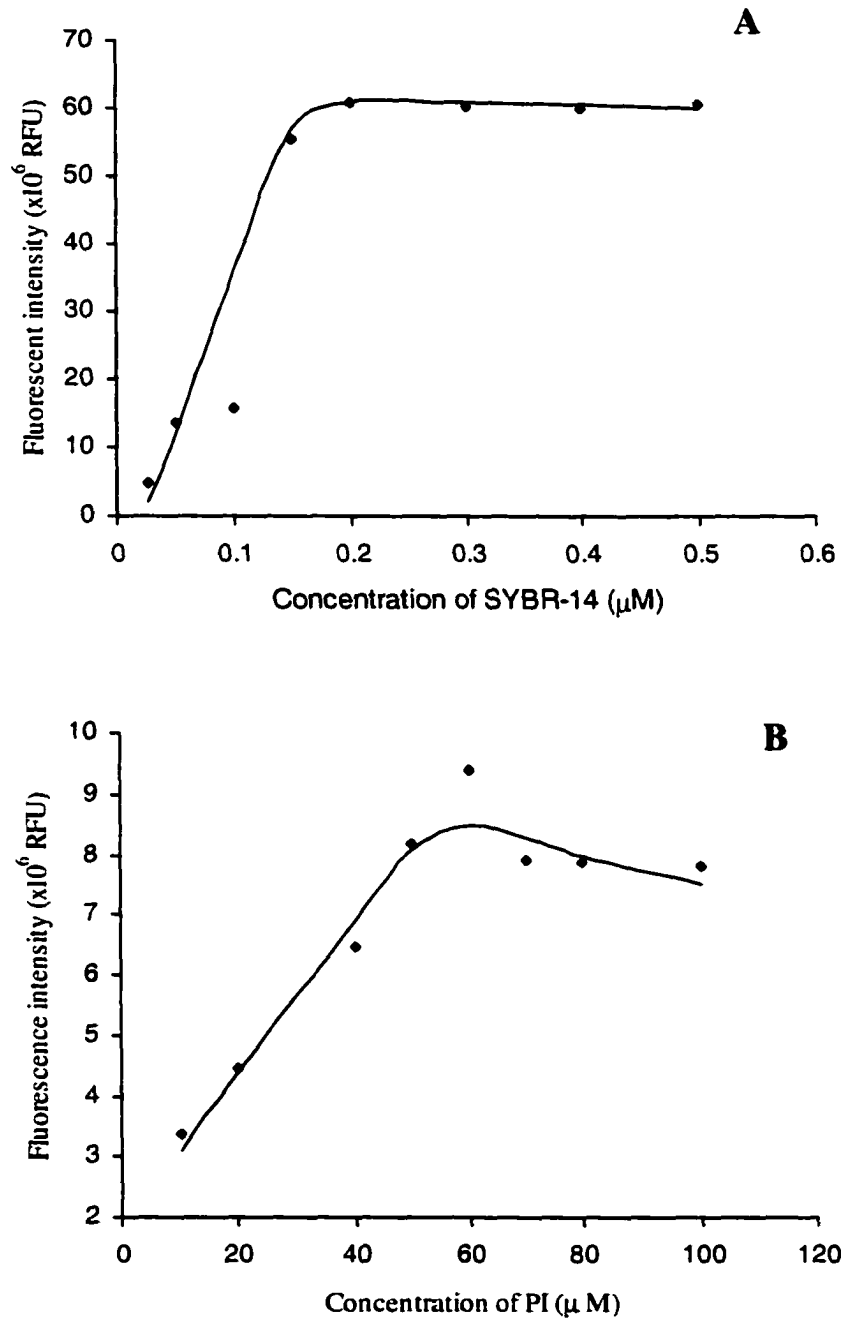
Figure 7.4. Boar sperm saturation curves for A) SYBR-14 live fluorescent stain and B) propidium iodide dead fluorescent stain. Semen samples used had sperm concentrations of 1.5 x 10^{7} /mL and 2.1 x 10^{7} /mL, respectively. The decreasing fluorescence intensity for PI is the result of an inner filter effect resulting from the excess dye in solution.

36]. One of the conclusions of these studies is that the surface charge of sperm is dependent on sample treatment (e.g., enzyme treatment or storage of sperm in seminal plasma) and on the source of sperm within the male reproductive tract [26]. The pH of the running buffer affects the electrophoretic mobility of sperm by affecting the dissociation of a variety of ionizable function groups on the sperm cell surfaces. The dependence of μ_{eff} on the running buffer pH value is shown in Figure 7.5. At pHs above 7, all ionizable function groups were fully dissociated, therefore, μ_{eff} reached constant value and didn't change with increasing buffer pH. Compared to bacteria, whose isoelectric points (pI) are generally in the range from 2 to 4 [37], mammalian sperm have relatively higher pI, varying from 3.9 for ejaculated human sperm to 8.55 for hamster caudal sperm pre-incubated in seminal vesicular fluid [25-28]. Seminal vesicular fluid was found to alter considerably the pI value of sperm, since the positively charged seminal plasma proteins adsorb to the sperm surface, thus changing the surface charge of spermatozoa [25]. For example, the spermatozoa released from normal boars with seminal vesicle glands focused at pH 6.5 ± 0.35, while the spermatozoa from vesiculectomized boars focused at pH 4.5 ± 0.25 [25]. Under our experimental conditions, the pI of boar sperm was found to be close to pH 5 (Figure 7.5), which is within the range of values mentioned above. The specific value can be attributed to the difference between sample treatments used in our experiments and those in previous studies. The data in Figure 7.5 also show that the variation of running buffer pH didn't affect the G/R ratio within the experimental error of our method. To avoid any detrimental effects from extremes of pH on the viability of sperm, the pH of the running buffer was maintained at ~ pH 6.9, which is close to the actual pH of boar semen (see Table 7.1).

7.3.5. Effect of Ionic Strength.

The ionic strength of the running buffer has a dramatic influence on the electropherogram of boar sperm. As can be seen in Figure 7.6, when the concentration of Tris and citric acid increased, two things happened. First, the relative positions of the sperm and background peaks changed (Figure 7.6B and C). The reversal occurred when the concentration of the running buffer approached 20 mM Tris and 6.67 mM citric acid. The second thing that occurred was that the background peak became much sharper (i.e., focused) when the buffer concentration increased. Interestingly, the peak shape of the background didn't change as dramatically when NaCl was used to adjust the ionic strength of running buffer instead of Tris and citric acid (data not shown). As stated earlier, the background peak is probably produced by other cellular particles or the debris of sperm containing nucleic acid. The focusing of these colloidal particles in the semen matrix might be induced and even
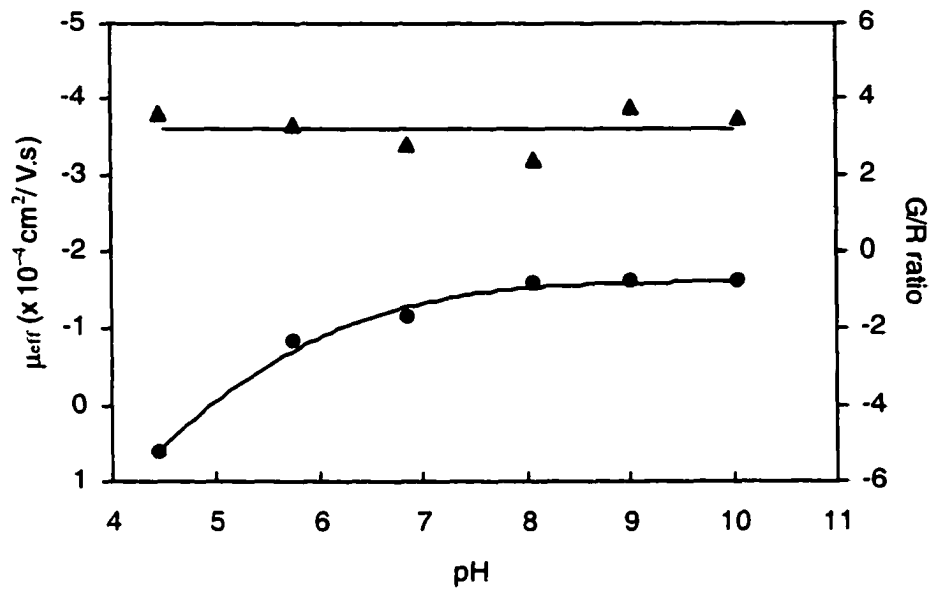
Figure 7.5. Effect of the pH of the running buffer on the electrophoretic mobility (μ_{eff}) (●) and the G/R ratio (▲) of the sperm peak. Boar semen was diluted with MR-A extender. The running buffer contained 30 mM NaCl, 1 mM Tris, 0.33 mM citric acid, and 1% fructose. Sample was injected for 10 seconds at 0.5 psi and the applied voltage was 5 kV.
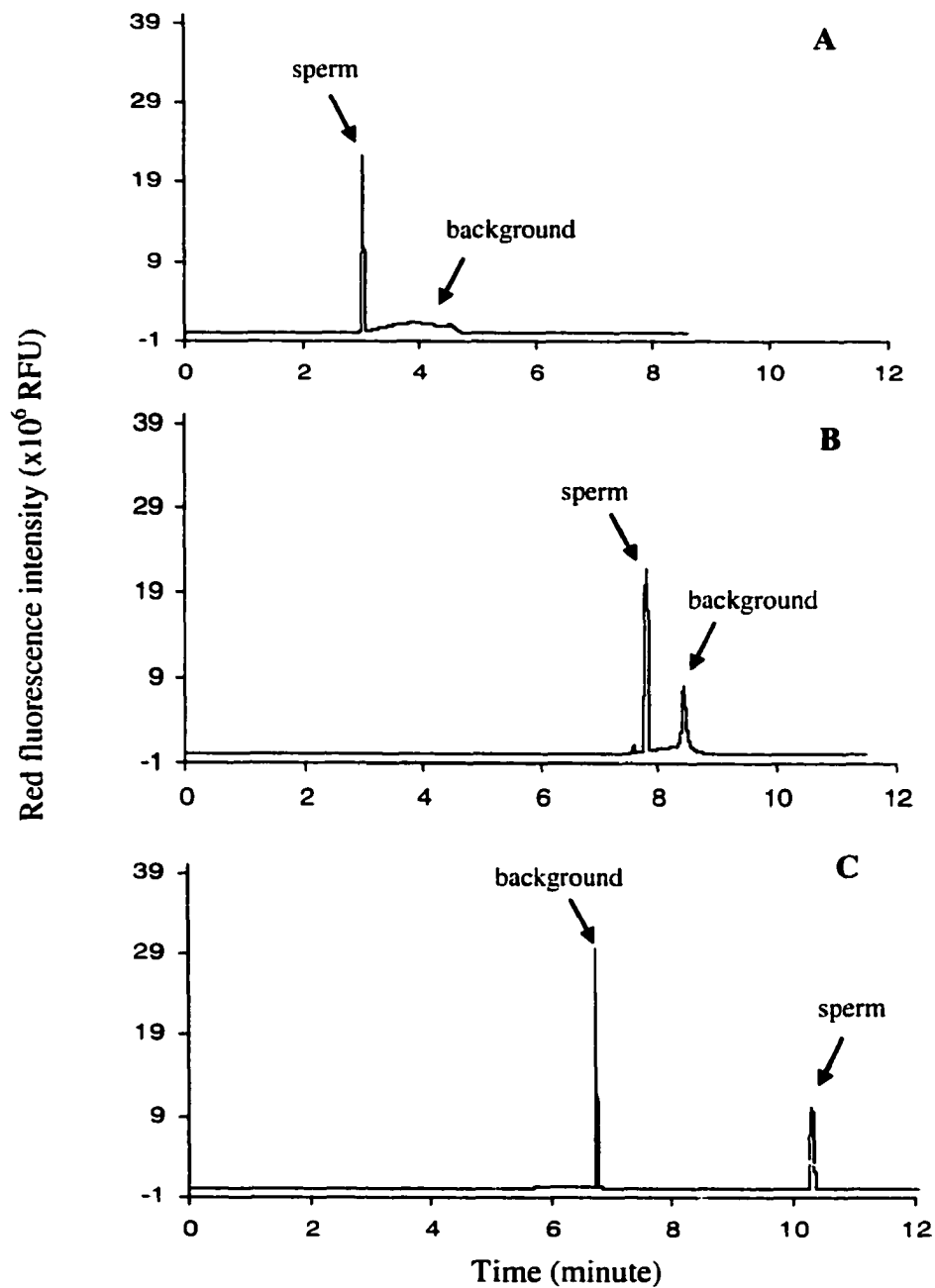
Figure 7.6. Electropherograms showing the effect of ionic strength in term of the concentration of Tris on the electrophoretic migration of sperm and background peak. The signal was collected after passing through a 630-nm band filter. In addition to 1% fructose, the running buffer consisted of A) 1mM Tris and 0.33 mM critic acid; B)10 mM Tris and 3.3 mM critic acid; C) 30 mM Tris and 10 mM critic acid with a pH of 6.9. Boar semen were diluted in Androhep Plus extender. Sample was injected for 10 seconds at 0.5 psi and the applied voltage was 5 kV.

enhanced under specific experimental conditions of ionic strength and the proper buffer system. A similar effect of higher ionic strength of the running buffer improving the peak shape of colloidal-sized analytes has been reported recently [24]. Different types of electrolytes in the running buffer were also found to significantly influence the mobility of colloidal-sized metal oxide fine particles and produce different selectivities in CZE separations of titania and alumina [21]. It should be noted that effects of ionic strength on the CE of colloids are expected to be more complex than for small molecules. This is because colloids in aqueous solution acquire charge not only by dissociation of their surface functional groups, but also by selective adsorption of ions and other species from solution. Thus the same colloidal particle can have a different surface charge and zeta potential if suspended in two solutions of the same pH and ionic strength, but different ionic compositions.

The ionic strength of the running buffer not only alters the appearance of the boar semen electropherogram, but also the G/R ratio of the sperm peak (Figure 7.7). Although the increase in the ionic strength of running buffer compresses the thickness of the double layers on both the capillary wall and the sperm cell surfaces, and slows the EOF slightly, the μ_{eff} of the sperm peak as shown by curve b in Figure 7.7 does not change appreciably (in the studied range of ionic strength). The running buffer ionic strength has a more complicated effect on the G/R ratio of the sperm peak. As can be seen from curve a in Figure 7.7, the G/R ratio initially remains constant and then changes sharply when the concentration of buffer is above 20 mM Tris and 6.67 mM citric acid. A similar effect of ionic strength was also observed when the ionic strength of the running buffer was adjusted with NaCl. This may be because the binding between SYBR-14 / PI and the nucleic acid of sperm can be affected by ionic strength. Previous studies showed that the binding constant between PI and free DNA diminishes markedly at higher ionic strength due to the electrostatic characteristic of the interactions between PI and DNA [38,39]. Although the mechanism by which the sperm nuclei stain with SYBR-14 has not been elucidated [3], ionic strength should have a similar influence on the binding between the sperm nuclei and SYBR-14 as it does for PI but to a different extent. For sperm with intact cell membranes, their cellular ionic strengths are well maintained; therefore, the interaction between dyes and nucleic acids should remain the same even though the ionic strength of the environment is changed. For dead sperm, however, the situation is different. Their compromised membranes allowed their cellular ionic compositions to be affected more easily by the surrounding solution. Since the sperm cells used in this part of study were all dead, it is expected that the G/R ratio of the sperm peak changes somewhat at high ionic strength. For accurate assessment of sperm viability, the same ionic strength must be used for both unknowns and standards.
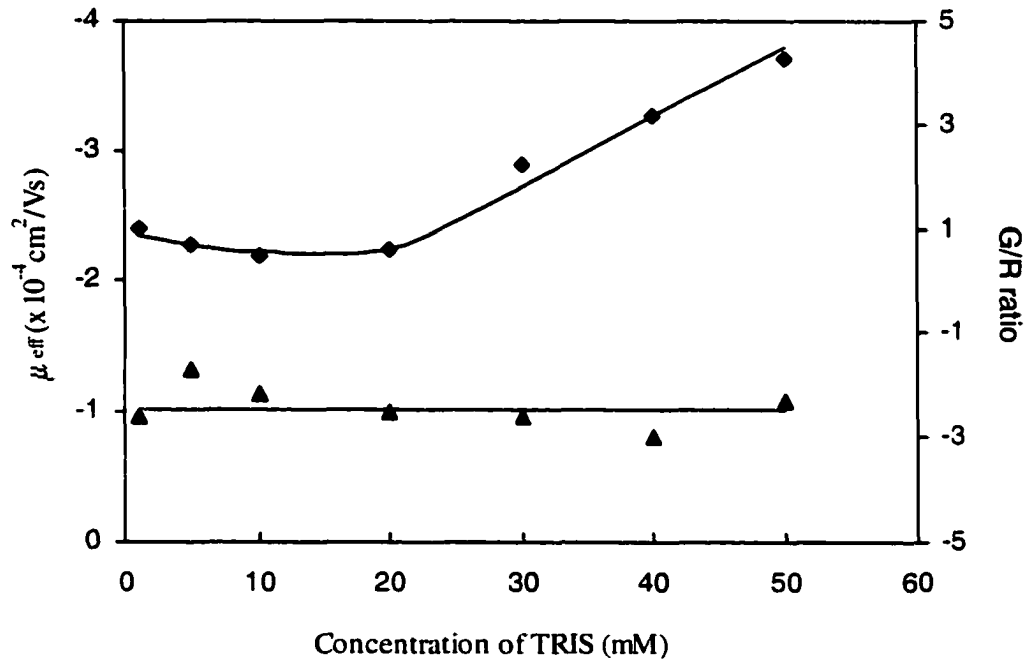
Figure 7.7. Effect of the ionic strength of the running buffer in term of the concentration of Tris on the electrophoretic mobility (♦) and the G/R ratio (▲) of the sperm peak. The ionic strength of the running buffer was adjusted by changing the concentration of Tris and citric acid. The rest conditions were the same as those in Figure 7.6.

7.3.6. Effect of Applied Voltage.

By definition, the electrophoretic mobility (μ_{eff}) of the charged analyte should remain constant as the applied voltage changes in CE. This is clearly shown by the data in Figure 7.8b. Because the μ_{app} of sperm and μ_{EOF} were measured separately (see experimental section), a small fluctuation of the μ_{eff} values, resulting from experimental error, was observed. We noticed that the boar semen matrix usually produced a sharp background peak at higher buffer concentrations (Figure 7.6C). This background peak could be used as an internal standard to correct the electrophoretic mobility of sperm at high buffer concentration. As a result, the μ_{eff} values of sperm (represented by the "▲" symbols in Figure 7.8) show much less fluctuation. Interestingly, the applied voltage had an effect on the G/R ratio of the sperm peak, namely, the G/R ratio increases with the applied voltage. This phenomenon is not yet well understood. Further investigation needs to be conducted in order to elucidate the mechanism behind this phenomenon.

7.3.7. Effect of PEO Additive.

In earlier studies, the addition of hydrophilic polymers to the running buffer played a key role in achieving highly efficient separations of microbes [15-19,24,29,31]. The dilute polymer additives slightly diminish the velocity of EOF, alter the electrophoretic mobility of microbes, and produce band narrowing during the separation. Similar effects of PEO additives were observed in the electrophoresis of boar sperm (Figure 7.9). The absolute value of the μ_{eff} of the sperm peak dramatically decreased as a small amount of PEO was added to the running buffer. The μ_{eff} tended to reach a minimum value as the PEO concentration further increased. However, it was noticed that the presence of polymer in the running buffer was not mandatory for obtaining an efficient single peak for sperm, as demonstrated in Figure 7.1 and 7.6. This is because boar semen extenders, which were used to suspended sperm cells, already contain polymeric components that can promote the focusing of the injected cells into a narrow zone. In spite of this, a polymer additive is still useful for the determination of sperm viability using the CE-LIF method. As can be seen in Figure 7.9, when the PEO concentration was below 0.1%, it had a minor effect on the G/R ratio of the sperm peak. The velocity of EOF, however, constantly decreased as the PEO concentration increased (data not shown). Therefore, PEO additives can be used to control the velocity of EOF and the electrophoretic mobility of sperm, while not affecting the fluorescence properties of stained sperm. The optimal PEO concentrations were found to be in the range of 0.01-0.05%. Using these conditions, both a better peak shape and short analysis times (less than 15 min) were obtained.
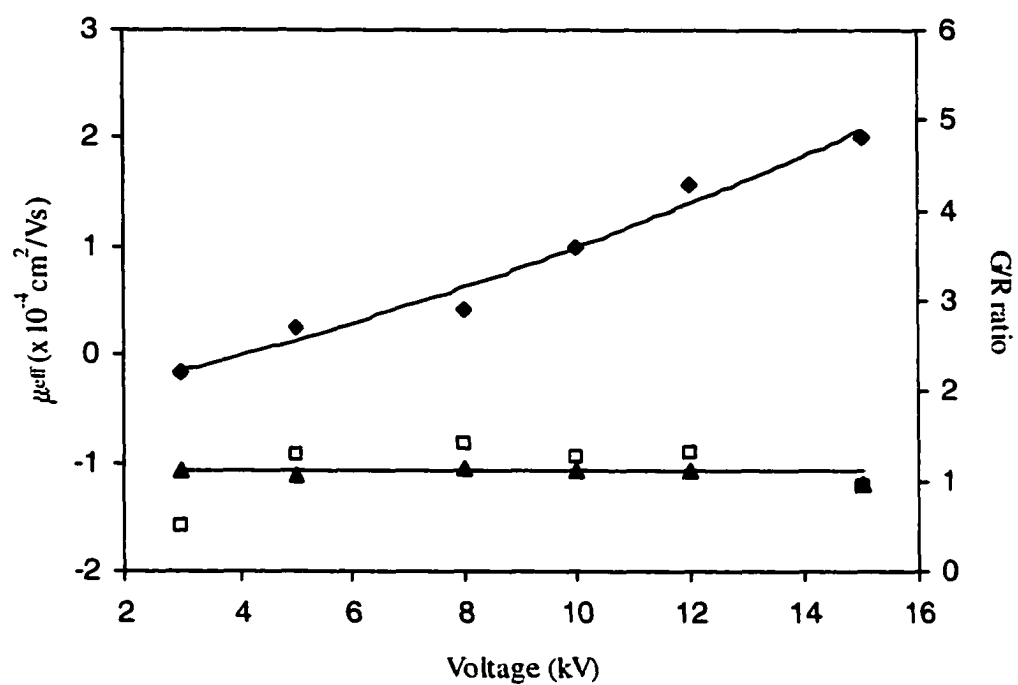
Figure 7.8. Effect of the applied voltage on the G/R ratio (♦) and μ_{eff} of the sperm peak. The μ_{eff} was corrected by subtracting (a) the velocity of EOF marker, represented by "□" data, and (b) the velocity of the background peak, represented by "▲" data. Boar semen was diluted with Androhep Plus extender. The running buffer contained 40 mM Tris, 13.3 mM citric acid, and 1% fructose with a pH of 7.26. Sample was injected for 10 seconds at 0.5 psi.

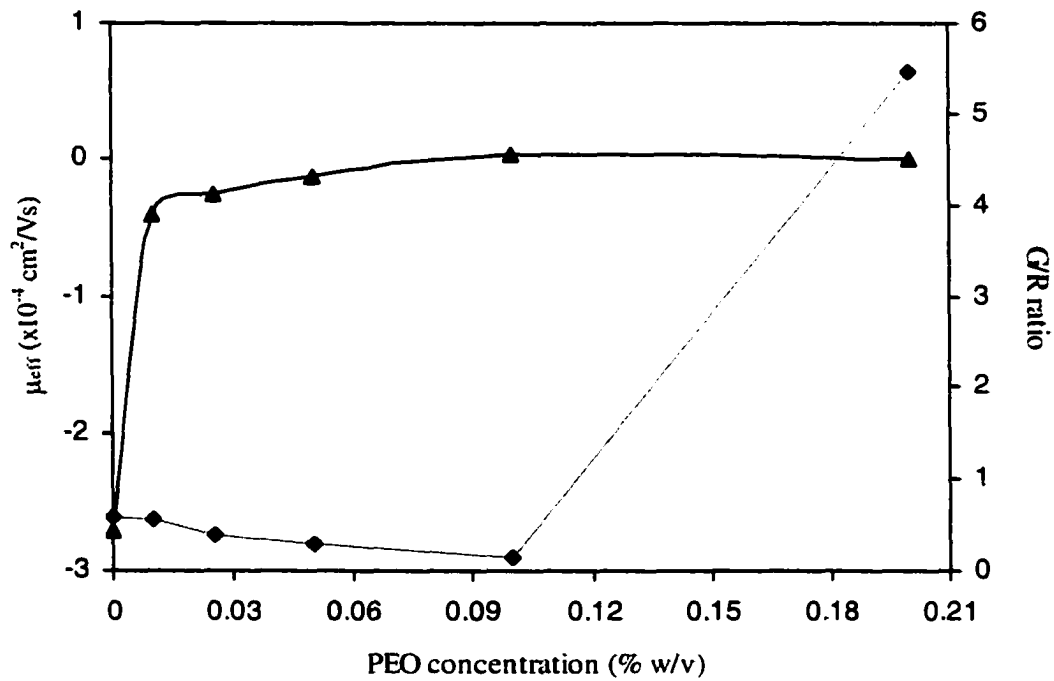Figure 7.9. Effect of the PEO concentration on μ_{eff} (▲) and the G/R ratio (♦) of sperm peak. The running buffer contains 1 mM Tris, 0.33 mM citric acid, and 1% fructose with a pH of 6.9. The rest experimental conditions were the same as those in Figure 7.8.
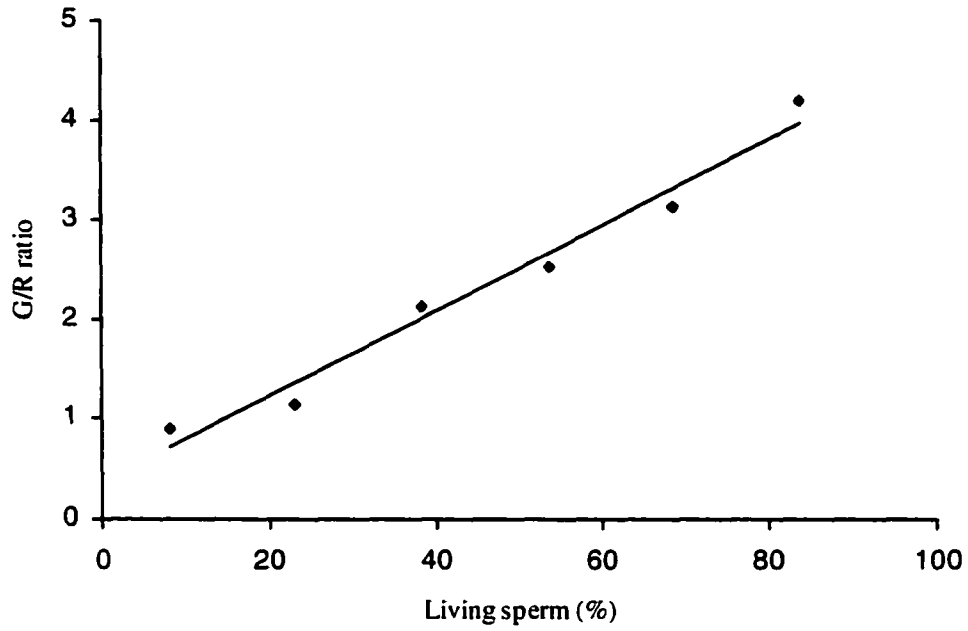
Figure 7.10. Standard viability curve for boar sperm (y = 0.043x + 0.3676, R^2 = 0.974). Semen sample was diluted with BTS extender.

8.3.8. Viability Calibration Curve of Boar Sperm.

Upon optimizing all the experimental conditions, the viability of sperm in a semen sample can be determined by constructing a calibration curve. Different boar semen extenders also have an impact on the electrophoresis and the G/R ratio of boar sperm due to their different compositions. Therefore, calibration curves should be constructed using the same extender that is used for analysis. The standard curve obtained when using BTS extender is shown in Figure 7.10. Using the G/R ratio in Figure 7.10, it was determined that the viabilities of sperm in two unknown boar semen samples were found to be 37% and 82%, respectively. These results are in agreement with those obtained in flow cytometry, within the experimental error, which were 46% and 75%, respectively.

8.4. CONCLUSIONS

CE-LIF is a valuable tool to study the electrophoretic behavior and evaluate the viability of boar sperm. A reproducible, sharp, single peak of sperm was easily obtained by diluting the boar semen samples in commercial boar semen extenders. The measured electrophoretic mobility (μ_{eff}) reflected the electrophoretic property of the aggregate of sperm rather than a population of individual sperm. The μ_{eff} of boar sperm was affected by pH, ionic strength and the polymer additive of the running buffer. Experimental results showed that the minimum amount of dye to saturate 10^7 sperm was 0.1 nmol for SYBR-14 and 25 nmol for PI. After staining by SYBR-14 and PI, the viability of boar sperm was determined by correlating the viability to the G/R ratio of the green fluorescence of living sperm to red fluorescence of dead sperm. The viability of boar semen samples determined with CE-LIF method was in agreement with that obtained with flow cytometry. Since the G/R ratio was affected by applied voltage, ionic strength and the polymer additives, it is critical to carefully control the experimental conditions so as to obtain accurate and reproducible results. The CE-LIF assay for sperm viability is not compromised by the presence of other cells, cell fragments and matrix contaminants as are some other methods, including flow cytometry. To our knowledge, this is the first report that the potency of mammalian sperm can be assessed by using a microfluidic electrokinetic technique.

ACKNOWLEDGEMENT

REFERENCES

1. Bearden, H.J.; Fuquay, J.W. *Applied animal reproduction*, 5th ed.; Prentice Hall: Upper Saddle River, NJ, **2000**; p 151.

2. Graham, E.F. In: Rinfret A. P., Petricciani J.C., eds. *The Integrity of Frozen Spermatozoa.* Washington, D.C.: National Academy of Science, **1978**; p 4-44.

3. Garner, D.L.; Johnson, L.A.; Yue, S.T.; Roth, B.L.; Haugland, R.P. *J. Androl.* **1994**, 16, 620-629.

4. McFeters, G.A.; Yu, F.P.; Pyle, B. H.; Stewart, P.S. *J. Microbiol. Meth.* **1995**, 21, 1-13.

5. Breeuwer, P.; Abee, T. *Int. J. Food Microbiol.* **2000**, 55, 193-200.

6. Garner, D.L.; Pinkel, D.; Johnson, L.A.; Pace, M.M. *Biol. Reprod.* **1986**, 34, 127-138.

7. Ericsson, S.A.; Garner, D.L.; Thomas, C.A.; Downing, T.W.; Marshall, C.E. *Theriogenology* **1993**, 39, 1009-1024.

8. Garner, D.L.; Dobrinsky, J.R.; Welch, G.R.; Johnson, L.A. *Theriogenology* **1996**, 45, 1103-1113.

9. Graham, J. K.; Kunze, E.; Hammerstedt, R.H. *Biol. Reprod.* **1990**, 43, 55-64.

10. Garner, D.L.; Johnson, L.A. *Biol. Reprod.* **1995**, 53, 276-284.

11. Garner, D.L.; Johnson, L.A.; Allen, C.H.; Palencia, D.D.; Chambers, C.S. *Theriogenology* **1996**, 45, 923-934.

12. Cerolini, S.; Maldjian, A.; Surai, P.; Noble, R. *Anim. Reprod. Sci.* **2000**, 58, 99-111.

13. Donoghue, A.M.; Garner, D.L.; Donoghue, D.J.; Johnson, L.A. *Poult. Sci.* **1995**, 1191-1200.

14. Arndt-Jovin, D.J.; Jovin, T.M. *J. Histochem Cytochem.* **1977**, 25, 585-589.

15. Armstrong, D.W.; Schneiderheinze, J.M.; Kullman, J.P.; He, L. *FEMS Microbiol. Lett.* **2001**, 194, 33-37.

16. Armstrong, D.W.; He, L. *Anal. Chem.* **2001**, 73, 4551-4557.

17. Armstrong, D.W.; Schulte, G.; Schneiderheinze, J.M.; Westenberg, D.J. *Anal.Chem.* **1999**, 71, 5465-5469.

18. Armstrong, D.W.; Schneiderheinze, J.M. *Anal. Chem.* **2000**, 72, 4474-4476.

19. Schneiderheinze, J.M.; Armstrong, D.W.; Schulte, G.; Westenberg, D.J. *FEMS Microbiol. Lett.* **2000**, *189*, 39-44.

20. Torimura, M.; Ito, S.; Kano, K.; Ikeda, T.; Esaka, Y.; Ueda, T. *J. Chromatogr. B*, **1999**, 721, 31-37.

21. Radko, S. P.; Chrambach, A. *J. Chromatogr. B*, **1999**, 722, 1-10.

22. Kenndler, E.; Blass, D. *Trends in Anal. Chem.* **2001**, 20, 543-551.

23. Van Der Mei, H.C.; Busscher, H. J. *Appl. Environ. Microbiol.* **2001**, 67, 491-494.

24. Shitani, T.; Yamada, K.; Torimura, M. *FEMS Microbiol. Lett.* **2002**, 210, 245-249.

25. Moore, H.D.M.; Hibbitt, K.G. *J. Repod. Fertl.* **1975**, 44, 329-332.

26. Hammerstedt, R.H.; Keith, A. D.; Boltz, Jr., R.C.; Todd, P.W. *Arch. Biochem. Biophys.* **1979**, 194, 565-580.

27. Moore, H.D.M. *Int. J. Androl.* **1979**, 2, 449-462.

28. Rahi, H.; Srivastava, P.N. *Gamete Res.* **1983**, 4, 325-329.

29. Girod, M.; Armstrong, D.W. *Electrophoresis* **2002**, 23, in press.

30. Zheng, J.; Yeung, E.S. *Anal. Chem.* **2002**, submitted.

31. Armstrong, D. W.; Girod, M.; He, L.; Rodriguez, M. A.; Wei, W.; Yeung, E.S.; Zheng, J. *Anal. Chem.* **2002**, in press.

32. Nichols, S.C.; Leowenberg, M.; Davis, R.H. *J. Colloid Interface Sci.* **1995**, 176, 342-351.

33. Grossman, P.D.; Soane, D.S. *Anal. Chem.* **1990**, 62, 1592-1596.

34. Haugland, R.P. Chapter 15 in *Handbook of Fluorescent Probes and Research Chemicals*, 8th ed., Molecular Probes, Eugene, OR.

35. Bey, E., *in "Cell Separation Methods"* (Ambrose, E.J., ed.), p. 142-151. Little, Brown and Co., Boston, **1965**.

36. Hafs, H.D.; Boyd, L.J. in *Sex Control at Birth-Prospects for Control* (Kiddy, C.A.; Hafs, H.D., eds), p. 85-97, American Society of Animal Sciences, Champaign, Illinois.

37. Harden, V.P.; Harris, J.O. *J. Bacteriol.* **1953**, 65, 198-202.

38. Chou, W.Y.; Marky, L.A.; Zaunczkowski, D.; Breslauer, K.J. *J. Biomol. Struct. Dyn.* **1987**, 5, 345-359.

39. Wilson, W. D.; Wang, Y.H.; Krishnamoorthy, C.R.; Smith, J.C. *Biochem.* **1985**, 24, 3991-3999.

CHAPTER 8

GENERAL CONCLUSIONS

The research outlined in the first part of this dissertation demonstrates several potential applications of imidazolium-based ionic liquids in the analytical chemistry field. The wetting ability and viscosity of room-temperature ionic liquids (RTILs) allow them to be used as GC stationary phases. The results based on 1-butyl-3-methylimidazolium hexafluorophosphate ([BuMIm][PF$_6$]) and the analogous chloride salt ([BuMIm][Cl]) show that ionic liquid stationary phases have a dual nature. They act as nonpolar stationary phases when separating nonpolar analytes or somewhat polar analytes that are not proton-donor or -acceptor molecules. However, they act in the opposite manner (i.e., are highly interactive and retentive) when used to separate molecules with somewhat acidic or basic functional groups. Thus, molecules with proton-donor or -acceptor characteristics tend to be spatially resolved, as a group, from nonpolar analytes. The dual nature of ionic liquid stationary phases also is evident from the Rohrschneider-McReynolds constants. Inverse GLC also is a good way to examine the nature of different ionic liquids. It is apparent that the chloride-containing ionic liquid interacted much more strongly with proton-donor and -acceptor molecules. The hexafluorophosphate-containing ionic liquid tended to be somewhat less polar and interacted more strongly with nonpolar solutes.

RTILs were found to be capable of solubilizing complex macrocyclic molecules such as cyclodextrins and their derivatives and macrocyclic antibiotics. This property enables RTILs to be used as stationary phase solvents for methylated cyclodextrins in GC. Our results establish that the [BuMI][Cl] is a useful solvent for GC stationary phases. It is able to dissolve a large amount of tested chiral selectors (more than 25% w/w) without intervening too much in the retention process of the derivatized analytes. It has a good viscosity producing a good kinetics in the solute-stationary phase exchange process and consequently, producing sharp peaks. It was also shown that methylated CDs were able to form inclusion complexes with 1-butyl-3-methylimidazolium, the cation of [BuMI][Cl]. The complexation of the CD cavity by the RTIL hindered the inclusion mechanism for the separation of the analyte enantiomers. Consequently, the CD-RTIL capillary columns were only able to separate enantiomers by external adsorption. This allows one to examine the inclusion complex formation and independent contributions to enantioselective GC involving CD-based CSPs. RTIL should be able to work well as GC stationary phase solvents with other molecules not able to make inclusion complexation.

Another potential application of ionic liquids is using as MALDI matrices, in which the vacuum stability and solubalizing power of ionic liquids are taken advantage of. With ionic matrixes, it is possible to combine the beneficial qualities of liquid and solid matrixes. Ionic liquids produce a much more homogeneous sample solution (as do all liquid matrixes) yet have greater vacuum stability than most solid matrixes. In many (most) cases, an ionic matrix can be found that produces greater spectral peak intensities and lower limits of detection than comparable solid matrixes. Most ionic liquids readily dissolve biological oligomers, proteins, and polymers. However, ionic liquids can vary tremendously in their ability to promote analyte ionization. Both the cationic and anionic portion of the ionic matrix must be chosen with a consideration for the special requirements of UV-MALDI. The ionic matrix must have significant absorbance at the desired wavelength, but also available protons. Most conventional ionic liquids that lack these properties are ineffective as MALDI matrixes.

The advent of high-efficiency microbial separations makes it possible to obtain qualitative and quantitative information on microbial systems with the accuracy, precision, speed, and throughput that currently is found for chemical systems. When this analytical separation-based approach is combined with dual fluorescence labeling techniques, it can be used to determine the viability of cells. For the first time, the feasibility and advantages of such an approach is demonstrated by separating, identifying, and determining the viability of two bacteria and yeast all in a single run. With this method each type of cells in a mixture could be analyzed individually without interference with each other. Living and dead cells are stained by fluorescent nucleic acid stain SYTO-9 and propidium iodide, respectively, and the viability of cells is obtained by establishing a standard curve that correlates the cell viability to the fluorescence response. The accuracy and reproducibility of results obtained in CE-LIF system are depended on the choice of suitable optical filters, properly staining the cells and carefully controlling other experimental conditions.

The usefulness of CE-LIF technique was further extended to the potency assay of boar sperm. In this study, it is essential to suspend sperm cells in commercial boar semen extenders in order to obtain single peak of sperm. The combination of fluorescent nucleic acid stains SYBR-14/PI was used to label sperm cells. The minimum amount of dye to saturate 10^7 sperm was 0.1 nmol for SYBR-14 and 25 nmol for PI. The viability of boar sperm was determined by correlating the viability to the G/R ratio of the green fluorescence of living sperm to red fluorescence of dead sperm. The viability of boar semen samples determined with CE-LIF method was in agreement with that obtained with flow cytometry. Since the G/R ratio was affected by applied voltage, ionic strength and the polymer additives,

it is critical to carefully control the experimental conditions so as to obtain accurate and reproducible results. The CE-LIF assay for sperm viability is not compromised by the presence of other cells, cell fragments and matrix contaminants as are some other methods, including flow cytometry.

Our study also shows that CE-LIF is a valuable tool to study the electrophoretic behavior of cell. Under our experimental conditions, the measured electrophoretic mobility (μ_{eff}) reflected the electrophoretic property of the aggregate of sperm rather than a population of individual sperm. The μ_{eff} of boar sperm was affected by pH, ionic strength and the polymer additive of the running buffer. To our knowledge, this is the first report that the potency of mammalian sperm can be assessed by using a microfluidic electrokinetic technique.